Adaptive Response of the Kidney to Metabolic Acid

Dissertation

zur

Erlangung der naturwissenschaftlichen Doktorwürde

(Dr. sc. nat.)

vorgelegt der Mathematisch-naturwissenschaftlichen Fakultät

der Universität Zürich

von

Marta Nowik

aus Polen

Promotionskomitee:

Prof. Dr. Carsten A. Wagner

Prof. Dr. Jürg Biber

Prof. Dr. André W. Brändli

Zürich, 2008

INDEX

SUMMARY.....1
DEUTSCHE ZUSAMMENFASSUNG DER DOKTORARBEIT..... 4
1. INTRODUCTION…..…….7
2. KIDNEYS CONTRIBUTION TO ACID-BASE BALANCE……..…… 9
   2.1. Reabsorption of bicarbonate…….…… 9
   2.2. Excretion of titratable acids……...…… 10
   2.3. Synthesis and secretion of ammonia……...…11
   2.4. Proton and bicarbonate transport in the collecting duct.……12
3. DISTURBANCES OF ACID-BASE BALANCE…… 14
   3.1. Metabolic acidosis……..…… 14
      3.1.1. Renal tubular acidosis……..……15
4. RENAL ADAPTATION TO METABOLIC ACIDOSIS…….……16
   4.1. Proximal tubule adaptation…… 16
   4.2. Distal nephron adaptation……..……18
   4.3. Hormonal adaptation……..…… 19
5. POTENTIAL MECHANISMS OF RENAL ACID-BASE SENSING……... 20
6. HIGH-THROUGHPUT TECHNIQUES FOR TRANSCRIPTOME SCANNING.....21
   6.1. High-throughput techniques used to study renal adaptation to metabolic acidosis…..…… 22
7. MOUSE MODELS USED IN THIS STUDY……..……24
   7.1. NaPi-IIa deficient mice…… 24
   7.2. Models of NH_4Cl-induced metabolic acidosis…….……24
8. AIM OF THE WORK…… 26
9. PUBLICATIONS THAT CONTRIBUTED TO THIS WORK……27
   9.1. Genome-wide gene expression profiling reveals renal genes regulated during metabolic acidosis……28

9.2. Renal phosphaturia during metabolic acidosis revisited: molecular mechanisms for decreased renal phosphate reabsorption……..... 29
9.3. Induction of metabolic acidosis with ammonium chloride (NH_4Cl) in mice and rats – species differences and technical considerations……..…… 30
10. SUMMARY OF THE RESULTS……..……31
10.1. Genome wide detection of renal genes regulated during metabolic acidosis……31
10.2. Molecular mechanisms for decreased renal phosphate reabsorption during metabolic acidosis…… 32
10.3. Induction of metabolic acidosis with ammonium chloride – some technical considerations…..……..……33
10.4. Renal adaptation to metabolic acidosis – outlook and an integrative view…….……33
11. PUBLICATIONS THAT DID NOT CONTRIBUTE TO THIS WORK…….35
11.1. Thyroid hormone deficiency alters expression of acid-base transporters in rat kidney…… 36
11.2. Role of Rhesus factor RhCG in renal ammonium excretion and male fertility……..……..…… 37
11.3. Calcium-sensing receptor-mediated urinary acidification prevents renal stone formation…….. 38
11.4. Proliferation of acid-secretory cells in the kidney during adaptive remodeling of the collecting duct…….…..…... 39
REFERENCES…… 40
ACKNOWLEDGMENTS…… 52
CURRICULUM VITAE……..…. 53
LIST OF PUBLICATIONS……..……..… 55

SUMMARY

The kidney is a central organ responsible for maintaining acid-base homeostasis, body fluid status, and electrolyte balance. During metabolic acid challenges or metabolic acidosis (MA) this homeostasis is disturbed leading to increased renal acid secretion, a process that requires the concerted regulation of metabolic and transport pathways, which are only partially understood. Therefore we aimed in this project to characterize adaptational changes occurring in the kidney during metabolic acidosis.

In the first part we investigated transcriptional changes in the kidney during 2 and 7 days NH_4Cl-induced MA performing a genome-wide scan using microarray technology. We identified 4,075 transcripts with altered expression in response to 2 and/or 7 day acid-load. The majority of genes (3,070) exhibited transient changes in expression levels responding only to 2 days NH_4Cl treatment that may indicate renal adaptation to MA or stress. Among regulated transcripts were genes involved in cell growth, proliferation, apoptosis, water homeostasis, and ammoniagenesis. The most represented group contained members of different solute carrier transporters (97 SLC members). Pathway analysis revealed that the most affected pathway was oxidative phosphorylation, which may indicate increased requirement for ATP in acidotic mice. Selected genes from ammoniagenic and gluconeogenic pathways (SNAT3, PEPCK, PDG) were found to be differentially regulated between early (S1/S2) and late (S3) parts of the proximal tubule. These findings suggest that the kidney responds to MA by temporally and spatially altering the expression of a large number of genes.

Among genes found by microarray screening was the Na^+-dependent phosphate (Pi) cotransporter NaPi-IIc that was strongly downregulated in kidneys of 2 and 7 days acidotic mice. Phosphate reabsorption in the proximal tubule is mediated by two cotransporters located in the brush border membrane (BBM), NaPi-IIa and NaPi-IIc. During metabolic acidosis urinary phosphate excretion is increased and contributes to acid removal. To further investigate the contribution of transporter regulation to phosphaturia, we induced MA for 2 and 7 days in

wildtype and NaPi-IIa KO mice and examined NaPi-IIa, IIc, Pit1, and Pit2 mRNA expression, changes in NaPi-IIa and IIc protein abundance, activity, and localization. We found that acidosis increased BBM abundance of NaPi-IIa and NaPi-IIc, although mRNA expression was significantly lower. Interestingly, no changes in localization of both cotransporters were found. These findings show that phosphaturia observed during MA is not due to reduced protein abundance of Na^+-dependent cotransporters and suggest a direct inhibitory effect of low pH, mainly on NaPi-IIa function.

The kidney is also an important organ to sustain body fluid homeostasis. Microarray screening of acidotic mice kidneys showed upregulation of several genes involved in renal water handling (the water channels AQP1, AQP2, AQP3, AQP4, the urea transporter UT-A1, and the vasopression receptor V2R), but acidotic mice consumed about 20% less water, which could contribute to the regulation. Therefore, in the third part of my PhD work, we compared two similar protocols to induce MA in mice and rats: standard 0.28M NH_4Cl in drinking water or an equivalent amount of NH_4Cl in food. Both treatments induced MA. However, mice and rats responded differently regarding mRNA and protein expression of AQP2, AQP3 and V2R, dependent on route of NH_4Cl application. Pendrin, SNAT3 and PEPCK, known to be regulated during MA, were regulated irrespectively of the route of NH_4Cl application. Thus, application of NH_4Cl in water but not MA per se induces dehydration causing regulation of various transport proteins involved in water homeostasis. These data demonstrate that the standard protocol inducing MA with NH_4Cl in drinking water is problematic and that application of NH_4Cl in food should be considered. Moreover, mice and rats respond differently to NH_4Cl loading, and increased water intake and diuresis may be a compensatory mechanism during MA.

In summary, using microarray technology, we identified genes and major pathways involved in both acute and chronic adaptation to metabolic acidosis. Among the genes downregulated was the Na^+-dependent Pi cotransporter NaPi-IIc, and we therefore studied its contribution to acidosis-induced phosphaturia.

Furthermore, we found a number of genes involved in water homeostasis to be affected by acid-loading. This led us to investigate different routes of NH_4Cl application in the context of induction of metabolic acidosis and dehydration.

More recently we employed the newly developed SILAC (stable isotope labeling with amino acids in cell culture) mouse to study proximal tubule (S1/S2 and S3 segment) specific changes in protein expression after 2 days of NH_4Cl-induced MA. Combination of large scale screening through microarray and proteomics will provide us with more complex information about adaptive responses of the kidney to metabolic acidosis.

DEUTSCHE ZUSAMMENFASSUNG DER DOKTORARBEIT

Die Niere spielt eine zentrale Rolle für das Aufrechterhaltung des Säure-Basengleichgewichtes, des Wasserhaushaltes, und der Elektrolytbalance. Diese Homöostase kann gestört werden durch vermehrten Bildung von Säuren im Metabolismus oder eine metabolische Azidose (MA). Dies führt wiederum zu einer vermehrten renalen Ausscheidung von Säuren, ein Prozess, der von der koordinierten Regulation von Stoffwechsel und Transportvorgängen abhängt. Die zugrundeliegenden Vorgänge sind allerdings nur bedingt untersucht und verstanden. Daher war es das Ziel dieser Arbeit adaptive Prozesse in der Niere während einer metabolischen Azidose zu charakterisieren.

Im ersten Teil der Arbeit untersuchten wir mittels Mikroarray-Technologie Genom-weit die transkriptionellen Veränderungen in der Niere nach 2 bzw. 7 Tagen Azidose, induziert durch Gabe von NH_4Cl. Wir fanden, dass 4,075 Transkripte eine veränderte Expression zeigten nach 2 und/oder 7 Tagen Säurebeladung. Die Mehrheit dieser Gene (3,070) zeigte nur einen transiente Veränderung der Expression nach 2 Tagen, ein möglicher Hinweis auf eine renale Adaptation oder Stress. Unter den regulierten Transkripten befanden sich Gene, die an der Regulation von Zellwachstum, Zellteilung, Apoptose, des Wasserhaushaltes, und der Ammoniagenese beteiligt sind. Am stärksten repräsentiert waren jedoch sogenannte Solute Carrier Transporter (SLC Familie) mit insgesamt 97 regulierten Transkripten. Die Analyse von Stoffwechselwegen zeigte, dass oxidative Phosphorylierung sehr stark reguliert war, was auf einen vermehrten Bedarf an ATP hinweisen könnte. Ausgewählte Gene aus der Ammoniagenese und Glukoneogenese (SNAT3, PEPCK, PDG) waren unterschiedlich im frühen (S1/S2) und späten (S3) Abschnitt des proximalen Tubulus reguliert. Dies deutet darauf hin, dass die Niere auf eine metabolische Azidose durch eine räumlich und zeitlich regulierte Antwort adaptiert.

Unter den durch Mikroarray entdeckten, regulierten Genen war auch der Na^+-abhängige Phosphat (Pi) Kotransporter NaPi-IIc, dessen mRNA in der Niere nach 2 und 7 Tagen Azidose stark herunterreguliert war. Die Phosphatreabsorption in der Bürstensaummembran des proximalen Tubulus wird durch mindestens zwei Kotransporter, NaPi-IIa und NaPi-IIc, vermittelt. Während metabolischer Azidose ist der Urinausscheidung von Phosphat erhöht and trägt zur Säureausscheidung aus. Um die Rolle der Regulation der Phosphattransporter zur Phosphaturie während metabolischer Azidose weiter zu untersuchen, wurde MA für 2 und 7 Tage in Wildtypmäusen und NaPi-Iia Knock-out Mäusen induziert. Die mRNA und Proteinexpression von NaPi-IIa, NaPi-IIc, Pit1, und Pit2, sowie die Lokalisierung von NaPi-IIa und NaPi-IIc, und die natrium-abhängige Phosphattransportraten wurden untersucht. Metabolische Azidose erhöhte die Proteinexpression von NaPi-IIa und NaPi-IIc, obwohl die mRNA Expression verringert wurde. Die Lokalisation beider Transporte änderte sich nicht. Diese Daten deuten darauf hin, dass die Phosphaturie nicht durch Herunterregulation der Phsophattransporter induziert wird, sondern vermutlich durch einen direkten Effekt des sauren Urin pH auf die Transportaktivität, hauptsächlich auf den Protonen-sensitiven NaPi-IIa Transporter.

Die Niere kontrolliert den Wasserhaushalt. Unsere Mikroarray Daten zeigten die Hochregulation verschiedener Gene, die in der Niere an der Urinkonzentration und damit der Regulation des Waserhaushaltes beteiligt sind (die Wasserkanäle AQP1, AQP2, AQP3, AQP4, der hHrnstofftransporter UT-A1, und der Vasopression-Rezeptor V2R). Allerdings tranken azidotische Mäuse auch 20% weniger Wasser. Daher untersuchten wir im dritten Teil dieser Arbeit zwei ähnliche Protokolle zur Induktion von Azidose mittels NH4Cl. Der wichitgste Unterschied war, dass in einem Protokoll die Mäuse frei Wasser trinken konnten: Standarddiät 0.28M NH_4Cl im Trinkwasser oder die äquivalente Menge von NH_4Cl im Futter. Beide Protokolle verursachten MA. Interessanterweise reagierten Mäuse und Ratten unterschiedlich und zeigten verschiedene Muster in der Regulation von mRNA und Proteinexpression von AQP2, AQP3 und V2R,

abhängig auch vom NH_4Cl Beladungsprotokoll. Die Regulation von Pendrin, SNAT3 und PEPCK, Kontrollgene, war unabhängig vom Protokoll. Die Beladung mit NH4Cl im Trinkwasser führt zu Azidose und Dehydrierung in Ratten und Mäusen. Azidose allein führt eher zu einer vermehrten Diurese und Herunterregulation von Wasserkanälen. Zukünftige Arbeiten sollten daher eher auf eine Beladung der Tiere mit NH_4Cl im Futter zurückgreifen, vermehrte Diurese stellt vermutlich einen kompensatorischen Mechanismus bei Azidose dar.

Zusammenfassend lässt sich sagen, dass wir mittels Mikroarray verschiedene Stoffwechselwege entdecken konnten, die während der Adaptation der Niere an akute oder chronische Säurebeladung eine Rolle spielen. Der NaPi-IIc Phosphatkotransporter war auf mRNA Ebene herunterreguliert und wir untersuchten seine Rolle bei Phosphaturie. Darüberhinaus fanden wir eine grosse Zahl von Genen, die an der Regulation des Wasserhaushaltes beteiligt sind. Wir haben daher auch untersucht inwiefern die die Art der Säurebladung der Tiere das Ausmass der Azidose und Dehydrierung beeinflusst.

Wir konnten kürzlich die neu entwickelte SILAC (stable isotope labeling with amino acids in cell culture) Proteomtechnologie in der Maus anwenden und Proteinexpression in isolierten frühen (S1/S2) und späten (S3) Segmenten des proximalen Tubulus während metabolischer Azidose untersuchen. Die Kombination der Transkriptomdaten aus den Mikoarray Experimenten und Proteomdaten aus diesem Ansatz erlauben uns nun komplexere Regulationsprozesse auf beiden Ebenen zu untersuchen und die räumliche/anatomische Auflösung zu verbessern.

1. INTRODUCTION

Systemic acid-base homeostasis is maintained within a tight physiological range of pH 7.36-7.45 by the cooperation of various body buffering systems. These are release of $CaCO_3$ from bone, regulated exhalation of CO_2 by the lungs, glutamine release from the liver, phosphate absorption in the intestine, and acid or base excretion by the kidney (32). Body buffering and CO_2 exhalation is important in the immediate response to changes in acid-base balance, whereas the kidney is crucial for the intermediate and long-term adaptation.

Tight regulation of acid-base status is necessary to sustain essential biochemical and metabolic functions of cells and organs. Therefore, a number of physiological buffering systems exist to control pH in various body compartments (47). A buffer is any substance that reversibly consumes or releases H^+ (15). Among intra- and extracellular buffers are proteins, organic and inorganic phosphates, hemoglobin, creatinine, urate, and ammonia. However, the most important physiological buffer in extracellular fluid is the carbonic acid – bicarbonate system (47):

(Eqn. 1) $$CO_2 + H_2O \leftrightarrow H_2CO_3 \leftrightarrow H^+ + HCO_3^-$$

The respiration and the kidney react to changes in acid-base status by controlling two major components of this system: respiration CO_2 and the kidneys HCO_3^- (47). The relationship between pH, pCO_2 and HCO_3^- is described by the Henderson-Hasselbalch equation (15, 38):

(Eqn. 2) $$pH = 6.1 + \log \frac{[HCO_3^-]}{0.03 \times pCO_2}$$

The Henderson-Hasselbalch equation describes that a shift in plasma pH can be caused either by change in the plasma concentration of HCO_3^- or the partial pressure of CO_2 (pCO_2) in blood (38).

Normal metabolism generates volatile and non-volatile acids. The largest source of acid is CO_2 that is a volatile acid produced during oxidation of carbohydrates, fats, and most amino acids in amount of approximately 15,000 mmol/day. Carbon dioxide could potentially act as an acid because in body fluids it is immediately converted to H^+ and HCO_3^- (Eqn. 1). However, this large amount is removed by exhalation by the lungs.

Dietary protein metabolism results also in production of so called non-volatile acids. A standard protein-rich western diet generates approximately 70 mmol of acid per day that cannot be exhaled from the body and must be removed by the kidney. These non-volatile acids are buffered primarily by the carbonic acid buffering system (Eqn. 1), which leads to its consumption and subsequent fall in plasma bicarbonate concentration. To avoid fall in plasma pH, the consumption of bicarbonate is balanced by the generation of new bicarbonate using two major mechanisms in the kidney: secretion of H^+ together with excretion of titratable acids, and synthesis and secretion of ammonia.

2. THE KIDNEYS CONTRIBUTION TO ACID-BASE BALANCE

The kidneys play a central role in maintaining acid-base homeostasis by applying three mechanisms: 1) reabsorption of virtually all filtered bicarbonate, 2) excretion of excess acid, 3) synthesis of ammonia and excretion of ammonia/ammonium and titratable acids.

2.1 Reabsorption of bicarbonate

The major buffering system for maintaining acid-base balance of the blood is bicarbonate. Daily approximately 4,500 mmol of bicarbonate is freely filtered at the glomerulus (47). To prevent loss of the buffer in the urine the kidney reabsorbs virtually all filtered bicarbonate, mainly in the proximal tubule and to a lesser extend in the thick ascending limb (21).

Up to 80% of filtered bicarbonate is reabsorbed in the proximal tubule via the concerted action of the apical Na^+/H^+ exchanger NHE3, vacuolar H^+-ATPases, and luminal and cytosolic carbonic anhydrases (CAIV and CA II, respectively) (Fig. 1). In the lumen CAIV catalyzes formation of CO_2 and H_2O from filtered HCO_3^- and excreted protons. Carbon dioxide rapidly diffuses into the tubular cell, where it is rehydrated by cytosolic CAII to HCO_3^- and H^+. Bicarbonate formed in this reaction is transported across the basolateral membrane into blood via a Na^+/HCO_3^- cotransporter, whereas H^+ is excreted into urine, mainly by NHE3 and to smaller extent by H^+-ATPases. The remaining 20% of bicarbonate is reabsorbed along the loop of Henle at the level of the thick ascending limb (TAL) in a similar process as in the proximal tubule (22).

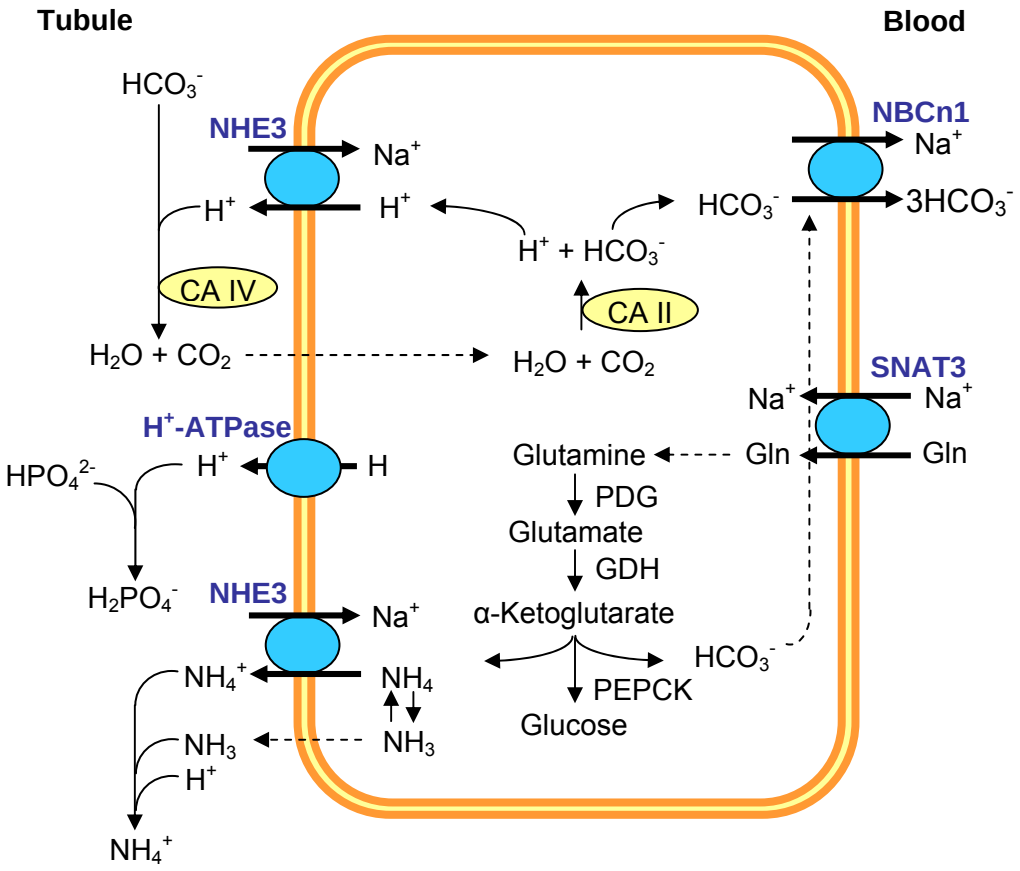

Fig. 1 Mechanisms of proximal tubule bicarbonate reclamation (modified after (40)). Detailed description in the text.

2.2 Excretion of titratable acids

Titratable acid (TA) by definition means the amount of base one must add to a sample of urine to bring its pH back up to the pH of blood plasma (47). The sum of excreted titratable acids and NH_4^+ minus bicarbonate lost in urine is described as net acid excretion (NAE) (47):

(Eqn. 3) $NAE = TA + NH_4^+ - \text{urinary } HCO_3^-$

Protons excreted into the tubule lumen can be buffered both by HCO_3^- or titratable acids, mainly phosphoric acid (HPO_4^{2-}), and to a smaller extent sulfuric acid, citric acid, and creatinine.

Phosphate is the main titratable acid in urine. Phosphate, in form of monohydrogen phosphate (HPO_4^{2-}), can be titrated by H^+ to dihydrogen phosphate ($H_2PO_4^-$) and excreted into urine with sodium (Fig. 1). Titration of HPO_4^{2-} has however limited capacity and only 30 mmol/day of H^+ can be removed that way (38, 47). Under normal physiological conditions the bulk of filtered phosphate is reabsorbed in the brush border membrane (BBM) of the proximal tubule via at least two Na^+-dependent phosphate cotransporters, NaPi-IIa (Slc34a1) and NaPi-IIc (Slc34a3) (83, 104).

2.3 Synthesis and secretion of ammonia

Ammonia (NH_3) is the only buffer synthesized by the kidney itself and is the main component of net acid excretion.

Renal ammoniagenesis takes place in the proximal tubule (84) and requires uptake of glutamine from the blood via a Na^+-dependent glutamine cotransporter, possibly SNAT3 (Slc38a3) (81, 108). Metabolism of glutamine in renal proximal cell requires activity of the intramitochondrial phosphate-dependent enzyme glutaminase (PDG) and glutamine dehydrogenase (GDH) and yields α-ketoglutarate and two ammonia molecules, which are secreted into urine. Further metabolism of α-ketoglutarate generates also two bicarbonate molecules that may help buffering protons in blood. Ammonia synthesized in the proximal tubule is secreted into the luminal fluid. Initially a diffusion-trapping mechanism was proposed (93). According to this model NH_3 diffuses freely across apical plasma membrane to the lumen, where it binds H^+ and is trapped as NH_4^+ (10, 90, 93). The non-diffusable ammoniac ion NH_4^+ is secreted into tubular lumen via Na^+/H^+ exchanger NHE3 substituting for H^+ (64). In the loop of Henle (in the thick ascending limb portion) ammonium is reabsorbed via the apical $Na^+/K^+/2Cl^-$ cotransporter (NKCC2) and transported to the medullary

interstitial fluid. This process generates high interstitial ammonia and ammonium concentrations creating favorable gradients for the transfer of NH_3/NH_4^+ into the collecting duct. Final excretion of ammonia takes place in the intercalated and principal cells of collecting duct (32, 84, 126). Previously secretion of ammonia along the collecting duct was thought to occur by passive diffusion. However recently two Rhesus glycoproteins have been identified, RhBG and RhCG, that may serve as ammonia transporters in the collecting duct. RhBg and RhCG are expressed in intercalated cells and principal cells on the apical and basolateral membrane, respectively (35, 96). RhCG deficient mice display abnormal urinary acidification caused by impaired transport of NH_3 in the collecting duct indicating the importance of RhCG in renal ammonia excretion (14).

2.4 Proton and bicarbonate transport in the collecting duct

The final tuning of urinary acidification takes place in the distal part of the nephron, the connecting tubule (CNT), cortical collecting duct (CCD), and medullary collecting duct (MCD) (114). In the collecting duct two types of cells are involved in acid-base transport: acid-secretory type A intercalated cells (A-IC) and bicarbonate-secretory type B intercalated cells (B-IC) (6, 63). A third population of cells in the distal nephron, principal cells, is involved in water reabsorption and maintenance of sodium and potassium homeostasis (46).

The two different subtypes of intercalated cells differ morphologically and functionally (Fig. 2). Type A-ICs express vacuolar H^+-ATPase on the apical membrane excreting protons into urine and the Cl^-/HCO_3^- exchanger AE1 basolaterally transporting bicarbonate into blood. In contrast, B-ICs secrete bicarbonate into the lumen through the apical Cl^-/HCO_3^- exchanger pendrin and express H^+-ATPases on the basolateral membrane. Both, A-ICs and B-ICs express the $Na^+/K^+/2Cl^-$ (NKCC1) cotransporter, which might play a role in the uptake of NH_4^+ from interstitial fluid which is then secreted to the lumen (41, 101). However, NKCC1 deficient mice display no apparent defect in NH_4^+ secretion (117).

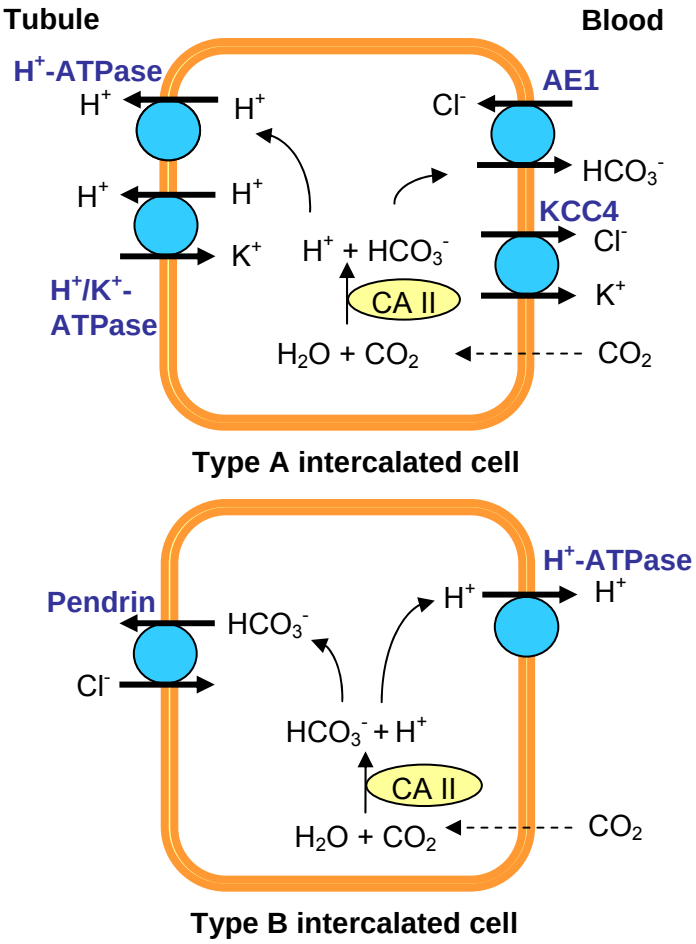

Fig. 2 Mechanisms of proton and bicarbonate transport in the collecting duct. Adapted from (116).

3. DISTURBANCES OF ACID-BASE BALANCE

Acid-base disturbances are either of metabolic origin (primary change in serum HCO_3^-) or respiratory based (primary change in serum pCO_2). They can be classified into four main types: metabolic acidosis and alkalosis and respiratory acidosis and alkalosis, respectively (Table 1). Further in the text the main focus is on metabolic acidosis.

Type	Primary disturbance	Compensation
Metabolic acidosis	↓ HCO_3^-	↓ pCO_2
Metabolic alkalosis	↑ HCO_3^-	↑ pCO_2
Respiratory acidosis	↑ pCO_2	↑ HCO_3^-
Respiratory alkalosis	↓ pCO_2	↓ HCO_3^-

Table 1. Classification of basic acid-base disorders. Modified from (94)

3.1 Metabolic acidosis

Metabolic acidosis (MA) is a severe disturbance of acid-base balance characterized by decreased plasma pH and bicarbonate concentration. MA is caused either by accumulation of H^+, due to the kidneys inability to excrete the basal metabolic acid load, an increased acid load, or loss of bicarbonate, due to inappropriate wasting by the kidney or the gastrointestinal tract.

The primary response to MA is titration of all available bases, mainly bicarbonate, which leads to a fall in plasma bicarbonate concentration (HCO_3^- < 24 mEq/l). Low plasma pH triggers a respiratory compensation manifesting as increased tidal volume and ventilatory rate that within minutes to hours drives the pCO_2 below normal values. The final correction is, however, renal. That includes maximal titration of all available buffers with secreted protons and increased

synthesis and secretion of ammonia (38). The more detailed adaptation mechanisms in the kidney during MA will be described later in the text.

3.1.1 Renal tubular acidosis (RTA)

Metabolic acidosis caused by impaired urinary acidification by the kidney is called renal tubular acidosis (RTA). Depending on the part of the nephron where the primary disturbance occurs, two types of RTA can be distinguished: distal renal tubular acidosis (dRTA) and proximal renal tubular acidosis (pRTA), either of which can be inherited or acquired (5, 40).

Type I RTA

Distal RTA is caused by the failure in proton secretion by A-ICs along the collecting duct. Mutations in two subunits of the vacuolar H^+-ATPase, a4 and B1, and the basolateral Cl^-/HCO_3^- exchanger AE1 lead to inherited dRTA (18, 59, 60, 107, 110, 111).

Type II RTA

Proximal RTA results from decreased bicarbonate reabsorption in the proximal tubule. In this type of disorder intercalated cells along the collecting duct function normally. Inherited pRTA is caused by mutations in the proximal tubule Na^+/HCO_3^- cotransporter NBCe1 (Slc4a4), which leads to excessive loss of bicarbonate in urine and subsequent MA. NBCe1 is also expressed in the eye; therefore this type of RTA is associated with blindness (73).

Mutations in the gene encoding carbonic anhydrase II (CAII) lead to mixed type of pRTA and dRTA, due to its expression in both, proximal tubule and collecting duct intercalated cells (106). Furthermore, aldosterone deficiency, such as in aldosterone synthase deficient mouse, leads to mild MA classified as so-called type IV RTA (79).

4. RENAL ADAPTATION TO METABOLIC ACIDOSIS

The final correction of acid-base disturbances requires a response of the kidney that activates adaptive pathways that include: increased synthesis of bicarbonate, increased ammoniagenesis, excretion of titratable acids, stimulation of proton secretion, changes in electrolyte and water handling, and also extensive remodeling of the nephron with cellular hypertrophy of various nephron segments (32).

4.1 Proximal tubule adaptation

During metabolic acidosis excessive acid is primarily buffered by bicarbonate, which leads to its consumption. To maintain stable bicarbonate concentration in the extracellular fluid (ECF) the kidneys have to reabsorb all filtered bicarbonate and produce new bicarbonate. It is achieved in two ways: enhancing secretion of H^+ together with excretion of titratable acids, and stimulating synthesis and secretion of ammonia.

Acid-loading enhances the proximal tubule's capacity to reabsorb bicarbonate (66), a process mediated by the concomitant increase in activity of the apical NHE3 and vacuolar H^+-ATPase (23) and the basolateral Na^+/HCO_3^- cotransporter NBCe1 (1). Increased brush border Na^+/H^+ exchange observed in MA is due to increased abundance of NHE3 protein but not mRNA (7, 125). In TAL acid-loading increases NHE3 protein abundance and functional activity, but also mRNA expression (68). Reabsorption of bicarbonate in the proximal tubule and TAL is also dependent on the activity of apical H^+-ATPases. Chan and Giebisch demonstrated that approximately 40% of the bicarbonate reabsorption in the proximal tubule is independent from luminal sodium and may reflect H^+-ATPase proton secretion (24). Metabolic acidosis increases activity and exocytic insertion of the H^+-ATPase in the brush border membrane (23, 102).

Elevated bicarbonate reabsorption observed during acute MA is concomitant with increased activity of the basolateral Na^+/HCO_3^- exchanger by

mechanisms that involve redistribution of the transporter from cytosol to the basolateral membrane (16). NBCe1 mutations cause proximal renal tubular acidosis (31, 53) and mice lacking basolateral Na^+/HCO_3^- exchanger exhibit severe metabolic acidosis (43) highlighting the importance of this transporter for maintaining normal acid-base status.

The kidney not only reabsorbs all filtered bicarbonate, but also regenerates bicarbonate via the process of ammonia synthesis and secretion (84). Ammonia is also necessary to buffer protons secreted along the collecting duct. Both, synthesis and secretion of ammonia are highly stimulated during metabolic acidosis (29). The adaptation involves increased uptake of glutamine into proximal tubule cells (123) mediated by upregulation of a basolateral Na^+-dependent glutamine transporter, possibly SNAT3 (Slc38a3) (81). Under normal conditions SNAT3 is expressed predominantly in the late portion of the proximal tubule (S3), however during MA its expression spreads into the early segment (S1/S2) (61, 81, 108). Also key enzymes involved in renal ammoniagenesis are stimulated during acute and chronic metabolic acidosis, namely the phosphate-dependent glutaminase (PDG), glutamate dehydrogenase (GDH) and phosphoenolpyruvate carboxykinase (PEPCK) (54, 55, 81, 100). Interestingly, the mechanisms of increased expression of mRNAs coding for ammoniagenesis enzymes seem to differ. Upregulation of PEPCK mRNA was reported to be due to increase in mRNA synthesis (54), whereas the increase in PDG and GDH mRNAs is mediated rather via increased stability of the transcript and not enhanced transcription (55, 56, 58). Both PDG and GDH mRNAs contain 8-nt AU sequences, so called pH responsive elements (pHRE), that bind multiple RNA-binding proteins (ζ-crystallin) and stabilize the transcript (56). In WKPT cells (rat proximal tubule cell line) grown on acidic medium ζ-crystallin is recruited to the stress granules formed in response to endoplasmic reticulum (ER) stress (56).

Hydrogen ions accumulated during MA are also partially buffered by bone (69). In response to acid-loading, phosphate is released from bone and excreted into urine, where it acts as a titratable acid and contributes to acid removal (19,

20, 48). As described before, the bulk of filtered phosphate is reabsorbed in the proximal tubule via action of Na^+-dependent Pi cotransporters, NaPi-IIa and NaPi-IIc (83, 104). During metabolic acidosis in rats Na/Pi cotransport activity, BBM NaPi-IIa protein, and mRNA abundance are decreased (8). In contrary, we found that in mice and rats acidosis-induced phosphaturia is not caused by reduction of sodium-dependent phosphate transport or protein expression of either NaPi-IIa or NaPi-IIc (88, 109).

4.2 Distal nephron adaptation

The renal response to acid-base disturbances involves not only the proximal part of the nephron but also adaptational changes in the distal tubule to maximize proton secretion.

The main transport protein involved in proton handling in the collecting duct is the vacuolar H^+-ATPase expressed in the apical membrane of A-ICs and the basolateral membrane of non-type A-ICs (17, 113). Interestingly, neither alkali nor acid-load affects mRNA nor protein levels of the proton pump (12, 110). However, depending on the acid-base status, the proton pump is redistributed within the cell. Acid-loading leads to insertion of vacuolar H^+-ATPase into the apical membrane, whereas alkalosis promotes trafficking into the basolateral membrane (12, 17, 110). The adaptation of the collecting duct involves also changes in the relative or absolute abundance of the two subtypes of intercalated cells, a phenomenon named “intercalated cell plasticity”. During chronic metabolic acidosis the relative number of acid-secretory A-ICs increases, whereas non-type A-ICs decreases. The underlying mechanisms of this phenomenon remain however unclear. Some investigators suggest conversion of non-type A-ICs into A-ICs (2, 4, 37, 103). Others propose a mechanism of basolateral Cl^-/HCO_3^- exchange activation in non-type A-ICs favoring bicarbonate reabsorption in response to intracellular acidification (80, 120). Observations from our group indicate that during chronic MA proliferation of acid-secretory A-ICs occurs and may contribute to the remodeling of the collecting duct (D. Bacic, M.

Nowik, CA. Wagner, manuscript in preparation). Also Duong et al. observed acidosis-induced proliferation of type A-ICs that was dependent on the overexpression of the growth differentiation factor 15 (GDF15) (34).

4.3 Hormonal regulation of urinary acidification

Transport of acid and base equivalents in the proximal tubule, TAL, and collecting duct, the main nephron segments involved in the adaptation to acid-base status, is affected by a number of hormones.

Among them the renin-angiotensin-aldosterone system (RAAS) seems to play a crucial role in renal acidification (77). Metabolic acidosis is associated with increased activity of the RAAS (50, 52). Increased levels of angiotensin II (ANGII) are observed during metabolic acidosis and modulate bicarbonate reabsorption in the proximal tubule and urinary acidification in the collecting duct (11, 42, 44, 77, 115, 120). Previous studies indicated that angiotensin II also stimulates renal ammoniagenesis (28), Na^+/H^+ exchange, and Na^+/HCO_3^+ cotransport in the proximal tubule (44), and vacuolar H^+-APase activity (115). Angiotensin also stimulates urinary acidification in the distal tubule and collecting duct by increasing H^+-ATPase activity in these segments (70, 98). Chronic blockade of ANGII type 1 (AT1)-receptor leads to decreased H^+-ATPase activity and protein abundance (71). Similarly, aldosterone is a potent regulator of acid-base homeostasis stimulating proton secretion by H^+-ATPases (3) and proton pump insertion into the membrane of type A-IC (124). Plasma aldosterone levels and expression of aldosterone synthase are also enhanced during metabolic acidosis (36). Aldosterone synthase deficient mice exhibit mild MA emphasizing the importance of aldosterone in regulation of acid-base homeostasis (79).

Further, a stimulatory effect of the potent vasoconstrictor endothelin on proton secretion was demonstrated (121). Endothelin is secreted from endothelial cells in response to acid-loading (122) and stimulates the Na^+/H^+ exchanger NHE3 and the vacuolar H^+-ATPase (68, 121).

5. POTENTIAL MECHANIMS OF RENAL ACID-BASE SENSING

Restoration of acid-base balance in response to acid-loading requires activation of number of metabolic and transport pathways described above. However, to date little is known about mechanisms of local pH sensing in the kidney.

Recently Preisig et al. proposed the Pyk2 kinase as the kidney's elusive acid sensor (74). The authors found that 24-hour exposure of opossum kidney cells leads to Pyk2 phosphorylation and activation of signaling pathways that increase NHE3 activity. However, it is still unclear whether Pyk2 itself is a proton sensor.

Another concept of renal acid sensing was proposed by Ludwig et al. (78) and Seuwen et al. (105). The authors identified a small subfamily of G protein coupled receptors, including OGR1 (ovarian cancer G-protein-coupled receptor 1), and GPR4 (G protein-coupled receptor 4), activated by extracellular protons. Both receptors sense extracellular protons through histidine residues (78). OGR1 and GPR4 are expressed in the kidney in the proximal tubule and most other nephron segments (N. Mohebbi, C. Benabbas, A. Velic, MG Ludwig, K. Seuwen, CA Wagner, unpublished results). The role of OGR1 and GPR4 in the renal regulation of acid-base homeostasis is still under investigation.

Recently, also evidence for a soluble adenylyl cyclase (sAC) as a bicarbonate sensor was provided. Chen et al. reported that HCO_3^- directly stimulates mammalian soluble adenylyl cyclase activity *in vivo* and *in vitro* in a pH-independent manner (26). Soluble adenyl cyclase is expressed in the kidney thick ascending limb, distal tubule, and A-IC and B-IC of the collecting duct, where it colocalizes with the H^+-ATPase (91, 92). In clear cells of the epididymis sAC regulates in a pH-dependent manner H^+-ATPase recycling (91).

6. HIGH-THROUGHPUT TECHNIQUES FOR TRANSCRIPTOME SCANNING

High-throughput techniques for measuring mRNA expression levels have become easily available and are therefore more extensively used in research over the last few years. These approaches include DNA microarray, serial analysis of gene expression (SAGE), sequencing of expressed sequence tags (ESTs), and high-throughput real-time PCR (75). Basic characteristics of main high-throughput scanning techniques are listed in Table 2.

	DNA Microarray	SAGE	EST	Real-time PCR
Number of genes	10,000s	10,000s	10,000s	10s
Number of samples	10s	A few	A few	100s
False positive	+	+	+	+/-
False negative	+	+	+	+/-
Equipment	Array laser scanner	DNA sequencer	Large-capacity DNA sequencer	Real-time PCR machine
Time	Days	> Weeks	> Months	Hours

Table 2. Characteristics of major high-throughput techniques for transcriptome analysis. Adapted from (75).

Among large-scale scanning techniques DNA microarrays have become most popular and widely used in life science research. A microarray, or gene chip is a matrix of thousands of cDNAs or oligonucleotides imprinted on a solid support (33, 67). The technology allows monitoring expression of thousands of genes in parallel in a single experiment without advanced specification which genes have to be studied (67, 99). The result of a microarray experiment is a “gene expression profile” (45).

DNA microarray technology is not only used to produce gene expression profiles of certain cells, tissues or disease states. More importantly, when combined with mathematical and computational analysis, it can be used to predict the function of novel genes, link various cell pathways, and common regulatory mechanisms within the pathway, analyze genetic variation, and identify novel therapeutic drug targets (for review: (67)).

Although DNA microarrays are a very powerful tool, the technique has a number of limitations. Still relatively large amounts of good quality RNA is required to obtain reliable results without an additional amplification step that increases the risk of false-positive calls. This makes profiling of certain organs or tissues very difficult (e.g. nephron segments). Another limitation is the accessibility and costs. Microarray profiling requires expensive hybridization and data analysis/mining equipment that can usually be provided only by specialized facilities.

6.1 High-throughput techniques used to study renal adaptation to metabolic acidosis

High-throughput techniques are becoming a standard tool in renal physiology. Recently two studies described identification of targets regulated during metabolic acidosis using two different approaches. The first one by Curthoys et al. used two-dimensional difference gel electrophoresis (DIGE) followed by MALDI-TOF/TOF mass spectrometry to identify proximal tubule proteins regulated during chronic adaptation (7 days) to MA (30). This approach allowed, however, the identification of only a small number of novel proteins (17 upregulated and 16 downregulated), all of which were cytosolic. No function was associated with proteins regulated. Also reproducibility of 2-DE gels is an important problem. The second study used outer medullary collecting ducts from 2 and 14 days acidotic mice and SAGE technology (27). This approach is problematic due to low sensitivity, time requirements, and the need for several amplification steps.

Recently the novel quantitative mass spectrometry (MS)-based proteomics approach was developed to study changes in protein abundance in mouse tissues (65). SILAC (stable isotope labeling by amino acids in cell culture) technology uses stable isotope-containing amino acids (e.g., $^{13}C_6$-lysine) that are incorporated into peptides that can be identified and quantified in the mass spectrometer (89). Important advantage of SILAC is a possibility to capture membrane proteins due to separation step over standard SDS-PAGE. Moreover, SILAC allows to calculate relative changes in protein abundance in two samples coming from untreated and treated cells or animals. In collaboration with B. Macek and M. Mann at the Max-Planck Institute for Biochemistry in Munich, our group had the chance to employ the SILAC mouse to study proximal tubule (S1/S2 and S3 segment) specific changes in protein expression after 2 days of NH_4Cl-induced MA. We identified and quantified more than 1,000 proteins in each of the two different subsegments of the proximal tubule, many of which were membrane proteins. Preliminary analysis indicates that the SILAC technology combined with cDNA microarray will provide us with complex information about renal adaptation to MA.

7. MOUSE MODELS USED IN THIS STUDY

7.1. NaPi-IIa deficient mice

NaPi-IIa is a primary sodium-dependent Pi cotransporter located in BBM of proximal tubule cells and responsible for a bulk of Pi reabsorption (13).

NaPi-IIa deficient mice were generated by Beck and colleagues by homologous recombination (13). NaPi-IIa$^{-/-}$ mice exhibited biochemical features of patients with hereditary hypophosphatemic rickets with hypercalcuria (HHRH). These are: increased urinary phosphate excretion, hypophosphatemia, and an adaptive increase in the circulating concentration of 1,25-dihydroxyvitamin D_3 concomitant with hypercalcemia, hypercalcuria, and decreased serum parathyroid hormone (PTH) levels. In contrary to patients with HHRH, no rickets or osteomalacia was observed. However, NaPi-IIa deficient mice exhibited a complex bone phenotype that was reversed with age. Interestingly, mice homozygous for the disrupted NaPi-IIa gene retain up to 30% BBM Na-dependent phosphate cotransport activity suggesting that at least one more Pi transporter, most probably NaPi-IIc, is involved in Pi reabsorption in the proximal tubule.

In our study NaPi-IIa deficient mice served as an additional tool to distinguish *in vivo* and *ex vivo* between type IIa and type IIc mediated transport activities and to test the contribution of renal mechanisms to acidosis induced phosphaturia.

7.2. Models of NH_4Cl-induced metabolic acidosis

Ammonium chloride (NH_4Cl) is widely used for inducing metabolic acidosis in experimental animals. The first study using NH_4Cl to induce MA was published in 1921 by Haldane (51).

The standard protocol involves application of NH_4Cl in the drinking water (7-9, 30, 36, 39, 54, 68, 85, 87, 97, 118). Another protocol involves addition of

NH_4Cl to the food or fixed amount of gelled diet (62, 82, 86, 95, 112, 123). Combination of both protocols is also used (57, 72).

Recently Amlal and colleagues described upregulation of the water channel AQP2 and a concomitant increase of circulating levels of vasopressin in response to NH_4Cl-induced (0.28M NH_4Cl in the drinking water) MA (9). A similar study, but with NH_4Cl in the food, confirmed upregulation of AQP2 in the collecting duct, however, showed no change in circulating levels of vasopressin (82). The authors suggested that the increased abundance of AQP2 observed by Amlal et al. was due to dehydration and not MA itself (86). These reports indicate that the route of application of NH_4Cl may affect the experimental outcome.

Therefore in our study we compared induction of MA in mice and rats using two different protocols: 0.28M NH_4Cl in the drinking water or equivalent amount of NH_4Cl in food.

8. AIM OF THE WORK

Renal adaptation to metabolic acidosis involves the increase in acid excretion that is mediated via activation/regulation of various pathways described earlier in the text. Two recent publications shed more light on the underlying mechanisms of renal adaptation to an acid-load. Cheval and colleagues searched for altered transcripts in the mouse outer medullary collecting duct using serial analysis of gene expression (SAGE) (27), whereas Curthoys et al. applied 2-dimensional gel electrophoresis and subsequent mass spectroscopy to detect altered protein expression in acidotic rat proximal tubules (30). However, these reports did not include all kidney structures into their analysis, and both technologies, SAGE and 2-D gels, are limited in terms of sensitivity as described above.

Therefore the aims of this study were:

1. Characterization of transcriptional changes in mammalian kidney during 2 and 7-days NH_4Cl-induced MA performing a genome wide scan using microarray technology, to gain insights into adaptive pathways.
2. Based on microarray results, investigation molecular mechanisms of phosphaturia during metabolic acidosis.
3. Investigation of the role of water-preserving mechanisms during metabolic acidosis: compare the induction of MA in mice and rats using two different protocols: standard 0.28M NH_4Cl in drinking water and equivalent amount of NH_4Cl in food.

9. PUBLICATIONS THAT CONTRIBUTED TO THAT WORK

9.1 Genome-wide gene expression profiling reveals renal genes regulated during metabolic acidosis

Marta Nowik, Rita M. Lecca, Ana Velic, Hubert, Rehrauer, Andrè W. Brändli, Carsten A. Wagner

Physiol Genomics (2008); 32(3): 322-34

Physiol Genomics 32: 322–334, 2008.
First published December 4, 2007; doi:10.1152/physiolgenomics.00160.2007.

Genome-wide gene expression profiling reveals renal genes regulated during metabolic acidosis

Marta Nowik,[1] M. Rita Lecca,[2] Ana Velic,[1] Hubert Rehrauer,[3] André W. Brändli,[2] and Carsten A. Wagner[1]

[1]*Institute of Physiology and Zurich Center for Human Integrative Physiology (ZIHP), University of Zurich;* [2]*Institute of Pharmaceutical Sciences, Department of Chemistry and Applied Biosciences, ETH Zurich; and* [3]*Functional Genomics Center Zurich, Zurich, Switzerland*

Submitted 18 July 2007; accepted in final form 21 November 2007

Nowik M, Lecca MR, Velic A, Rehrauer H, Brändli AW, Wagner CA. Genome-wide gene expression profiling reveals renal genes regulated during metabolic acidosis. *Physiol Genomics* 32: 322–334, 2008. First published December 4, 2007; doi:10.1152/physiolgenomics.00160.2007.— Production and excretion of acids are balanced to maintain systemic acid-base homeostasis. During metabolic acidosis (MA) excess acid accumulates and is removed from the body, a process achieved, at least in part, by increasing renal acid excretion. This acid-secretory process requires the concerted regulation of metabolic and transport pathways, which are only partially understood. Chronic MA causes also morphological remodeling of the kidney. Therefore, we characterized transcriptional changes in mammalian kidney during MA to gain insights into adaptive pathways. Total kidney RNA from control and 2- and 7-days NH_4Cl treated mice was subjected to microarray gene profiling. We identified 4,075 transcripts significantly ($P < 0.05$) regulated after 2 and/or 7 days of treatment. Microarray results were confirmed by qRT-PCR. Analysis of candidate genes revealed that a large group of regulated transcripts was represented by different solute carrier transporters, genes involved in cell growth, proliferation, apoptosis, water homeostasis, and ammoniagenesis. Pathway analysis revealed that oxidative phosphorylation was the most affected pathway. Interestingly, the majority of acutely regulated genes after 2 days, returned to normal values after 7 days suggesting that adaptation had occurred. Besides these temporal changes, we detected also differential regulation of selected genes (SNAT3, PEPCK, PDG) between early and late proximal tubule. In conclusion, the mammalian kidney responds to MA by temporally and spatially altering the expression of a large number of genes. Our analysis suggests that many of these genes may participate in various processes leading to adaptation and restoration of normal systemic acid-base and electrolyte homeostasis.

kidney; microarray; acid-base; ammoniagenesis; remodeling

SYSTEMIC pH in extracellular fluids is maintained within the physiological range through the cooperation of various body buffering systems including regulated exhalation of CO_2 by the lungs, release of buffers from bone, and acid or base excretion by the kidney (16), whereby the kidney plays a central role in maintaining systemic acid-base homeostasis. Chemical buffering and ventilation contribute to the immediate and chronic response to changes in systemic acid-base status, whereas the kidney is rather responsible for both intermediate and chronic adaptation. The kidney participates in maintaining pH homeostasis by excreting the net excess of acid in urine (23). This is achieved by three main processes: *1*) the reabsorption of filtered bicarbonate, *2*) the excretion of acids/protons, and *3*) the synthesis of ammonia and use of ammonia, phosphate, and citrate as titratable acids increasing the kidneys' ability to excrete protons. These processes take place in different segments of the nephron and are precisely regulated and coordinated (23).

Disturbances in acid-base balance lead to and require an adaptive increase in renal acid excretion that involves activation and/or regulation of various pathways (16). These pathways include increased ammoniagenesis, changes in electrolyte and water handling, excretion of titratable acids, increased synthesis of bicarbonate, stimulation of proton secretion, and also extensive remodeling of the nephron with cellular hypertrophy of various nephron segments (16).

However, these adaptive changes are only partially understood. Two recent publications employed different experimental approaches to identify changes in renal gene or protein expression in chronically acidotic animals. Cheval and colleagues (12) searched for altered transcripts in the mouse outer medullary collecting duct using serial analysis of gene expression (SAGE), whereas Curthoys et al. (15) applied two-dimensional gel electrophoresis and subsequent mass spectroscopy to detect altered protein expression in rat proximal tubules after acidosis. Here, we used microarray-based gene expression profiling as an alternative approach to perform a genome-wide analysis of altered transcripts in response to acute (2 days) and chronic (7 days) metabolic acidosis in mouse kidneys. Our data demonstrate a massive regulation of various transcripts after 2 days of NH_4Cl-loading with most genes returning to normal levels after 7 days. Several pathways including ammoniagenesis, oxidative phosphorylation, and general transport processes were highly overrepresented. Furthermore, gene regulation was spatially and temporally regulated in dissected early and late proximal tubules. Thus, our data suggest a concerted, spatially and temporally regulated, response of the kidney to systemic metabolic acidosis that may contribute to the kidneys' ability to restore systemic acid-base balance.

METHODS

Animals. All experiments were performed on 12-wk-old C57BL/6J male mice and according to Swiss Animal Welfare laws, with approval of the local veterinary authority (Kantonales Veterinäramt Zürich).

Metabolic cages. To induce metabolic acidosis, C57BL/6J mice (10 animals per group) were given 0.28 M NH_4Cl/2% sucrose in drinking water for 2 or 7 days, whereas the control group received

Article published online before print. See web site for date of publication (http://physiolgenomics.physiology.org).

Address for reprint requests and other correspondence: C. A. Wagner, Inst. of Physiology and Zurich Center for Integrative Human Physiology, Univ. of Zurich, Winterthurerstr. 190, CH-8057 Zurich, Switzerland (e-mail: Wagnerca@access.uzh.ch).

only 2% sucrose in drinking water. All animals were adapted to metabolic cages for 3 days before data collection. Forty-eight hours before death, mice were housed in metabolic cages and had free access to standard mouse chow and drinking water. Daily chow, water intake, and body weights were measured, and urine was collected under mineral oil. At the end of the experiment, mice were anesthetized, and heparinized venous blood was collected and analyzed immediately for pH, blood gases, and electrolytes on a Radiometer ABL 505 (Radiometer, Copenhagen, Denmark) blood gas analyzer. Serum was collected and frozen until further analysis. Both kidneys were harvested, immediately frozen in liquid nitrogen, and stored at −80°C until mRNA extraction.

Urinary pH was measured using a pH microelectrode (691 pH-meter, Metroholm). Urinary creatinine was measured by the Jaffe method (42). Ammonium in urine was measured by the method of Berthelot (5). Urinary and serum phosphate was measured using a commercial kit (Sigma Diagnostics, Munich, Germany). Urinary electrolytes (Na^+, K^+, Ca^{2+}, Mg^{2+}, Cl^-, SO_4^{2-}) were measured by ion chromatography (Metrohm ion chromatograph, Herisau, Switzerland).

Preparation of isolated proximal tubule segments. Control animals received 2% sucrose in their drinking water for 2 days, whereas the acidotic group received 0.28 M NH_4Cl plus 2% sucrose in their drinking water for 2 days. Animals were otherwise housed in standard cages and had free access to standard rodent chow. Mice were anesthetized and perfused through the left heart ventricle with 20 ml of a solution containing 140 mM sucrose, 28 mM Na_2HPO_4, and 112 mM NaH_2PO_4. Kidneys were immediately removed, the capsule removed, and thin coronal slices containing both cortex and medulla were prepared. The inner medulla was removed. The tissue was dissected under a stereo microscope at 4°C using two fine forceps (Dumont no. 5). The total number of 50 S1 and S2 segments, followed by 50 S3 segments, was collected and placed in 300 μl RLT-Buffer (Qiagen, Basel, Switzerland) containing 3 μl 2-mercaptoethanol. S1/S2 and S3 segments of proximal tubules were dissected separately from six controls and six acidotic animals. Collected tissue was immediately frozen at −80°C until mRNA extraction.

RNA extraction from total kidney. Snap-frozen kidneys (10 kidneys for each condition) were homogenized in RLT-Buffer (Qiagen) supplemented with 2-mercaptoethanol to a final concentration of 1%. Total RNA was extracted from 200 μl aliquots of each homogenized sample using the RNeasy Mini Kit (Qiagen) according to the manufacturer's instructions. Quality and concentration of the isolated RNA preparations were analyzed by electrophoresis and spectroscopically using the 2100 Bioanalyzer (Agilent Technologies) and the ND-1000 spectrophotometer (NanoDrop Technologies), respectively. Total RNA samples were stored at −80°C.

RNA extraction from microdissected nephron segments. After thawing on ice, each sample was vortexed and total RNA was extracted using the RNeasy Micro Kit (Qiagen) according to the manufacturer's instructions. Quality and concentration of the isolated RNA preparations were analyzed using the ND-1000 spectrophotometer (NanoDrop Technologies). Total RNA samples were stored at −80°C.

Quantitative real-time PCR. Each RNA sample was diluted to 100 ng/μl, and 3 μl was used as a template for reverse transcription using the TaqMan Reverse Transcription Kit (Applied Biosystems, Forster City, CA). Quantitative real-time (qRT-PCR) was performed on the ABI PRISM 7700 Sequence Detection System (Applied Biosystems). Primers for all genes of interest were designed using Primer Express from Applied Biosystems (Supplementary Table S1).[1] Probes were labeled with the reporter dye FAM at the 5′ end and the quencher dye TAMRA at the 3′ end (Microsynth, Balgach, Switzerland). The specificity of all primers was first tested in a standard PCR and always resulted in a single product of the expected size on 1% agarose gels (data not shown). Real-time PCR reactions were performed using the TaqMan Universal PCR Master Mix (Applied Biosystems). Briefly, 3.5 μl cDNA, 1 μl of each primer (25 μM), 0.5 μl labeled probe (5 μM), 6.5 μl RNase-free water, 12.5 μl TaqMan Universal PCR Master Mix reached 25 μl of final reaction volume. Reaction conditions were: denaturation at 95°C for 10 min followed by 40 cycles of denaturation at 95°C for 15 s and annealing/elongation at 60°C for 60 s with autoramp time. All reactions were run in duplicate. To analyze the data, we set the threshold to 0.06 as this value had been determined to be in the linear range of the amplification curves for all mRNAs in all experimental runs. The expression of gene of interest was calculated in relation to hypoxanthine guanine phosphoribosyl transferase (HPRT) or β-actin. Relative expression ratios were calculated as $R = 2^{[Ct(HPRT/\beta\text{-actin}) - Ct(\text{test gene})]}$, where Ct represents the cycle number at the threshold 0.06.

Labeling of cRNA, microarray hybridization, and image processing. Digoxigenin (DIG)-UTP-labeled cRNA was generated and linearly amplified from total RNA using the Nano Amp RT-IVT Labeling Kit (Applied Biosystems) and the manufacturer's protocol. Briefly, 1 μg of total RNA was used to perform the 1st- and 2nd-strand synthesis of cDNA. The purified cDNA was transcribed in vitro in presence of 200 nM DIG-11 UTP to produce DIG-labeled cRNA, followed by purification. The quality and amount of labeled cRNA were assessed with the Agilent 2100 Bioanalyzer and the ND-1000 spectrophotometer, respectively. Labeled cRNA preparations were hybridized to mouse microarrays (Mouse Genome Survey Microarray, 33,148 features; Applied Biosystems). Microarray hybridization, chemiluminescence detection, image acquisition, and analysis were performed using the Applied Biosystems Chemiluminescence Detection Kit and Applied Biosystems 1700 Chemiluminescent Microarray Analyzer following the manufacturer's protocols. Each microarray was first prehybridized at 55°C for 1 h in hybridization buffer with blocking agent. The DIG-labeled cRNA targets (20 μg) were first fragmented to 100–400 bases by incubation with fragmentation buffer at 60°C for 30 min, mixed with internal control target (ICT, 24-mer oligo labeled with LIZ fluorescent dye), and hybridized to each prehybridized microarray in 1.5-ml volume at 55°C for 16 h using an Minitron Incubator Shaker (Infors HT). After hybridization, the microarrays were washed with hybridization wash buffer and chemiluminescence rinse buffer. Enhanced chemiluminescent signals were generated by first incubating the microarrays with antidigoxigenin Fab fragment antibodies coupled to alkaline phosphatase (150 U, Roche Applied Science) for 20 min, then washing with Chemiluminescence Enhancing Solution, and finally adding Chemiluminescence Substrate. Images were collected for each microarray using Applied Biosystems 1700 Chemiluminescent Microarray Analyzer. Images were autogridded, and the chemiluminescent signals were quantified, corrected for background, and spatially normalized using the Expression Array System Analyzer Software Version 1.1.1 (Applied Biosystems).

Membrane preparation and western blot analysis. Mice were anesthetized with ketamine-xylazine intraperitoneally, and kidneys were removed and rapidly frozen in liquid nitrogen. For total membranes isolation kidneys were homogenized in an ice-cold K-HEPES buffer (200 mM mannitol, 80 mM K-HEPES, 41 mM KOH, pH 7.5) with pepstatin, leupeptin, K-EDTA, and phenylmethylsulfonyl fluoride as protease inhibitors. Samples were centrifuged at 1,000 *g* for 10 min at 4°C, and the supernatant was saved. Subsequently, the supernatant was centrifuged at 41'000 *g* for 1 h at 4°C, and the pellet was resuspended in K-HEPES buffer containing protease inhibitors. Brush border membranes (BBM) were prepared as described previously using the Mg^{2+}-precipitation technique (6). After measurement of the total protein concentration (Bio-Rad, Hercules, CA), 50 μg of crude membrane proteins or 10 μg of BBM proteins were solubilized in Laemmli sample buffer, and SDS-PAGE was performed on 10%

[1] The online version of this article contains supplemental material.

polyacrylamide gels. For immunoblotting, the proteins were transferred electrophoretically to polyvinylidene fluoride membranes (Immobilon-P; Millipore, Bedford, MA). After blocking with 5% milk powder in Tris-buffered saline/0.1% Tween-20 for 60 min, the blots were incubated with the primary antibodies and mouse monoclonal anti-β-actin antibody (42 kDa; Sigma, St. Louis, MO) 1:5,000 either for 2 h at room temperature or overnight at 4°C. The primary antibodies were: rabbit anti-mouse NHE3 (1:5,000) (generated against a KLH-linked peptide, Pineda Antibody Services, Berlin, Germany), rabbit anti-mouse SNAT3 previously described (32), rabbit anti-aquaporin 2 (1:5,000) (kindly provided by J. Loffing, University of Fribourg, Switzerland), rabbit anti-pendrin (1:5,000). The membranes were then washed three times, blocked for 1 h, and again incubated for 1 h at room temperature with the secondary goat anti-rabbit or donkey anti-goat antibodies (1:5,000) linked to alkaline phosphatase (Promega). The protein signal was detected with the CDP Star chemiluminescence system (Roche Diagnostics, Basel, Switzerland) using the DIANA III-chemiluminescence detection system (Raytest, Straubenhardt, Germany). All images were analyzed using appropriate software (Advanced Image Data Analyser AIDA, Raytest) to calculate the protein of interest/actin ratio.

Microarray data analysis. RNA samples (four biological replicates per condition) were transcribed into DIG-labeled cRNAs and hybridized to Mouse Genome Survey Arrays (32,996 probes representing 32,389 curated genes) from Applied Biosystems. The arrays were scanned and quantified using Expression Array System Analyzer Software Version 1.1.1 (Applied Biosystems). Intensity readouts were normalized across arrays with Bioconductor's *vsn* package (24). Genes were defined as present and used in the subsequent analysis if they satisfied the intensity threshold of 2,000 in all four replicates of at least one condition. Among the present genes, the differentially expressed ones were identified by applying Student's *t*-test to the log-intensity data. For the significant genes fold-changes between the treated and untreated conditions were also computed on log-intensity data.

Hierarchical clustering. Clustering was performed using Gene Spring GX Version 7.3 software (Agilent Technologies). Microarray data were normalized by dividing the expression values of each gene by the median of its expression values across all samples. To remove genes that do not show significant expression changes, we first applied a one-way ANOVA analysis to select among the present genes only those that showed a significant variation across the time points (P value threshold: 0.05). The selected genes were then clustered using Spearman correlation as distance measure and the average linkage algorithm for merging clusters.

Identification of genes and biological processes involved in kidney adaptation to metabolic acidosis. PANTHER (Protein ANalysis THrough Evolutionary Relationships) Classification System (1) (http://www.pantherdb.org) was used to classify significantly regulated transcripts. Pathway analysis of significantly regulated genes was performed using MetaCore (GeneGo, St. Joseph, MI) and WebGestalt toolkit (http://bioinfo.vanderbilt.edu/webgestalt). MetaCore is a web-based software suite for functional analysis of experimental data based on a manually curated database of human protein-protein, protein-DNA and protein compound interactions, and metabolic and signaling pathways. Gene Ontology (GO) annotations were used as indicators of biological function. Associations with GO biological process, molecular function, and cellular component groups were obtained through MetaCore. WebGestalt includes information from Kyoto Encyclopedia of Genes and Genomes (KEGG) database and organizes genes based on the KEGG biochemical pathway.

Statistical analysis. Results are expressed as means ± SE. All data were tested for significance using ANOVA and unpaired Student's test where appropriate. Only values with $P < 0.05$ were considered as significant.

RESULTS

Acid-base status of animals. Animals were given 0.28 M NH_4Cl with 2% sucrose in the drinking water for the 48 h or 7 days to induce metabolic acidosis. The control group received only 2% sucrose in the drinking water for 2 or 7 days. This treatment has been previously shown to induce metabolic acidosis (32, 45). As we did not detect any difference in the 2- or 7-day control groups, all data were subsequently pooled. Blood and urine samples were analyzed to monitor systemic acid-base status and renal acid excretion (Table 1).

Addition of 0.28 M NH_4Cl to the drinking water resulted in metabolic acidosis in both treated groups as was evident from the reduction of blood pH and bicarbonate levels and increase in chloride and sodium concentrations (Table 1). Potassium levels remained unchanged. As expected, urine pH values of both treated groups were more acidic compared with the control group, and urinary ammonium excretion was increased accordingly. Urine output was significantly reduced in both treated groups. Thus, the treatment with NH_4Cl resulted in the expected hyperchloremic metabolic acidosis and its consequences.

Genome-wide comparison of renal gene expression profiles of control and acidotic mice reveals large number of differentially regulated genes. Transcriptional changes in the total kidney during metabolic acidosis were investigated by genome-wide gene expression profiling using Applied Biosystems Mouse Genome Survey Arrays (32,996 probes representing 32,389 curated genes that target 44,498 transcripts). In a first step, changes in the expression of SNAT3 (Slc38a3) and

Table 1. *Summary of blood and urine analysis*

	Control	2 Days NH_4Cl	7 Days NH_4Cl
	Blood		
pH	7.24±0.03	7.10±0.02	7.19±0.03^{ns}
pCO_2, mmHg	47.1±2.2	40.9±2.7^{ns}	46.1±3.7^{ns}
$[HCO_3^-]$, mM	17.0±0.9	12.1±0.9‡	16.5±0.8*
$[Na^+]$, mM	144.2±0.6	148.7±0.7†	145.5±1.2^{ns}
$[K^+]$, mM	5.2±0.5	4.9±0.7^{ns}	5.16±0.3^{ns}
$[Cl^-]$, mM	113.4±0.5	128.5±1.3‡	121.8±1.5‡
Osmolality, mOsm/kg H_2O	274±5	279±6^{ns}	285±5^{ns}
	Urine		
pH	6.50±0.15	5.40±0.05‡	5.43±0.04‡
Creatinine, mg/dl	51.3±5.1	73.0±2.8‡	60.8±3.9^{ns}
NH_3/NH_4^+/(mM)/crea, mg/dl	0.9±0.5	6.5±0.5‡	7.1±0.6‡
Na^+(mM)/crea, mg/dl	2.4±0.5	2.3±0.2^{ns}	2.6±0.1^{ns}
K^+(mM)/crea, mg/dl	5.4±0.8	5.2±0.4^{ns}	6.1±0.3^{ns}
Ca^{2+}(mM)/crea, mg/dl	0.05±0.02	0.09±0.01^{ns}	0.08±0.01^{ns}
Mg^{2+}(mM)/crea, mg/dl	0.44±0.10	0.53±0.03^{ns}	0.63±0.02^{ns}
Cl^-(mM)/crea, mg/dl	4.1±0.7	8.8±0.4‡	11.0±0.7‡
Pi (mM)/crea, mg/dl	2.4±0.4	2.5±0.4^{ns}	2.3±0.3^{ns}
SO_4^{2-} (mM)/crea, mg/dl	0.7±0.1	0.7±0.1^{ns}	0.7±0.1^{ns}
Osmolality, mOsm/kg H_2O	1577±142	3770±285‡	3332±232‡
Urine volume, ml	2.4±0.4	0.8±0.1‡	1.2±0.2†
Urine volume/BW	0.09±0.02	0.03±0.01†	0.05±0.01^{ns}
Weight change, %	+1.9±3.0	−5.3±0.04*	−2.5±0.6^{ns}
Water intake, ml/g BW	0.23±0.01	0.15±0.01‡	0.18±0.01†
Food intake, mg/g BW	0.13±0.01	0.12±0.00^{ns}	0.15±0.01^{ns}

Summary of blood and urine data from mice receiving 0.28 M NH_4Cl plus 2% sucrose in drinking water for 2 or 7 days or only 2% sucrose (control group); $n = 10$ per group. Urinary excretion was normalized against creatinine (crea). BW, body weight; ns, not significant. *$P < 0.05$, †$P < 0.01$, ‡$P < 0.001$.

PEPCK, two genes known to be upregulated in mouse kidney during metabolic acidosis (32), were tested using quantitative real-time PCR. As expected, SNAT3 and PEPCK mRNA levels were elevated three- to fourfold after 2 and 7 days (data not shown). Subsequently, four animals from each group with the highest degree of similarity in terms of SNAT3 and PEPCK expression were selected for microarray analysis. In the 12 samples hybridized on the microarrays (four biological replicates per condition) we detected a total of 12,984 genes (40% of the total number present on the array) expressed in kidneys of all groups of mice. We found that 4,075 transcripts were significantly ($P < 0.05$) regulated in response to the acid load after 2 and/or 7 days (Supplementary Tables S2 and S3). The majority of transcripts (3,070) responded only to 2 days NH_4Cl treatment, and only 322 responded exclusively to the chronic acid load (7 days). Out of the 3,070 genes acutely regulated, 1,475 were upregulated (69 with fold change ≥ 2) and 1,595 were downregulated (108 with fold change ≤ 2). Out of the 322 genes regulated only after 7 days treatment, 142 were upregulated (7 with fold change ≥ 2) and 180 were downregulated (3 with fold change ≤ 2). We found that 675 transcripts were similarly regulated in response to acute and chronic acid load. Moreover, 333 genes were consistently upregulated and 342 were downregulated. Seven transcripts showed decreased expression after 2 days acidosis and increased expression after 7 days. Only one gene coding for fucosyltransferase 11 (Fut11) was upregulated after 2 days and downregulated after 7 days. Selected genes affected by 2 and/or 7 days of NH_4Cl-loading are listed in Tables 2–5.

Pathway analysis. Pathway analysis using two different web-based softwares (MetaCore and WebGestalt) revealed that the most affected pathway in acidotic mice was oxidative phosphorylation (41 upregulated genes assigned to KEGG "mmu00190" pathway; 35 upregulated genes assigned to MetaCore's metabolic map "oxidative phosphorylation pathway"). As expected, in acid-loaded animals we found upregulation of a number of genes coding for enzymes and transporters important for ammonia synthesis (SNAT3, PDG, PEPCK, Glud1). Interestingly, increased ammoniagenesis was concomitant with activation of the TCA (tricarboxylic acid) cycle pathway (10 upregulated and 2 downregulated genes assigned to KEGG "mmu00020" pathway) and glycolysis/gluconeogenesis pathway (8 upregulated and 5 downregulated genes assigned to KEGG "mmu00010" pathway).

The largest group of transcripts affected by metabolic acidosis encoded solute carrier (Slc) transporters (62 genes downregulated, 35 genes upregulated). Monocarboxylic acid transporters (Slc16 family) and mitochondrial carriers (Slc25 family) were the most represented with 13 and 16 genes significantly regulated after 2 and/or 7 days of acid-loading, respectively.

Co-regulated gene clusters. Hierarchical clustering (17) was performed on 4,389 acidosis-responsive genes obtained after one-way ANOVA test. This allowed the identification of at least six distinct clusters of genes sharing similar expression profiles across the three experimental conditions (Fig. 1). Most genes were either found in *cluster 1* or *3*. Genes of *cluster 1* were upregulated more than twofold after 2 days and less than twofold after 7 days of metabolic acidosis (Fig. 1). This cluster included 1,278 genes, which encode gene products mainly involved in glutamine and glutamate metabolism: glutamate dehydrogenase 1 (Gluld1), glutamine transporter SNAT3 (Slc38a3), asparagine synthetase (Asns), glutamate-cysteine ligase (Gclm), guanine nucleotide binding protein, alpha 11 (Gna11), citrate synthase (Cs), glycolytic pathway, and ATP synthesis (hexokinase, phosphor-fructo-kinase, ATP synthase, NADH dehydrogenase, cytochrome c) (Supplementary Table S5). These findings are in good accordance with the observed increased utilization of glutamine, lactate, and citrate to generate ammonia and ATP during kidney metabolic acidosis. The increased production of ATP

Table 2. *Genes upregulated after 2 days acid-loading*

Gene Symbol	Gene Name	Fold Change	GenBank Acc. No.
Ugt8a	UDP galactosyltransferase 8A	11.38	NM_011674
1700047E16Rik	RIKEN cDNA 1700047E16 gene	10.84	NM_173431
Fgfrl1	fibroblast growth factor receptor-like 1	7.65	XM_983846; NM_054071
Grem2	gremlin 2 homolog, cysteine knot superfamily (*Xenopus laevis*)	5.26	NM_011825
Slc25a25	solute carrier family 25 (mitochondrial carrier, phosphate carrier), member 25	4.32	NM_146118
Slc38a3	solute carrier family 38, member 3; SNAT3	3.75	NM_023805
Slc4a7	solute carrier family 4, sodium bicarbonate cotransporter, member 7	3.33	NM_001033270
Slc13a2	solute carrier family 13 (sodium-dependent dicarboxylate transporter), member 2	3.29	NM_022411
Pck2	phosphoenolpyruvate carboxykinase 2 (mitochondrial)	3.28	NM_028994
AQP2	aquaporin 2	3.20	NM_009699
Slc14a2	solute carrier family 14 (urea transporter), member 2	2.94	NM_030683; NM_207651
Slc16a6	solute carrier family 16 (monocarboxylic acid transporters), member 6	2.62	NM_001029842; NM_134038
Mdh2	malate dehydrogenase 2, NAD (mitochondrial)	2.38	NM_008617
AQP4	aquaporin 4	2.12	NM_009700
Car2	carbonic anhydrase 2	1.69	NM_009801
PDG	glutaminase	1.63	NM_001081081
Slc16a7	solute carrier family 16 (monocarboxylic acid transporters), member 7	1.56	NM_011391
Avpr2	arginine vasopressin receptor 2	1.50	NM_019404
Slc13a3	solute carrier family 13 (sodium-dependent dicarboxylate transporter), member 3	1.49	NM_054055
AQP3	aquaporin 3	1.41	NM_016689
Cs	citrate synthase	1.36	NM_026444
Aco2	aconitase 2	1.30	NM_080633
Mdh1	malate dehydrogenase 1 (soluble)	1.19	NM_008618

List of selected genes upregulated after 2 days of NH_4Cl-loading. For each gene, the symbol, name, fold change, and GenBank Reference Sequence are given.

Table 3. *Genes upregulated after 7 days acid-loading*

Gene Symbol	Gene Name	Fold Change	GenBank Acc. No.
2200001I15Rik	RIKEN cDNA 2200001I15 gene	3.89	NM_183278
Slc38a3	solute carrier family 38, member 3; SNAT3	3.86	NM_023805
Cul7	cullin 7	3.78	NM_025611
Slc25a25	solute carrier family 25 (mitochondrial carrier, phosphate carrier), member 25	3.44	NM_146118
Pck2	phosphoenolpyruvate carboxykinase 2 (mitochondrial)	3.04	NM_028994
Pck1	phosphoenolpyruvate carboxykinase 1, cytosolic	2.71	NM_011044
Slc13a2	solute carrier family 13 (sodium-dependent dicarboxylate transporter), member 2	2.41	NM_022411
Slc16a6	solute carrier family 16 (monocarboxylic acid transporters), member 6	2.11	NM_001029842; NM_134038
AQP2	aquaporin 2	1.72	NM_009699
Car2	carbonic anhydrase 2	1.53	NM_009801
Slc13a3	solute carrier family 13 (sodium-dependent dicarboxylate transporter), member 3	1.52	NM_054055
PDG	glutaminase	1.48	NM_001081081
Aco2	aconitase 2	1.38	NM_080633
Slc25a10	solute carrier family 25 (mitochondrial carrier, dicarboxylate transporter), member 10	1.37	NM_013770
Cs	citrate synthase	1.16	NM_026444
Mdh1	malate dehydrogenase 1 (soluble)	1.20	NM_008618

List of selected genes upregulated after 7 days of NH_4Cl-loading. For each gene, the symbol, name, fold change, and GenBank Reference Sequence are given.

may be used to reabsorb sodium in the proximal convoluted tubule either during acute or chronic acidosis (22).

Cluster 3 contains 2,044 genes, whose expression levels were induced (>2-fold) after 2 days but returned to control levels during chronic acid load (Fig. 1). These genes, were mainly represented by genes encoding cytoskeletal proteins (α-tubulin, destrin), solute carrier transporters (mainly sodium and glutamate transporters), transcription factors (Foxp4, Foxp1, Wt1, Krüppel-like factors 5 and 7), chloride transporting proteins: chloride channel 3 (Clcn3), potassium/chloride transporter KCC3 (Slc12a4), and TGF-β and Wnt signaling molecules: MAD homolog 7 (Smad7), frizzled homolog 2 (Fzd2) (Supplementary Table S7).

Interestingly, only a small group of transcripts (214 genes) showed a late response with increased gene expression levels after 7 days of NH_4Cl loading (*cluster 2*, Fig. 1). *Cluster 2* includes, along with signaling molecules of the small GTPase family and G protein signaling pathway, genes encoding cytoskeleton and Wnt signaling modulators such as the mammalian counterpart of *Drosophila* pygopus1 (Supplementary Table S6). Of note, the recently identified $(Na^+,K^+)/H^+$ exchanger NHE7 (SLC9A7) was highly upregulated during chronic acidosis; the latter localizes predominantly to the *trans*-Golgi network (34), and it has been suggested to play a pivotal role in the control of organellar ion homeostasis, of which the molecular mechanisms are still largely unknown (29).

Moreover, we found three small clusters of genes (*clusters 4–6*) with the following characteristics: *cluster 4* contains 226 genes, which include the aspartate/glutamate transporter Slc1a6, the sodium/glucose cotransporter (Slc5a11), the sodium bicarbonate cotransporter Slc4a9, the gulonolactone oxidase (Gulo), and a member of the organic anion transporters (Slc22a19) (Supplementary Table S8). These genes showed a gradual decrease in expression levels during metabolic acidosis. *Cluster 5* consists of 442 genes that are transiently repressed after 2 days of acidosis but returned to control levels

Table 4. *Genes downregulated after 2 days acid-loading*

Gene Symbol	Gene Name	Fold Change	GenBank Acc. No.
Dst	dystonin	0.11	NM_133833; NM_134448
Angptl4	angiopoietin-like 4	0.23	NM_020581
Slc7a7	solute carrier family 7 (cationic amino acid transporter, y+ system), member 7	0.29	NM_011405
Slc34a3	solute carrier family 34 (sodium phosphate), member 3; NaPiIIc	0.32	NM_080854
GPI	glucose phosphate isomerase	0.38	NM_008155
Dpp7	dipeptidylpeptidase 7	0.39	NM_031843
Slc5a12	solute carrier family 5 (sodium/glucose cotransporter), member 12	0.39	NM_001003915
ASS1	argininosuccinate synthetase 1	0.42	NM_007494
Slc2a2	solute carrier family 2 (facilitated glucose transporter), member 2	0.43	NM_031197
Fbp2	fructose bisphosphatase 2	0.46	NM_007994
Gatm	L-arginine:glycine amidinotransferase	0.46	NM_025961
Slc5a11	solute carrier family 5 (sodium/glucose cotransporter), member 11	0.48	NM_146198
G6pc	glucose-6-phosphatase, catalytic	0.54	NM_008061
Asl	argininosuccinate lyase	0.54	NM_133768
Slc5a2	solute carrier family 5 (sodium/glucose cotransporter), member 2	0.56	NM_133254
Slc25a15	ORNT1, solute carrier family 25 (mitochondrial carrier ornithine transporter), member 15	0.59	NM_011017, NM_181325
Dao1	D-amino acid oxidase 1	0.61	NM_010018
Slc16a10	solute carrier family 16 (monocarboxylic acid transporters), member 10, TAT1	0.61	NM_028243
Slc16a2	solute carrier family 16 (monocarboxylic acid transporters), member 2	0.68	NM_009197
Slc26a4	solute carrier family 26, member 4; pendrin	0.70	NM_011867
Agmat	agmatine ureohydrolase (agmatinase)	0.77	XM_915401, XM_980293, XM_983114

List of selected genes dowregulated after 2 days of NH_4Cl-loading. For each gene, the symbol, name, fold change, and GenBank Reference Sequence are given.

Table 5. *Gene downregulated after 7 days acid-loading*

Gene Symbol	Gene Names	Fold Change	GenBank Acc. No.
Ces1	carboxylesterase 1	0.07	NM_021456
Slc7a12	solute carrier family 7 (cationic amino acid transporter, y+ system), member 12	0.25	NM_080852
Angptl4	angiopoietin-like 4	0.40	NM_020581
Fbp2	fructose bisphosphatase 2	0.43	NM_007994
Slc34a3	solute carrier family 34 (sodium phosphate), member 3; NaPiIIc	0.44	NM_080854
Slc7a7	solute carrier family 7 (cationic amino acid transporter, y+ system), member 7	0.45	NM_011405
Dpp7	dipeptidylpeptidase 7	0.47	NM_031843
Slc5a11	solute carrier family 5 (sodium/glucose cotransporter), member 11	0.56	NM_146198
Slc26a4	solute carrier family 26, member 4; pendrin	0.56	NM_011867
Slc2a2	solute carrier family 2 (facilitated glucose transporter), member 2	0.65	NM_031197
ASS1	argininosuccinate synthetase 1	0.66	NM_007494
Gatm	L-arginine:glycine amidinotransferase	0.71	NM_025961

List of selected genes downregulated after 7 days of NH_4Cl-loading. For each gene, the symbol, name, fold change, and GenBank Reference Sequence are given.

after 7 days (Supplementary Table S9). This cluster was characterized by genes encoding carbonic anhydrase 4 (Car4) as well as proteins involved in regulation of cell growth such as Fas apoptotic molecule 3 (Faim3), growth arrest specific 2 (Gas2), growth differentiation factor 3 (Gdf3), cytoskeleton-associated protein 2 (Ckap2), nibrin (Nbn), insulin-like growth factor binding protein 4 (Igfbp4), and angiopoietin-like gene (Angptl4). Many members of the SLC family were also represented in this cluster: sodium/glucose cotransporter Slc5a12, the facilitated glucose transporter Slc2a2, the cation transporters (Slc7a2, Slc7a9, Slc22a5), monocarboxylic transporters (Slc16a10, Slc16a2), the acetyl-CoA transporter Slc33a1, and many others (Slc1a6, Slc5a1, Slc2a2, Slc34a3, Slc7a7). Finally, *cluster 6* included 185 genes with increased expression levels in 7 days-treated mice but decreased expression in 2 days-treated mice (Supplementary Table S10). These gene transcripts include the amiloride-sensitive cation channel Accn1, the potassium channel Kcnk4, the glucose 6-phosphatase (G6pc), and an uncharacterized carbohydrate kinase. In addition, many genes encoding gene products of unknown function are also present in this cluster. Further characterization of these orphan genes may provide novel insights into the mechanisms of adaptation to metabolic acidosis.

Taken together, our findings highlight and confirm the pivotal role of ammoniagenesis, ATP synthesis, and sodium reabsorption as major players during acute and chronic metabolic acidosis. Furthermore, they address the potential adaptive mechanisms during chronic metabolic acidosis, which may be represented by complex signaling networks involving the fine-tuning of cytoskeleton organization, cell proliferation, cell differentiation, and apoptotic responses. Further investigations are needed to characterize not only the metabolic pathways directing these cellular modifications during chronic acidosis, but also the large number of differentially regulated genes, of which the structure and the function are still unknown.

Validation of candidate genes by quantitative real-time PCR. Candidate genes emerging from the microarray analysis were validated by qRT-PCR in a separate group of mice treated identically as the mice used above. Fifteen differently regulated genes were selected for further validation, including SNAT3 (Slc38a3/SN1), phospho-enol-pyruvate-carboxy kinase (PEPCK), aquaporin-2 (AQP2), aquaporin-3 (AQP3), vasopressin 2 receptor (Avrp2), carbonic anhydrase 2 (Car2), phosphate-dependent glutaminase (PDG), the sodium-dependent phosphate cotransporter NaPiIIa (Slc34a1), the sodium-dependent phosphate cotransporter NaPiIIc (Slc34a3), the monocarboxylate transporters MCT8 (Slc16a2) and MCT2 (Slc16a7), the sodium-dependent bicarbonate transporter NBCn1 (Slc4a7), the Cl^-/HCO_3^- exchanger pendrin (Slc26a4), malate dehydrogenase 2 (Mdh2), and fructose bisphosphatase 2 (Fbp2). These genes represented transcripts, which showed positive or negative regulation over a wide range. All genes, except Mdh2, showed the predicted changes in expression level (Fig. 2), similar in fold change to microarray data (slope of line 0.89, $R^2 = 0.73$ for 2 days acidosis vs. control, slope of 0.97, $R^2 = 0.94$ for 7 days acidosis vs. control, respectively). Thus, the regulation of all but one selected genes could be confirmed by qRT-PCR using a separate group of animals. This demonstrates a remarkably high degree of reproducibility and sensitivity of the gene expression profiles obtained by microarray analysis.

Validation of candidate genes by Western blotting. It has been previously demonstrated that changes in mRNA expression levels do not necessarily translate into changes in the corresponding protein levels (21). Therefore, we investigated whether the mRNA levels as determined by microarray analysis and validated by qRT-PCR correlate with changes in protein levels assessed by Western blotting.

Crude membrane fractions prepared from total kidney of control and acidotic animals were used to test the expression levels of the glycosylated and nonglycosylated forms of the aquaporin 2 water channel, the Cl^-/HCO_3^- exchanger pendrin, and the glutamine transporter SNAT3 (Fig. 3). The protein levels of SNAT3 (Slc38a3) were significantly increased after 2 and 7 days of NH_4Cl treatment (268.7 ± 17.9%, 257.6 ± 32.9%, respectively), that was in good agreement with the strong increase found at the mRNA level (3.8, 3.9-fold by microarray; 5.4, 3.9-fold by qRT-PCR). Similarly, the expression levels of the glycosylated (224.1 ± 20.7%, 323.2 ± 34.7%) and nonglycosylated (218.4 ± 15%, 275.9 ± 29.6%) AQP2 were significantly increased in acidotic animals (3.2, 1.7-fold by microarray; 2.2, 1.8-fold by qRT-PCR). Downregulation of mRNA levels of Cl^-/HCO_3^- exchanger pendrin observed in microarray experiments in the kidneys of 2 and 7 days treated animals (0.73- and 0.58-fold, respectively) and further confirmed by qRT-PCR (0.51- and 0.42-fold, respectively) was in agreement with decreased abundance of the protein (84.0 ± 6.0% and 67.8 ± 5.8%, respectively). Thus,

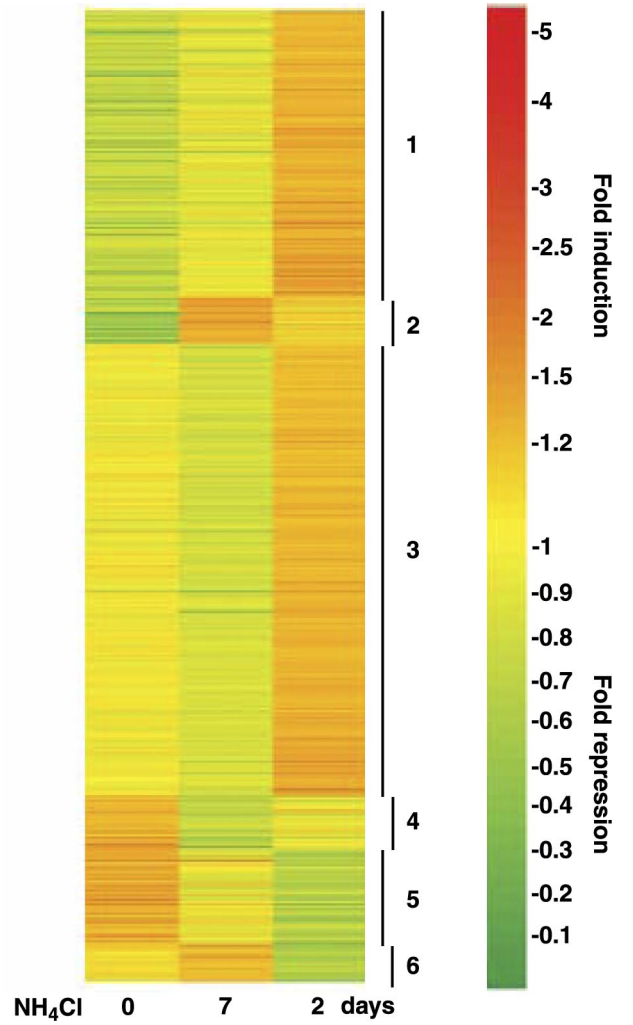

Fig. 1. Hierarchical clustering reveals 6 distinct clusters of coexpressed genes. The cluster image shows the different classes of gene expression profiles identified. We selected 4,389 genes, whose expression levels changed in response to 2 and 7 days of NH_4Cl administration. The expression pattern of each gene is displayed here as a horizontal stripe. For each gene, the ratio of the transcript expression level to the median of its expression level across the three time points is represented by a color, according to the color scale on the right. Experiments relative to each time point are shown in columns. Numbers indicate the identified clusters.

regulation of transcripts by acidosis could be confirmed for at least some selected genes suggesting that the transcriptional changes observed may translate into altered protein expression and may eventually alter functional properties of cells and nephron segments.

Spatial regulation of genes: qRT-PCR of dissected nephron segments. Microarray analysis and consecutive real-time PCR had been performed on the total kidney, which may mask even stronger changes in transcript levels, if occurring only in a subpopulation of cells along the nephron. Pathway analysis of regulated transcripts suggested a strong representation of genes involved in ammoniagenesis, the Krebs cycle, and gluconeogensis, processes known to be highly active in the proximal tubule (Fig. 4). Additionally we found a large number of genes involved in arginine metabolism that were downregulated in acidotic mice (Fig. 5). Renal arginine synthesis and metabolism take place in the proximal tubule (7). Therefore, we analyzed dissected early (S1/S2 convoluted) and late (S3 straight) proximal tubule segments from control mice and animals acid-loaded for 2 days (n = 3–6 animals for each group). Total RNA was extracted and used to assess abundance of several transcripts by qRT-PCR. Analysis was performed for PEPCK, SNAT3 (Slc38a3), PDG, Mdh2, and Fbp2, genes involved in ammoniagenesis, the Krebs cycle, and gluconeogenesis, and for ORNT1 (Slc25a15), y^+-LAT-1, and Gatm, which are genes important in arginine metabolism (Figs. 6 and 7). Under control conditions, we observed similar expression of PEPCK in early and late parts of the proximal tubule that was highly elevated in acidotic mice (10-fold in early, 3.6-fold in late proximal tubule). The glutamine transporter SNAT3 (Slc38a3) was in very low abundance in the early proximal tubule compared with the late segment in control mice; however, in acidotic animals mRNA expression was increased to a similar level in both proximal tubule segments. Under control condi-

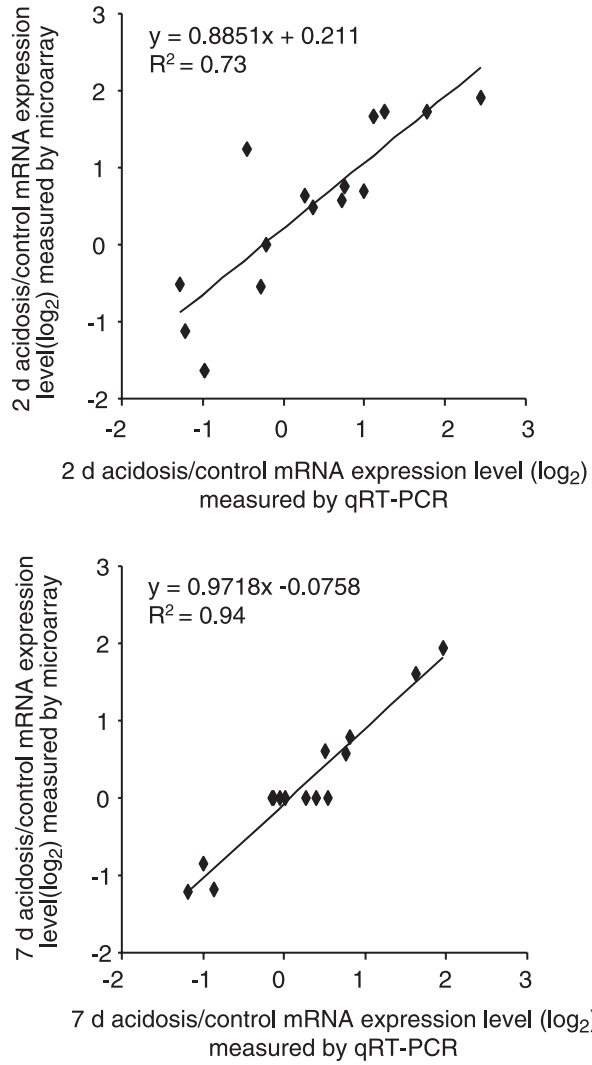

Fig. 2. Validation of microarray by qRT-PCR. Comparison of the relative changes in expression levels for 15 genes as determined by qRT-PCR and microarray analysis. The ratio of expression levels for each gene in response to 2 or 7 days acid loading compared with control was $\log_2$ transformed. The values obtained for 2 and 7 days show a high degree of correlation demonstrating that the changes in transcript levels as determined by microarray and qRT-PCR are largely comparable.

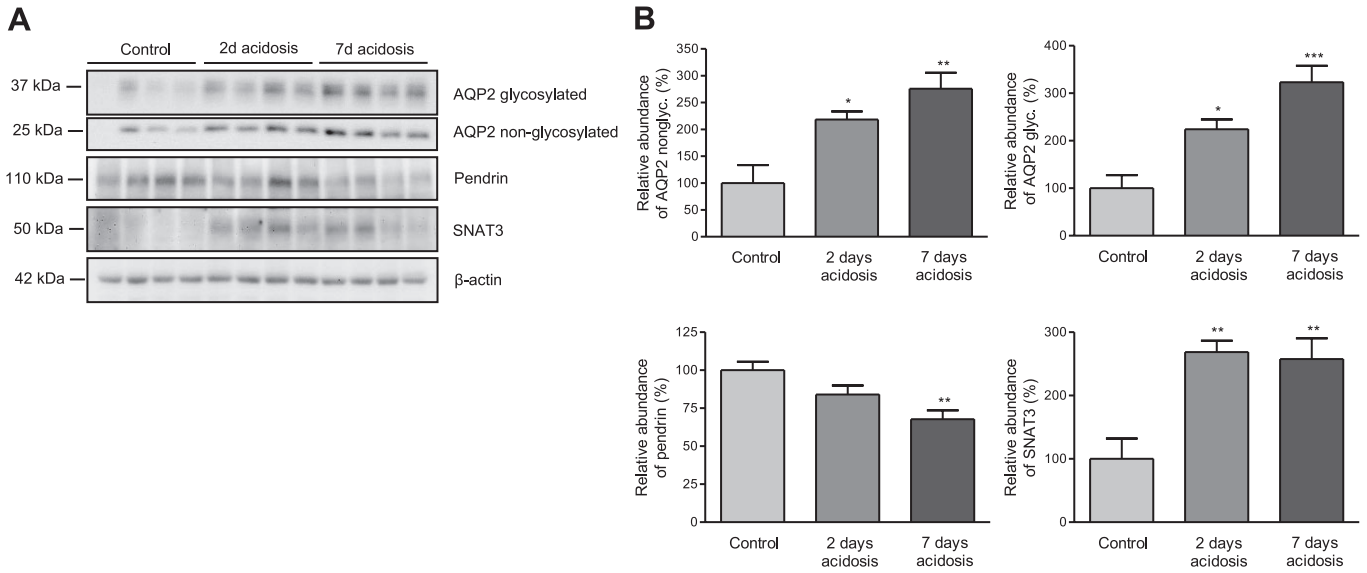

Fig. 3. Metabolic acidosis affects protein expression levels. Expression of selected proteins in total kidney membrane fractions after 2 and 7 days acid loading. *A*: abundance of glycosylated and nonglycosylated variants of aquaporin 2 water channel (AQP2), the chloride/anion exchanger pendrin (SLC26A4), and the glutamine transporter SNAT3 (SLC38A3). The immunoblots were stripped and reprobed for all proteins and β-actin to control for equal loading. *B*: bar graphs summarizing data from immunoblotting. All data were normalized against actin. $*P < 0.05$, $**P < 0.01$, $***P < 0.001$.

tions expression of PDG was similar in both, early and late proximal tubules, and was further increased 3.1-fold in the S1/S2 segment and 1.9-fold in the S3 segment from acid-loaded animals. In contrast, in control animals Fbp2 was 3.5-fold higher expressed in the early proximal tubule; however, in acidotic animals its expression was reduced to a similar extent. We did not observe any changes in Mdh2 expression, which was in agreement with qRT-PCR data from the total kidney but in contrast to the data from microarray analysis.

We also tested genes involved in proximal tubule arginine metabolism and transport and found that under control conditions expression of all analyzed transcripts (ORNT1, y^+-

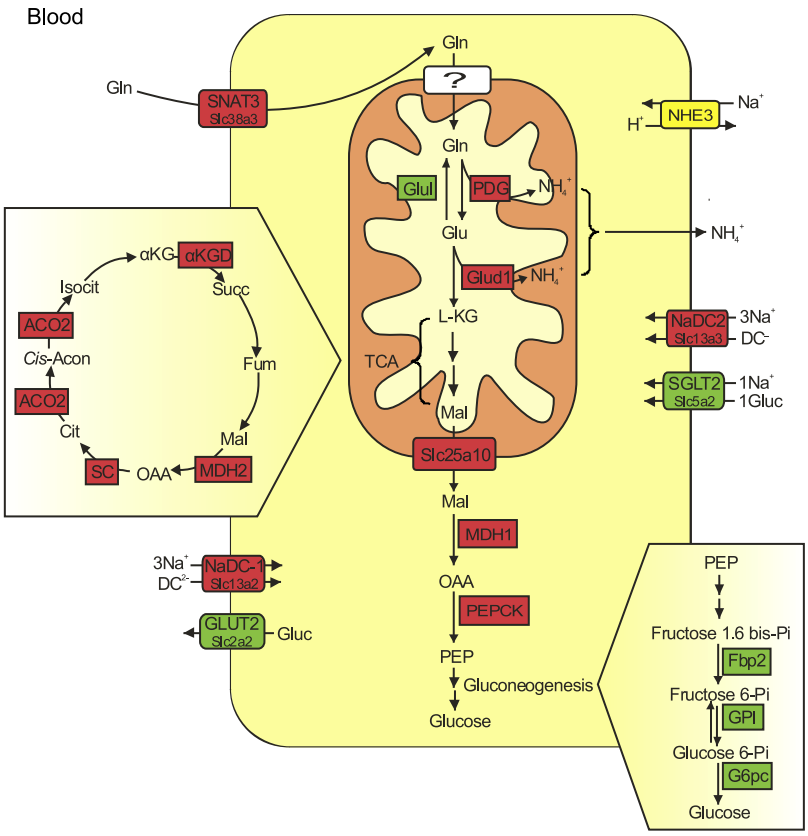

Fig. 4. The kidney ammoniagenesis pathway. Glutamine (Gln) is transported across the basolateral plasma membrane via the Na^+/glutamine transporter SNAT3 (Slc38a3) and then taken up into mitochondria via a yet unknown carrier. In mitochondria, Gln is converted to glutamate (Glu) by the phosphate-dependent glutaminase (PDG) and then to α-ketoglutarate (α-KG) by action of the glutamine dehydrogenase (Glud1) to fuel into the TCA (Krebs) cycle. These 2 reactions result in production of 2 NH_4^+ molecules that are secreted into the luminal fluid through a mechanism involving transport via the apical Na^+/H^+ exchanger NHE3. Eventually, glucose is produced by the cytosolic phosphoenolpyruvate carboxykinase (PEPCK). Green rectangles denote transporters and enzymes upregulated, red downregulated, yellow not regulated on microarrays. The white rectangle denotes a putative glutamine transporter not identified yet on a molecular basis. Other abbreviations used: ACO2, aconitase 2; Cit, citrate; CS, citrate synthase; Fbp2, fructose bisphosphatase 2; Fum, fumarate; Glul, glutamine synthase; Glut2 (Slc2a2), glucose transporter; GPI, glucose phosphate isomerase; G6pc, glucose-6-phosphatase; Isocit, isocitrate; Mal, malate; MDH1/2, malate dehydrogenase 1/2; NaDC1 (Slc13a2), Na^+/dicarboxylate cotransporter, NaDC3 (Slc13a3), Na^+/dicarboxylate cotransporter; OAA, oxoloacetate; PEP, phosphoenolpyruvate; Succ, succinate.

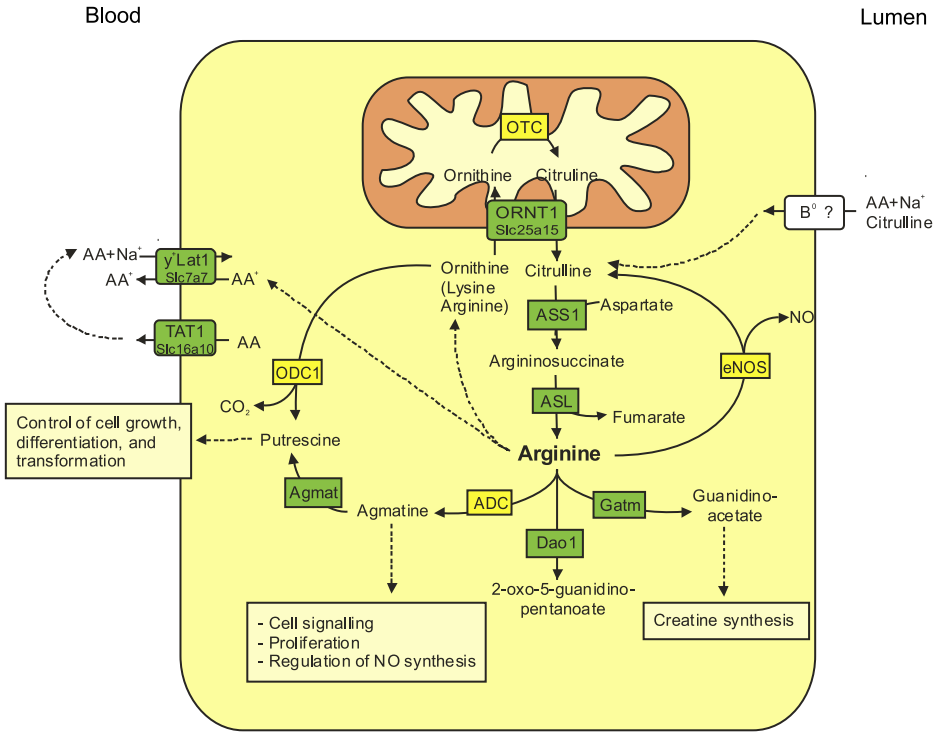

Fig. 5. The arginine metabolism pathway in proximal tubules. L-arginine is synthesized from L-citrulline via action of argininosuccinate synthetase (ASS1) and argininosuccinate lyase (ASL). Arginine may be also converted by the enzyme glycine amidinotransferase (Gatm) to guanidinoacetate or by argininodecarboxylase (ADC) to agmatine. Agmatine is then converted to putrescine by an agmatinase (Agmat). Arginine may be also metabolized to 2-oxo-5-guanidinopentanoate by D-amino acid oxidase 1 (Dao1). In addition, arginine is also a precursor of nitric oxide (NO) while converted back to citrulline via action of nitric oxide synthase (eNOS). The bulk of reabsorbed and newly synthesized arginine is, however, transported out of the proximal tubule cell via the basolateral system y^+L amino acid transporter y^+-LAT1 (Slc7a7) and is metabolized in other organs. Other abbreviations used: B^0 Na^+-dependent neutral amino acid transporter; ORNT1 (Slc25a15), mitochondrial ornithine (citrulline transporter); OTC, ornithine carbamoyltransferase; TAT1 (Slc16a10), monocarboxylic acid transporter. Green rectangles denote transporters and enzymes upregulated, red downregulated, yellow not regulated on microarrays. White rectangle denotes not identified transporters.

LAT1, and Gatm) was higher in the proximal convoluted tubule than proximal straight tubule. Furthermore, acid load decreased expression of these genes only in the early segment.

Thus, analysis of two consecutive segments of the proximal tubule from control and acidotic animals demonstrated a spatial arrangement of transcript expression levels and that acidosis differently affected transcript levels of the same genes in adjacent segments. In the case of SNAT3, similar results had been obtained recently by immunohistochemistry in kidneys from control and acidotic animals (32).

DISCUSSION

The renal adaptation to metabolic acidosis involves the regulation of various enzymes and transport proteins. Despite the identification of proteins and mechanisms regulated during metabolic acidosis, the processes involved in the adaptation of the kidney remain only partially understood. Here we used a microarray-based genome-wide gene expression profiling approach to characterize transcriptional changes in total kidney during metabolic acidosis.

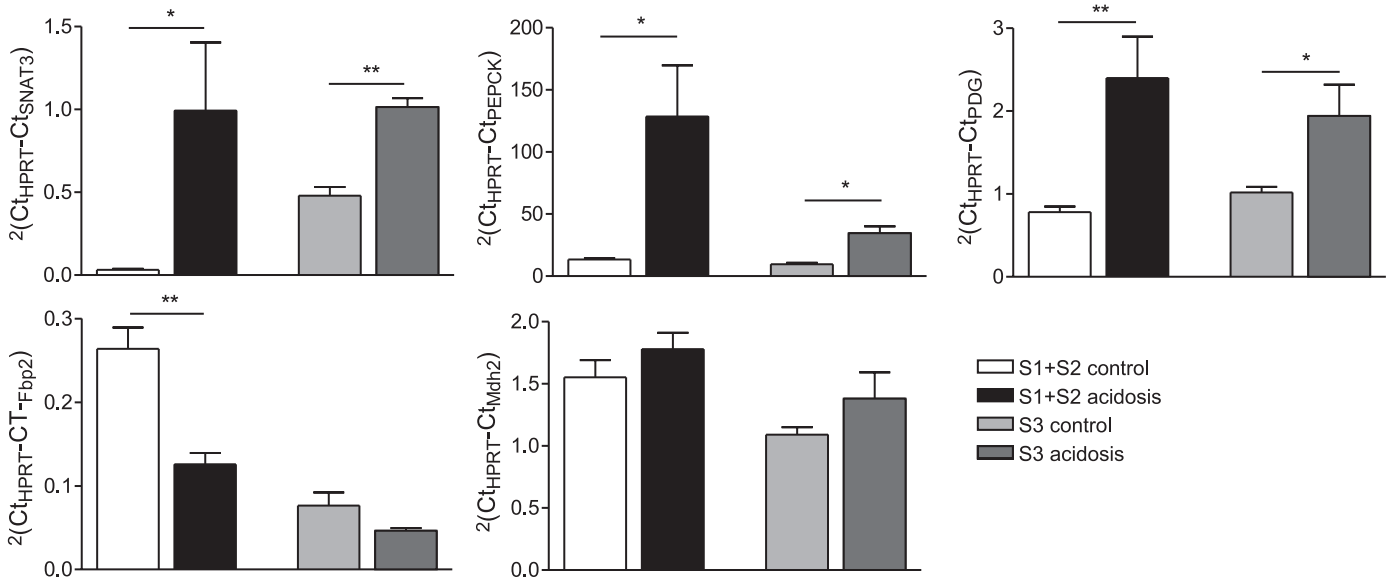

Fig. 6. Spatial expression and regulation of genes in the proximal tubule. Expression of mRNA for PEPCK, SNAT3, phosphate-dependent glutaminase (PDG), malate dehydrogenase 2 (Mdh2), and fructose bisphosphatase 2 (Fbp2) in microdissected early (S1/S2) or late (S3) segments of the proximal tubules from control and 2 days acidotic mice. HPRT, hypoxanthine guanine phosphoribosyl transferase. Data are given as means ± SE; $n = 3–6$. *$P < 0.05$, **$P < 0.01$.

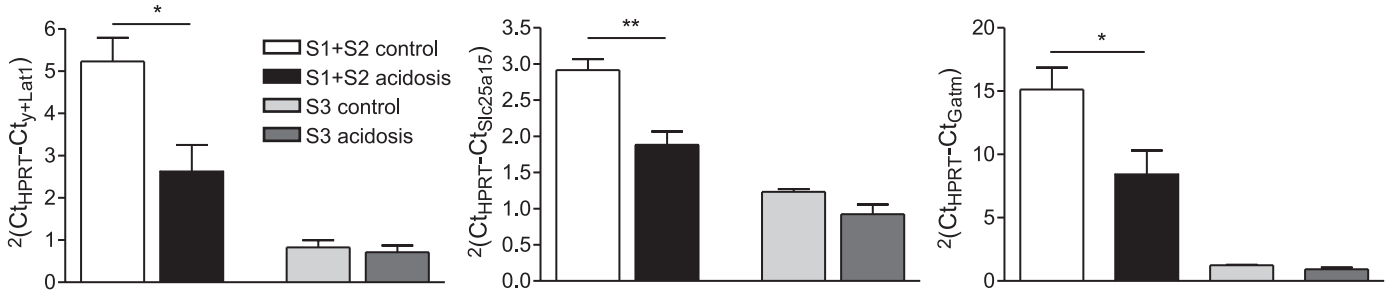

Fig. 7. Spatial expression and regulation of genes involved in arginine synthesis and metabolism in the proximal tubule. Expression of mRNA coding for glycine amidinotransferase (Gatm), the arginine efflux system y^+ L amino acid transporter y^+-LAT1 (Slc7a7), and the ornithine transporter (Slc25a15) in microdissected early (S1/S2) or late (S3) segments of the proximal tubules from control and 2 days acidotic mice. Data are given as means ± SE; $n = 3–6$ animals. $^*P < 0.05$, $^{**}P < 0.01$.

Analysis of microarrays revealed that nearly one-third of all genes present on the chip could be detected in kidney tissue at significant levels. This number is considerably higher than previous reports on total kidney using microarrays that covered the mouse genome only partly (40, 47) or using microdissected nephron segments analyzed by SAGE (11, 50). However, these reports did not include all kidney structures into their analyses, which may explain this discrepancy (44).

The relative expression of >4,000 genes was affected by acid loading for 2 or 7 days, representing almost one third of all expressed genes. Interestingly, cluster analysis detected a clear time course of changes with the majority of transcripts regulated only after 2 days treatment and only a smaller number responded to 7 days acid loading. This temporal change in gene expression was paralleled by the return of systemic acid-base parameters toward control values. It remains to be examined whether this apparent normalization of acid-base status and transcript levels is mediated by posttranscriptional changes, i.e., protein expression levels or posttranslational protein modifications. Quantitative real-time RT-PCR of 15 differentially regulated candidate transcripts validated the microarray findings. Correlation between microarray and qRT-PCR data was remarkably high, confirming the accuracy and reliability of the microarray technology used here. Moreover, protein abundance of AQP2, pendrin, and SNAT3 was in agreement with microarray and qRT-PCR findings. Many of the genes known to be regulated in response to acid loading (e.g., Slc38a3, PEPCK, Slc13a2) could be detected in our lists of regulated genes providing an additional and independent confirmation (Table 6). We further compared our data with a list of proteins detected by proteome analysis of rat proximal tubule during metabolic acidosis (15). Curthoys et al. (15) identified 21 proteins to be upregulated during acidosis of which 10 were also significantly upregulated on mRNA level in our set of data [i.e., transketolase, dimethyl glycine dehydrogenase, phosphoenolpyruvate carboxykinase, glutamate dehydrogenase, and glutathione S-transferases (Pi-class and Mu-1, selenium binding protein, glutaminase)]. Nine mRNAs were not regulated, and two RNAs (phenylalanine-4-hydroxylase, acetoacetyl-CoA thiolase) were downregulated as determined by microarray analysis. Similarly, out of the 16 proteins decreased in acidotic rat proximal tubule, we confirmed three candidates on mRNA level (argininosuccinate synthetase, transglutaminase, Arg-Gly amidinotransferase), one was found to be upregulated (enolase), the other mRNAs were not identified or found to be not regulated. This high degree of similarity between proteome and microarray data may encourage further efforts to decipher the renal response to acidosis on mRNA and protein levels.

Table 6. *Previously reported acidosis-regulated genes*

Gene Symbol	Gene Name	Fold Change		Reference No.	GenBank Acc. No.
		2 Days	7 Days		
Slc38a3	SNAT3	3.75	3.86	(27, 32)	NM_023805
Slc4a7	NBCn1	3.33		(28)	NM_001033270
AQP2	aquaporin 2	3.20	1.75	(3)	NM_009699
Slc13a2	NaC1, NaDC-1, SDCT1	3.29	2.41	(4)	NM_022411
Glud1	glutamate dehydrogenase	2.04	2.13	(39, 52)	NM_008133
Car2	carbonic anhydrase 2	1.69	1.53	(12, 41, 48)	NM_009801
PDG	phosphate-dependent glutaminase	1.63	1.48	(14, 25, 26)	NM_001081081
Fxyd4	CHIF (channel inducing factor)	1.49		(9, 10)	NM_033648
Slc7a7	y(+)-LAT1	0.279	0.468	(32)	NM_011405
Slc26a4	pendrin	0.70	0.56	(19, 36)	NM_011867
Slc7a9	$b^{0,+}$AT	0.47		(32)	NM_021291
Car4	carbonic anhydrase 4	0.466	0.748	(51)	NM_007607
Glul	glutamine synthase	0.79		(13)	NM_008131
Slc13a1	NaSi-1	0.58	0.63	(37)	NM_019481
Pck1	phosphoenolpyruvate carboxykinase 1, cytosolic	nd	2.71	(25, 32)	NM_011044

List of genes reported previously by others to be regulated by metabolic acidosis and also detected here by microarray analysis. For each gene, the symbol, name, fold change after 2 and/or 7 days acidosis as detected by microarray analysis, references, and GenBank Reference Sequence are given.

Pathway analysis revealed that regulated genes represent a large variety of GO categories and KEGG pathways, suggesting that the kidney is strongly affected as a whole and responds at many different levels. Analysis of statistically significant transcripts revealed that expression of 97 genes coding different solute carrier transporters was affected by acid loading. Mitochondrial carriers (Slc25) and monocarboxylic acid transporters (Slc16) were the most represented. Membrane transporters are important in maintaining cellular homeostasis and mediate the reabsorptive and excretory processes along the nephron. Thus, regulation of such a large number of solute carriers is not unexpected. However, the most represented pathway in both analyses was oxidative phosphorylation. The apparent overrepresentation of oxidative phosphorylation together with regulation of mitochondrial transporters may indicate the requirement of kidney cells for energy substrates such as ATP to adapt to acid-loading. Transport pathways involved in acid excretion or bicarbonate reclamation such as H^+-ATPases, Na^+/HCO_3^- cotransporter or Na^+/H^+-exchangers, and Na^+/K^+-ATPase are driven directly by ATP hydrolysis or depend on the sodium gradient and membrane potential generated by ATP-dependent processes. Along the same line, we detected 13 genes of the mitochondrial transporter family (Slc25) to be regulated by metabolic acidosis. Interestingly, the mitochondrial phosphate carrier (Slc25a25) was one of the genes with the highest elevation of expression during metabolic acidosis. These transporters participate in the import of substrates and release of metabolites from mitochondria (35). Also, expression of genes that belong to metabolism of amino acids, lipids, and carbohydrates was affected by metabolic acidosis.

Increased ammoniagenesis is a major process contributing to the renal response to metabolic acidosis (14). Ammonia is synthesized mainly in the proximal tubule from glutamine taken up from blood possibly by the Na^+-dependent amino acid transporter SNAT3 (Slc38a3). During metabolic acidosis SNAT3 is upregulated on mRNA and protein levels, and its expression spreads from the late proximal tubule to the early proximal tubule (27, 32, 43). In our experiments, the expression of SNAT3 was strongly elevated after 2 and 7 days of acid loading, which was confirmed by qRT-PCR and Western blotting. We also observed upregulation of many additional genes involved in renal ammoniagenesis namely the phosphate-dependent glutaminase (PDG), glutamate dehydrogenase (Glud1), mitochondrial malate transporter (Slc25a10), malate dehydrogenase 1 (Mdh1), and phospho-enolpyruvate carboxykinase (PEPCK), combined with downregulation of glutamine synthetase (Glul) (Supplementary Tables S2 and S3, Fig. 5). Effects of metabolic acidosis on expression of PDG, Glud1, PEPCK, and Glul were previously reported in other studies (Table 6); however, our data expand the list of genes considerably and suggest a concerted regulation of the whole pathway. Activation of ammoniagenesis was concomitant with increased expression of TCA cycle enzymes: α-ketoglutarate dehydrogenase (αKGD), malate dehydrogenase 2 (MDH2), citrate synthase (CS), and aconitase 2 (Aco2). The enhanced efflux of malate from mitochondria during acidosis has been described previously (33). However, in contrast to our data it has been reported that flux through citrate synthase is reduced. The apparent activation of the TCA observed here is in agreement with upregulation of the sodium-dependent citrate transporters NaDC1 (Slc13a2) (4) and NaDC3 (Slc13a3), NaDC1 and NaDC3 transport succinate, citrate and α-ketoglutarate, TCA cycle intermediates, and it has been suggested that NaDC1 regulation may provide more substrate for bicarbonate production.

Previous studies linked metabolic acidosis to increased renal gluconeogenesis (18, 39). Others have found no evidence for increased glucose release from kidney during acidosis (20). Our data indicate that gluconeogenesis may be reduced given that the key enzymes of glucose synthesis, glucose 6-phosphatase and fructose bisphosphatase, were severely downregulated (Fig. 5, Supplementary Table S2). It remains to be clarified if these apparent discrepancies are due to the different animal species used. Moreover, our data reflect only changes on the transcriptional level but not on the level of enzyme activity.

Both ammoniagenesis and gluconeogenesis take place in proximal tubule cells (14). Since the proximal tubule can be subdivided into at least two distinct subsegments, the early or convoluted tubule (S1/S2 segment) and the late or straight proximal tubule (S3 segment), we asked whether there is a differential transcriptional response to acidosis. Interestingly, qRT-PCR of S1/S2 and S3 segments demonstrated both spatial and temporal patterns of gene expression and regulation. Under control conditions, components of the gluconeogenic pathway were mostly found in the early proximal tubule, where downregulation during metabolic acidosis was more pronounced. In contrast, key transporters and enzymes of ammoniagenesis were mostly localized to the late proximal tubule and were strongly upregulated both in the early and late proximal tubule during metabolic acidosis. The very low mRNA expression of SNAT3 in the early proximal tubule is in agreement with the low abundance of the protein in this part of the nephron as detected by immunohistochemistry (32). Adaptation to metabolic acidosis involves also nephron remodeling increasing the number of acid-secretory type A intercalated cells and leading to hypertrophy of various cell types along the nephron (2, 30, 31, 49). In the present study we observed a large number of transcripts (both up- and downregulated) that are involved in cell death/apoptosis, growth, and differentiation. Therefore, it may be possible that the increased number of type A intercalated cells during chronic acidosis may involve proliferation combined with apoptotic removal of type B intercalated cells. In fact, we have observed during preliminary experiments that type A intercalated cells stain positive for various markers of proliferation, whereas type B intercalated were devoid of such markers (D. Bacic, M. Nowik, M. LeHir, B. Kaissling, and C. A. Wagner, unpublished results). Similarly, Cheval et al. (12) observed by SAGE analysis transcripts of proliferative pathways in isolated mouse outer medullary collecting duct. Moreover, proximal tubular cells also show prominent staining of proliferative markers during chronic acidosis (D. Bacic, M. Nowik, M. LeHir, B. Kaissling, and C. A. Wagner, unpublished observations).

We also observed upregulation of several genes involved in renal water handling, among them the water channels AQP1, AQP2, AQP3, AQP4, the urea transporter UT-A1, and the vasopression receptor V2R. Regulation of AQP2 during NH_4Cl-loading has been previously reported (3). Acidotic mice, however, consumed ~20% less water than control animals (data not shown). Thus, we cannot exclude that the addition of NH_4Cl to drinking water induced also a mild

dehydration that may contribute to the regulation observed. Water homeostasis in metabolic acidosis deserves further investigation as deranged water homeostasis has also been observed in inborn or acquired syndromes of renal tubular acidosis (8, 38, 46).

In summary, in our study >4,000 transcripts were significantly ($P < 0.05$) regulated during metabolic acidosis, which was ~40% of all genes expressed in the kidney. Major pathways regulated affect energy homeostasis, acid excretion, water and electrolyte balance, as well as pathways involved in apoptosis and cell proliferation. The latter may contribute to the remodeling of the kidney. Our data provide a genome-wide view on the complex regulatory and adaptive processes during metabolic acidosis and will allow elucidating the exact role of regulated pathways.

ACKNOWLEDGMENTS

The use of the ZIHP Core Facility for Rodent Physiology is gratefully acknowledged.

GRANTS

This study was supported by the 6th Framework EU project EuReGene (005085) to A. W. Brändli and C. A. Wagner. M. Nowik is supported by a PhD student fellowship from the Zurich Center for Integrative Physiology (ZIHP).

REFERENCES

1. **SRI International.** Panther classification system, www.pantherdb.org.
2. **Al-Awqati Q.** Plasticity in epithelial polarity of renal intercalated cells: targeting of the H^+-ATPase and band 3. *Am J Physiol Cell Physiol* 270: C1571–C1580, 1996.
3. **Amlal H, Sheriff S, Soleimani M.** Upregulation of collecting duct aquaporin-2 by metabolic acidosis: role of vasopressin. *Am J Physiol Cell Physiol* 286: C1019–C1030, 2004.
4. **Aruga S, Wehrli S, Kaissling B, Moe OW, Preisig PA, Pajor AM, Alpern RJ.** Chronic metabolic acidosis increases NaDC-1 mRNA and protein abundance in rat kidney. *Kidney Int* 58: 206–215, 2000.
5. **Berthelot M.** Violet d'aniline. *Rep Chim App* 1: 284, 1859.
6. **Biber J, Stieger B, Haase W, Murer H.** A high yield preparation for rat kidney brush border membranes. Different behaviour of lysosomal markers. *Biochim Biophys Acta* 647: 169–176, 1981.
7. **Brosnan ME, Brosnan JT.** Renal arginine metabolism. *J Nutr* 134: 2791S–2795S, 2004.
8. **Bruce LJ, Cope DL, Jones GK, Schofield AE, Burley M, Povey S, Unwin RJ, Wrong O, Tanner MJ.** Familial distal renal tubular acidosis is associated with mutations in the red cell anion exchanger (Band 3, AE1) gene. *J Clin Invest* 100: 1693–1707, 1997.
9. **Capurro C, Coutry N, Bonvalet JP, Escoubet B, Garty H, Farman N.** Cellular localization and regulation of CHIF in kidney and colon. *Am J Physiol Cell Physiol* 271: C753–C762, 1996.
10. **Capurro C, Coutry N, Bonvalet JP, Escoubet B, Garty H, Farman N.** Specific expression and regulation of CHIF in kidney and colon. *Ann NY Acad Sci* 834: 562–564, 1997.
11. **Chabardes-Garonne D, Mejean A, Aude JC, Cheval L, Di Stefano A, Gaillard MC, Imbert-Teboul M, Wittner M, Balian C, Anthouard V, Robert C, Segurens B, Wincker P, Weissenbach J, Doucet A, Elalouf JM.** A panoramic view of gene expression in the human kidney. *Proc Natl Acad Sci USA* 100: 13710–13715, 2003.
12. **Cheval L, Morla L, Elalouf JM, Doucet A.** The kidney collecting duct acid-base "regulon". *Physiol Genomics* 27: 271–281, 2006.
13. **Conjard A, Komaty O, Delage H, Boghossian M, Martin M, Ferrier B, Baverel G.** Inhibition of glutamine synthetase in the mouse kidney: a novel mechanism of adaptation to metabolic acidosis. *J Biol Chem* 278: 38159–38166, 2003.
14. **Curthoys NP, Gstraunthaler G.** Mechanism of increased renal gene expression during metabolic acidosis. *Am J Physiol Renal Physiol* 281: F381–F390, 2001.
15. **Curthoys NP, Taylor L, Hoffert JD, Knepper MA.** Proteomic analysis of the adaptive response of rat renal proximal tubules to metabolic acidosis. *Am J Physiol Renal Physiol* 292: F140–F147, 2007.
16. **DuBose T Jr, Alpern RJ.** Renal tubular acidosis. In: *The Metabolic and Molecular Bases of Inherited Disease*, edited by Scriver CR, Beaudet AL, Sly WS, Valle D. New York: McGraw-Hill, 2001, p. 4983–5021.
17. **Eisen MB, Spellman PT, Brown PO, Botstein D.** Cluster analysis and display of genome-wide expression patterns. *Proc Natl Acad Sci USA* 95: 14863–14868, 1998.
18. **Ekberg K, Landau BR, Wajngot A, Chandramouli V, Efendic S, Brunengraber H, Wahren J.** Contributions by kidney and liver to glucose production in the postabsorptive state and after 60 h of fasting. *Diabetes* 48: 292–298, 1999.
19. **Frische S, Kwon TH, Frokiaer J, Madsen KM, Nielsen S.** Regulated expression of pendrin in rat kidney in response to chronic NH4Cl or NaHCO3 loading. *Am J Physiol Renal Physiol* 284: F584–F593, 2003.
20. **Goldstein L.** Renal substrate utilization in normal and acidotic rats. *Am J Physiol Renal Fluid Electrolyte Physiol* 253: F351–F357, 1987.
21. **Greenbaum D, Colangelo C, Williams K, Gerstein M.** Comparing protein abundance and mRNA expression levels on a genomic scale. *Genome Biol* 4: 117, 2003.
22. **Halperin ML, Vinay P, Gougoux A, Pichette C, Jungas RL.** Regulation of the maximum rate of renal ammoniagenesis in the acidotic dog. *Am J Physiol Renal Fluid Electrolyte Physiol* 248: F607–F615, 1985.
23. **Hamm LL, Alpern RJ.** Cellular mechanisms of renal tubular acidification. In: *The Kidney (3rd ed.)*, edited by Seldin DW, Giebisch G. Philadelphia, PA: Lippincott, 2001, p. 1995–2013.
24. **Huber W, von Heydebreck A, Sultmann H, Poustka A, Vingron M.** Variance stabilization applied to microarray data calibration and to the quantification of differential expression. *Bioinformatics (Oxford)* 18, *Suppl* 1: S96–S104, 2002.
25. **Hwang JJ, Curthoys NP.** Effect of acute alterations in acid-base balance on rat renal glutaminase and phosphoenolpyruvate carboxykinase gene expression. *J Biol Chem* 266: 9392–9396, 1991.
26. **Hwang JJ, Perera S, Shapiro RA, Curthoys NP.** Mechanism of altered renal glutaminase gene expression in response to chronic acidosis. *Biochemistry* 30: 7522–7526, 1991.
27. **Karinch AM, Lin CM, Wolfgang CL, Pan M, Souba WW.** Regulation of expression of the SN1 transporter during renal adaptation to chronic metabolic acidosis in rats. *Am J Physiol Renal Physiol* 283: F1011–F1019, 2002.
28. **Kwon TH, Fulton C, Wang W, Kurtz I, Frokiaer J, Aalkjaer C, Nielsen S.** Chronic metabolic acidosis upregulates rat kidney Na-HCO cotransporters NBCn1 and NBC3 but not NBC1. *Am J Physiol Renal Physiol* 282: F341–F351, 2002.
29. **Lin PJ, Williams WP, Luu Y, Molday RS, Orlowski J, Numata M.** Secretory carrier membrane proteins interact and regulate trafficking of the organellar $(Na^+,K^+)/H^+$ exchanger NHE7. *J Cell Sci* 118: 1885–1897, 2005.
30. **Madsen KM, Tisher CC.** Response of intercalated cells of rat outer medullary collecting duct to chronic metabolic acidosis. *Lab Invest* 51: 268–276, 1984.
31. **Madsen KM, Verlander JW, Kim J, Tisher CC.** Morphological adaptation of the collecting duct to acid-base disturbances. *Kidney Int Suppl* 33: S57–S63, 1991.
32. **Moret C, Dave MH, Schulz N, Jiang JX, Verrey F, Wagner CA.** Regulation of renal amino acid transporters during metabolic acidosis. *Am J Physiol Renal Physiol* 292: F555–F566, 2007.
33. **Nissim I, Nissim I, Yudkoff M.** Adaptation of renal tricarboxylic acid cycle metabolism to various acid-base states: study with [3-13C,5-15N]glutamine. *Miner Electrolyte Metab* 17: 21–31, 1991.
34. **Numata M, Orlowski J.** Molecular cloning and characterization of a novel $(Na^+,K^+)/H^+$ exchanger localized to the trans-Golgi network. *J Biol Chem* 276: 17387–17394, 2001.
35. **Palmieri L, Lasorsa FM, Vozza A, Agrimi G, Fiermonte G, Runswick MJ, Walker JE, Palmieri F.** Identification and functions of new transporters in yeast mitochondria. *Biochim Biophys Acta* 1459: 363–369, 2000.
36. **Petrovic S, Wang Z, Ma L, Soleimani M.** Regulation of the apical Cl-/HCO-3 exchanger pendrin in rat cortical collecting duct in metabolic acidosis. *Am J Physiol Renal Physiol* 284: F103–F112, 2003.
37. **Puttaparthi K, Markovich D, Halaihel N, Wilson P, Zajicek HK, Wang H, Biber J, Murer H, Rogers T, Levi M.** Metabolic acidosis regulates rat renal Na-Si cotransport activity. *Am J Physiol Cell Physiol* 276: C1398–C1404, 1999.

38. **Rodriguez-Soriano J, Vallo A, Castillo G, Oliveros R.** Natural history of primary distal renal tubular acidosis treated since infancy. *J Pediatr* 101: 669–676, 1982.
39. **Schoolwerth AC, deBoer PA, Moorman AF, Lamers WH.** Changes in mRNAs for enzymes of glutamine metabolism in kidney and liver during ammonium chloride acidosis. *Am J Physiol Renal Fluid Electrolyte Physiol* 267: F400–F406, 1994.
40. **Schwab K, Patterson LT, Aronow BJ, Luckas R, Liang HC, Potter SS.** A catalogue of gene expression in the developing kidney. *Kidney Int* 64: 1588–1604, 2003.
41. **Schwartz GJ, Winkler CA, Zavilowitz BJ, Bargiello T.** Carbonic anhydrase II mRNA is induced in rabbit kidney cortex during chronic metabolic acidosis. *Am J Physiol Renal Fluid Electrolyte Physiol* 265: F764–F772, 1993.
42. **Seaton B, Ali A.** Simplified manual high performance clinical chemistry methods for developing countries. *Med Lab Sci* 41: 327–336, 1984.
43. **Solbu TT, Boulland JL, Zahid W, Lyamouri Bredahl MK, Amiry-Moghaddam M, Storm-Mathisen J, Roberg BA, Chaudhry FA.** Induction and targeting of the glutamine transporter SN1 to the basolateral membranes of cortical kidney tubule cells during chronic metabolic acidosis suggest a role in pH regulation. *J Am Soc Nephrol* 16: 869–877, 2005.
44. **Soutourina O, Cheval L, Doucet A.** Global analysis of gene expression in mammalian kidney. *Pflügers Arch* 450: 13–25, 2005.
45. **Stehberger PA, Schulz N, Finberg KE, Karet FE, Giebisch G, Lifton RP, Geibel JP, Wagner CA.** Localization and regulation of the ATP6V0A4 (a4) vacuolar H+-ATPase subunit defective in an inherited form of distal renal tubular acidosis. *J Am Soc Nephrol* 14: 3027–3038, 2003.
46. **Stehberger PA, Shmukler BE, Stuart-Tilley AK, Peters LL, Alper SL, Wagner CA.** Distal renal tubular acidosis in mice lacking the AE1 (band3) Cl^-/HCO_3^- exchanger (slc4a1). *J Am Soc Nephrol* 18: 1408–1418, 2007.
47. **Stuart RO, Bush KT, Nigam SK.** Changes in global gene expression patterns during development and maturation of the rat kidney. *Proc Natl Acad Sci USA* 98: 5649–5654, 2001.
48. **Tsuruoka S, Kittelberger AM, Schwartz GJ.** Carbonic anhydrase II and IV mRNA in rabbit nephron segments: stimulation during metabolic acidosis. *Am J Physiol Renal Physiol* 274: F259–F267, 1998.
49. **Verlander JW, Madsen KM, Cannon JK, Tisher CC.** Activation of acid-secreting intercalated cells in rabbit collecting duct with ammonium chloride loading. *Am J Physiol Renal Fluid Electrolyte Physiol* 266: F633–F645, 1994.
50. **Virlon B, Cheval L, Buhler JM, Billon E, Doucet A, Elalouf JM.** Serial microanalysis of renal transcriptomes. *Proc Natl Acad Sci USA* 96: 15286–15291, 1999.
51. **Winkler CA, Kittelberger AM, Schwartz GJ.** Expression of carbonic anhydrase IV mRNA in rabbit kidney: stimulation by metabolic acidosis. *Am J Physiol Renal Physiol* 272: F551–F560, 1997.
52. **Wright PA, Packer RK, Garcia-Perez A, Knepper MA.** Time course of renal glutamate dehydrogenase induction during NH4Cl loading in rats. *Am J Physiol Renal Fluid Electrolyte Physiol* 262: F999–F1006, 1992.

9.2 Renal phosphaturia during metabolic acidosis revisited: molecular mechanisms for decreased renal phosphate reabsorption

Marta Nowik, Nicolas Picard, Gerti Stange, Paola Capuano, Harriet S. Tenenhouse, Jürg Biber, Heini Murer, Carsten A. Wagner

Pflugers Arch, manuscript in press

Pflugers Arch - Eur J Physiol
DOI 10.1007/s00424-008-0530-5

TRANSPORT PHYSIOLOGY

Renal phosphaturia during metabolic acidosis revisited: molecular mechanisms for decreased renal phosphate reabsorption

Marta Nowik · Nicolas Picard · Gerti Stange · Paola Capuano · Harriet S. Tenenhouse · Jürg Biber · Heini Murer · Carsten A. Wagner

Received: 15 April 2008 / Accepted: 8 May 2008

Abstract During metabolic acidosis (MA), urinary phosphate excretion increases and contributes to acid removal. Two Na^+-dependent phosphate transporters, NaPi-IIa (Slc34a1) and NaPi-IIc (Slc34a3), are located in the brush border membrane (BBM) of the proximal tubule and mediate renal phosphate reabsorption. Transcriptome analysis of kidneys from acid-loaded mice revealed a large decrease in NaPi-IIc messenger RNA (mRNA) and a smaller reduction in NaPi-IIa mRNA abundance. To investigate the contribution of transporter regulation to phosphaturia during MA, we examined renal phosphate transporters in normal and Slc34a1-gene ablated (NaPi-IIa KO) mice acid-loaded for 2 and 7 days. In normal mice, urinary phosphate excretion was transiently increased after 2 days of acid loading, whereas no change was found in *Slc34a1−/−* mice. BBM Na/Pi cotransport activity was progressively and significantly decreased in acid-loaded KO mice, whereas in WT animals, a small increase after 2 days of treatment was seen. Acidosis increased BBM NaPi-IIa abundance in WT mice and NaPi-IIc abundance in WT and KO animals. mRNA abundance of NaPi-IIa and NaPi-IIc decreased during MA. Immunohistochemistry did not indicate any change in the localization of NaPi-IIa and NaPi-IIc along the nephron. Interestingly, mRNA abundance of both Slc20 phosphate transporters, Pit1 and Pit2, was elevated after 7 days of MA in normal and KO mice. These data demonstrate that phosphaturia during acidosis is not caused by reduced protein expression of the major Na/Pi cotransporters NaPi-IIa and NaPi-IIc and suggest a direct inhibitory effect of low pH mainly on NaPi-IIa. Our data also suggest that Pit1 and Pit2 transporters may play a compensatory role.

Keywords NaPi-IIa · NaPi-IIc · Pit1 · Pit2 · Phosphate · Metabolic acidosis

Electronic supplementary material The online version of this article (doi:10.1007/s00424-008-0530-5) contains supplementary material, which is available to authorized users.

M. Nowik · G. Stange · P. Capuano · J. Biber · H. Murer · C. A. Wagner (✉)
Institute of Physiology and Zurich Center for Human Integrative Physiology (ZHIP), University of Zurich,
Winterthurerstrasse 190,
8057 Zurich, Switzerland
e-mail: Wagnerca@access.uzh.ch

N. Picard
Institute of Anatomy, University of Zurich,
Zurich, Switzerland

H. S. Tenenhouse
Departments of Pediatrics and Human Genetics,
McGill University and Montreal Children's Hospital Research Institute, Montreal, QC, Canada

Introduction

Body inorganic phosphate (Pi) homeostasis is the product of intestinal absorption and renal excretion or reabsorption, respectively. The bulk of filtered phosphate is reabsorbed at the brush border membrane (BBM) of proximal tubular cells via action of sodium-dependent phosphate (Na/Pi) transporters, NaPi-IIa (Slc34a1) [23], and to a smaller extent, NaPi-IIc (Slc34a3) [30]. Abundance and activity of NaPi-IIa are regulated by a variety factors, including dietary Pi intake, parathyroid hormone, as well as other hormones [18, 22, 24], and FGF23 [21]. In contrast, less is known about the regulation of NaPi-IIc, which appears to be modulated by dietary phosphate intake, growth, and FGF-23 [26, 30–32]. Intestinal Pi absorption appears to be mediated by one

sodium-dependent cotransporter NaPi-IIb (Slc34a2) that may be also altered by dietary Pi intake, 1,25 (OH)2-dihydroxy-vitamin D3, and FGF-23 [8, 14, 28].

Recently, a different class (type III) of Na^+-dependent Pi transporters were identified in rat kidney: Pit1 (Glvr-1, Slc20a1) and Pit2 (Ram-1, Slc20a2) [15, 16]. Both Pit1 and Pit2 are widely distributed in many tissues, suggesting that they serve as housekeeping Na/Pi cotransporters in mammalian cells [15].The exact cellular and subcellular localization of Pit1 and Pit2 in the kidney remains to be determined, although in situ hybridization suggests expression along the proximal nephron [35].

The bulk of apical Na/Pi cotransport activity in the proximal tubule is accounted for by the type IIa Na/Pi cotransporter, as evident from murine NaPi-IIa gene ablation studies [3]. NaPi-IIc has been suggested to be growth-related and important only during weaning in rodents [30]. However, recent studies identified SLC34A3 mutations in patients with hereditary hypophosphatemic rickets with hypercalciuria, indicating that NaPi-IIc may play a more prominent role in maintaining body phosphate homeostasis than previously thought [4, 19].

During metabolic acidosis, phosphate is released from bone together with Ca^{2+} and carbonate [17] and is excreted into urine in large amounts [12]. Phosphate, together with ammonia and citrate, acts as so-called titratable acid that binds protons and increases the kidney's ability to excrete protons. Ambuhl et al. reported previously that induction of metabolic acidosis in a rat model caused massive downregulation of sodium-dependent phosphate transport activity in brush border membrane vesicles associated with reduced NaPi-IIa messenger RNA (mRNA) and protein abundance [1]. In contrast, we failed to find a clear reduction in brush border membrane Na^+/phosphate cotransport activity and NaPi-IIa expression both in rat and mouse kidney despite massive phosphaturia [33].

During complementary DNA (cDNA) microarray screening of mouse kidneys 2 and 7 days after the induction of metabolic acidosis, we found strong downregulation of NaPi-IIc mRNA abundance, which may contribute to the phosphaturia observed [25]. To further investigate the contribution of phosphate transporter regulation to phosphaturia, we induced metabolic acidosis for 2 and 7 days in C57BL/6 and NaPi-IIa KO mice and examined NaPi-IIa, NaPi-IIc, Pit1, and Pit2 mRNA expression, changes in NaPi-IIa and NaPi-IIc protein abundance, transport activity, and cotransporter localization.

Materials and methods

Animals

All experiments were performed on 12-week-old C57BL/6J and homozygous NaPi-IIa-deficient (*Slc34a1*−/−) male mice. The generation, breeding, and genotyping of these mice have been described previously [3]. All experiments were performed according to Swiss Animal Welfare laws and approved by the local veterinary authority (Veterinäramt Zürich).

Metabolic studies

To induce metabolic acidosis, male C57BL/6J and NaPi-IIa deficient mice were given 0.28 M NH_4Cl/ 2% sucrose in drinking water for 2 or 7 days. The control group received only 2% sucrose in drinking water for 7 days. Each group consisted of five animals for each time point, treatment, and genotype. Forty-eight hours prior to sacrifice, mice were housed in metabolic cages (single mouse metabolic cages, Tecniplast, Buguggiate, Italy) and had free access to standard mouse chow and drinking water ad libitum. Daily chow (standard rodent chow GLP3433, Kliba AG, Switzerland: 0.8 % phosphate, 1.05 % calcium, 0.2 % magnesium), water intake, and body weights were measured, and urine was collected under mineral oil. For the acute induction of metabolic acidosis, mice were trained over 5 days to receive food only for 6 h in the morning. Two days before the actual experiment, mice were adapted to metabolic cages. On the day of the experiment, mice received either standard chow or 2 g NH_4Cl/100g standard chow over a period of 6 h with free access to water. Urine was collected over 6h. Before and after the collection period, urinary bladders were emptied by abdominal massage. At the end of all metabolic cage experiments, mice were anesthetized with ketamine–xylazine, and heparinized mixed arterial-venous blood was collected and analyzed immediately for pH, blood gases, and electrolytes on a Radiometer ABL 800 (Radiometer, Copenhagen, Denmark) blood gas analyzer. Plasma was collected and frozen until further analysis. Both kidneys were harvested and rapidly frozen in liquid nitrogen and stored at −80°C.

Urinary pH was measured using a pH microelectrode (691 pH-meter, Metroholm). Urinary creatinine was measured by the Jaffe method [29]. Ammonium in urine was measured by the method of Berthelot [5]. Urine and plasma phosphate were measured using a commercial kit (Sigma Diagnostics, Munich, Germany). Urinary electrolytes (Na^+, K^+, Ca^{2+}, Mg^{2+}, Cl^-) were measured by ion chromatography (Metrohm ion chromatograph, Herisau, Switzerland).

RNA extraction and reverse transcription

Snap-frozen kidneys (five kidneys for each condition) were homogenized in RLT-Buffer (Qiagen, Basel, Switzerland) supplemented with β-mercaptoethanol to a final concentration of 1%. Total RNA was extracted from 200 μl aliquots

of each homogenized sample using the RNeasy Mini Kit (Qiagen) according to the manufacturer's instructions. Quality and concentration of the isolated RNA preparations were analyzed by the ND-1000 spectrophotometer (NanoDrop Technologies). Total RNA samples were stored at −80°C. Each RNA sample was diluted to 100 ng/μl and 3 μl used as a template for reverse transcription using the TaqMan Reverse Transcription Kit (Applied Biosystems, Forster City, CA, USA). For reverse transcription, 300 ng of RNA template were diluted in a 40-μl reaction mix that contained (final concentrations) RT buffer (1×), $MgCl_2$ (5.5mM), random hexamers (2.5 μM), RNase inhibitor (0.4U/μl), the multiscribe reverse transcriptase enzyme (1.25U/μl), dNTP mix (500 μM each), and RNase-free water.

Real-time quantitative PCR

Quantitative real-time qRT-PCR was performed on the ABI PRISM 7700 Sequence Detection System (Applied Biosystems). Primers for all genes of interest (Table 1) were designed using Primer Express software from Applied Biosystems. Primers were chosen to result in amplicons no longer than 150bp spanning intron-exon boundaries to exclude genomic DNA contamination. The specificity of all primers was first tested on mRNA derived from kidney and always resulted in a single product of the expected size (data not shown). Probes were labeled with the reporter dye FAM at the 5' end and the quencher dye TAMRA at the 3' end (Microsynth, Balgach, Switzerland). Real-Time PCR reactions were performed using TaqMan Universal PCR Master Mix (Applied Biosystems). Briefly, 3.5 μl cDNA, 1 μl of each primer (25 μM), 0.5 μl labeled probe (5 μM), 6.5 μl RNAse-free water, and 12.5 μl TaqMan Universal PCR Master Mix reached 25 μl of final reaction volume. Reaction conditions were denaturation at 95°C for 10 min followed by 40 cycles of denaturation at 95°C for 15s and annealing/elongation at 60°C for 60s with auto ramp time. All reactions were run in duplicate. For analyzing the data, the threshold was set to 0.06 as this value had been determined to be in the linear range of the amplification curves for all mRNAs in all experimental runs. The expression of gene of interest was calculated in relation to hypoxanthine guanine phosphoribosyl transferase (HPRT). Relative expression ratios were calculated as $R = 2^{(Ct(HPRT) - Ct(test\ gene)}$, where Ct represents the cycle number at the threshold 0.06.

BBM vesicles preparation

NH_4Cl-treated WT and KO mice were anesthetized with ketamine–xylazine intraperitoneally, and kidneys were removed and rapidly frozen in liquid nitrogen. Brush border membranes vesicles (BBMV) were prepared as described previously using the Mg^{2+}-precipitation technique [6, 7] and further used for western blotting and transport studies.

Table 1 Primers and probes used for quantitative real-time PCR

Gene	Acc. No.	Primers	Probe
NaPi-IIa (Slc34a1)	NM_011392	F: 5′-TGATCACCAGCATTGCCG-3′ (907–924) R: 5′-GTGTTTGCAAGGCTGCCG-3′ (1,022–1,039)	5′-CCAGACACAACAGAGGCTTCCACTTCTATGTC-3′ (975–1,006)
NaPi-IIc (Slc34a3)	NM_080854	F: 5′-TAATCTTCGCAGTTCAGGTTGCT-3′ (1,399–1,421) R: 5′-CAGTGGAATTGGCAGTCTCAAG-3′ (1,478–1,499)	5′-CCACTTCTTCTTCAACCTGGCTGGCATACT-3′ (1,427–1,456)
Pit-1 (Slc20a1)	NM_015747	F: 5′-CGC TGC TTT CTG GTA TTA TGT CTG-3′ (972,995) R: 5′-AGA GGT TGA TTC CGA TTG TGC A-3′ (1,085–1,106)	5′-TTG TTC GTG CGT TCA TCC TCC GTA AGG-3′ (1,011–1,037)
Pit-2 (Slc20a2)	NM_011394	F: 5′-AGG AGT GCA GTG GAT GGA GC-3′ (813–832) R: 5′-ATT AGT ATG AAC AGC ACG CCG G-3′ (887–908)	5′-ATT GTC GCC TCC TGG TTT ATA TCG CCA C-3′ (841–868)
HPRT	NM_013556	F: 5′TTATCAGACTGAAGAGCTACTGTAAGATC-3′ (442–471) R: 5′-TTACCAGTGTCAATTATATCTTCAACAATC-3′ (539–568)	5′-TGAGAGATCATCTCCACCAATAACTTTTATGTCCC-3′ (481–515)

All primers and probes were designed using Primer Express software (Applied Biosystems). The nucleotide numbers of the primers and probes are given in brackets.

Transport studies

The transport rate of phosphate into renal BBMV was determined at 30s and 120min (equilibrium value) as described [14] at 25°C in the presence of inward gradients of 100mM NaCl or 100mM KCl and 0.1mM K_2HPO_4. All measurements were performed in triplicates.

Western blot analysis

After measurement of the protein concentration (Bio-Rad, Hercules, CA, USA), 10 μg of brush border membrane proteins were solubilized in Laemmli sample buffer, (2 % 2-mercaptoethanol), and SDS-PAGE was performed on a 10 % polyacrylamide gel. For immunoblotting, the proteins were transferred electrophoretically to polyvinylidene fluoride membranes (Immobilon-P, Millipore, Bedford, MA, USA). After blocking with 5% milk powder in Tris-buffered saline/0.1% Tween-20 for 60 min, the blots were incubated with the primary antibodies: rabbit polyclonal anti-NaPi-IIa (1:6,000) [10], rabbit affinity-purified anti-NaPi-IIc (1:1,000) raised against the C-terminal amino acids 588–601 (NH_2–CYENPQVIASQQL–COOH; Pineda Antibody Services, Berlin, Germany) and mouse monoclonal anti-β-actin antibody (42kDa; Sigma, St. Louis, MO; 1:5,000) either for 2 h at room temperature or overnight at 4°C. The specificity of the NaPi-IIc antibody was tested by western blotting and immunohistochemistry (see supplementary Figs. 1 and 2). The membranes were then washed three times, blocked for 1 h, and again incubated for 1 h at room temperature with the secondary goat anti-rabbit or donkey anti-mouse antibodies 1:5,000 linked to alkaline phosphatase (Promega, USA). The protein signal was detected with the CDP Star chemiluminescence system (Roche Diagnostics, Basel, Switzerland) using the DIANA III-chemiluminescence detection system (Raytest, Straubenhardt, Germany). All images were analyzed using appropriate software (Advanced Image Data Analyser AIDA, Raytest) to calculate the protein of interest/β-actin ratio.

Immunohistochemistry

Mouse kidneys were perfusion-fixed through the right ventricle with a fixative solution, and subsequent immunohistochemistry was performed as described previously [11]. Serial cryosections (5 μm) were taken and incubated at 4°C overnight with a rabbit anti NaPi-IIa 1:1,000 as described previously [10] or immunopurified rabbit anti NaPi-IIc 1:1,500. The specificity of the immunopurified anti-NaPi-IIc antibody was characterized as shown in the supplementary figures (supplementary Fig. 2). Binding sites of the primary antibodies were detected using Alexa 555-conjugated goat/anti-rabbit antibodies (Invitrogen, Basel, Switzerland). F-actin was visualized using fluorescein-coupled phalloidin (Invitrogen, Basel, Switzerland). Sections were studied by epifluorescence with a Polyvar microscope (Reichert Jung, Vienna, Austria), and digital images were acquired with a charged coupled device camera.

Statistical analysis

Results are expressed as mean ± SEM. All data were tested for significance using the ANOVA and unpaired Student's test where appropriate. Only values with $p < 0.05$ were considered as significant.

Results

Induction of metabolic acidosis

NH_4Cl-induced metabolic acidosis was achieved after 48h and 7 days in both WT and NaPi-IIa KO mice, as evident from the reduction in blood pH and bicarbonate concentration and the increase in serum chloride concentration (Table 2). Urinary pH was decreased only in NH_4Cl-loaded WT mice. In NaPi-IIa-deficient animals, urine pH, which was significantly lower than that of WT mice under control conditions (5.27 ± 0.07 vs. 6.85 ± 0.30, respectively), was not changed by NH_4Cl treatment (Table 2). Urinary ammonium excretion was increased in WT and KO acid-loaded animals. As expected, the plasma phosphate concentration was lower in NaPi-IIa KO mice compared to WT mice under all conditions examined; however, metabolic acidosis did not significantly affect blood Pi concentration either in WT or in KO animals (Table 2). Urinary Pi excretion was higher in KO mice compared to WT mice under all conditions examined and was further increased only in WT animals after 2 days of NH_4Cl loading (Table 2; Fig. 1). In KO animals, acid loading reduced renal phosphate excretion non-significantly. Metabolic acidosis was more pronounced in animals receiving NH_4Cl for 2 days, as evident from blood pH and plasma bicarbonate concentrations, indicating partial adaptation of these animals to acid-base disturbances after 7 days of acid loading (Table 2).

Acidosis alters mRNA expression of renal Na^+/phosphate cotransporters

To investigate the effect of metabolic acidosis on mRNA expression of renal phosphate transporters, real-time quantitative RT-PCR was performed for NaPi-IIa, NaPi-IIc, Pit1, and Pit2 and the housekeeping gene HPRT. Induction of metabolic acidosis with NH_4Cl resulted in a decrease in renal NaPi-IIa mRNA abundance in WT mice after 2 days but not after 7 days (Fig. 2a). In contrast, a strong decrease in the

Table 2 Summary of blood and urine data from WT and NaPi-IIa KO mice under control conditions and after 2 or 7 days oral acid loading (0.28M NH_4Cl + 2% sucrose in drinking water)

	CBL57/6 WT			NaPi-IIa KO		
	Control	2 days acidosis	7 days acidosis	Control	2 days acidosis	7 days acidosis
Blood						
pH	7.18 ± 0.03	6.99 ± 0.02*	7.12 ± 0.04	7.20 ± 0.03	7.04 ± 0.05*	7.12 ± 0.03
pCO_2 (mmHg)	40.7 ± 0.5	34.0 ± 0.9***	36.7 ± 0.7**	42.3 ± 1.8	39.0 ± 1.8	35.4 ± 2.7
[HCO_3^-] (mM)	14.0 ± 0.9	8.2 ± 0.3*	11.5 ± 0.9	15.7 ± 1.3	10.5 ± 1.7*	10.9 ± 0.8
[Na^+] (mM)	151.2 ± 1.0	150.0 ± 1.1	148.2 ± 1.9	147.8 ± 1.5	156.6 ± 1.8*	158.4 ± 2.8**##
[K^+] (mM)	6.8 ± 0.5	7.3 ± 0.4	7.1 ± 0.3	6.6 ± 0.2	7.0 ± 0.5	6.3 ± 0.3
[Cl^-] mM	114.8 ± 1.0	128.5 ± 1.4***	125.6 ± 0.4**	118.6 ± 2.2	128.6 ± 1.9**	143.8 ± 2.7***###
[Pi] (mM)	3.2 ± 0.2	3.1 ± 0.1	3.0 ± 0.2	2.4 ± 0.6#	1.9 ± 0.2#	2.3 ± 0.1#
Urine						
pH	6.85 ± 0.30	5.46 ± 0.02***	5.47 ± 0.02***	5.27 ± 0.07###	5.39 ± 0.03	5.16 ± 0.03
Creatinine (mg/dl)	25.2 ± 2.3	57.7 ± 2.0**	60.6 ± 3.3***	47.1 ± 5.0#	50.3 ± 6.6	54.5 ± 7.5
NH_3/NH_4^+/(mM)/crea (mg/dl)	0.8 ± 0.3	6.3 ± 0.7***	7.2 ± 0.4***	1.2 ± 0.7	7.1 ± 1.1***	6.7 ± 0.8 ***
Na^+ (mM)/crea (mg/dl)	2.6 ± 0.2	3.2 ± 0.2	3.0 ± 0.2	1.8 ± 0.2	1.7 ± 0.2###	1.6 ± 0.2###
K^+ (mM)/crea (mg/dl)	5.4 ± 0.2	7.4 ± 0.4	6.5 ± 0.3	5.1 ± 0.5	4.2 ± 0.7 ###	4.9 ± 0.4
Ca^{2+} (mM)/crea (mg/dl)	0.06 ± 0.03	0.12 ± 0.02	0.07 ± 0.01	0.33 ± 0.05##	0.26 ± 0.05	0.29 ± 0.07#
Mg^{2+} (mM)/crea (mg/dl)	0.31 ± 0.11	0.71 ± 0.05*	0.68 ± 0.02*	0.76 ± 0.08##	0.57 ± 0.10	0.56 ± 0.06
Cl^- (mM)/crea (mg/dl)	3.8 ± 0.3	11.9 ± 0.1***	13.9 ± 0.9***	3. ± 0.3	10.3 ± 1.4***	11.2 ± 1.2***
Pi (mM)/crea (mg/dl)	0.31 ± 0.07	0.61 ± 0.09*	0.34 ± 0.05	1.36 ± 0.06###	1.06 ± 0.10##	1.52 ± 0.16###
24 h Pi (μmol/l)	23.8 ± 3.2	55.2 ± 10.3*	27. ± 4.1	129.2 ± 18.1###	87.7 ± 14.2	93.3 ± 9.3##
Urine volume (ml)	3.4 ± 0.5	1.6 ± 0.1	1.3 ± 0.1	2.1 ± 0.3	1.8 ± 0.4	1.4 ± 0.4
Food intake (mg/g BW)	0.15 ± 0.01	0.11 ± 0.01	0.13 ± 0.01	0.14 ± 0.01	0.07 ± 0.02	0.08 ± 0.0

All data are presented as mean ± SEM, $n = 5$ per group. *$p < 0.05$, **$p < 0.01$, ***$p < 0.001$; # significantly different between WT and KO (#$p < 0.05$, ##$p < 0.01$, ###$p < 0.001$)

relative mRNA abundance of NaPi-IIc was evident in both WT and KO mice after 2 and 7 days (Fig. 2b). Under control conditions, NaPi-IIc mRNA expression was 2-fold higher in KO mice compared to WT animals. Metabolic acidosis resulted in increased mRNA expression of Pit1, which reached significance in WT and KO mice only after 7 days of acid loading (Fig. 2c). mRNA abundance of Pit2 was not affected by NH_4Cl treatment in WT mice and increased after 7 days of metabolic acidosis in NaPi-IIa KO mice (Fig. 2d).

Metabolic acidosis increases protein expression of renal Na^+/phosphate cotransporters

Western blotting of brush border membranes prepared from kidneys of control and acid-loaded mice demonstrated that in contrast to mRNA expression, NH_4Cl loading resulted in a greater abundance of both NaPi-IIa and NaPi-IIc, immunoreactive protein in WT mice after 2 and 7 days of treatment (Fig. 3). In NaPi-IIa KO mice expression of NaPi-IIc was elevated only after 2 days acid loading and returned to normal values after 7 days (Fig. 3). Effects of NH_4Cl loading on Pit1 and Pit2 protein abundance could not be investigated due to the lack of specific antibodies against these two transporters.

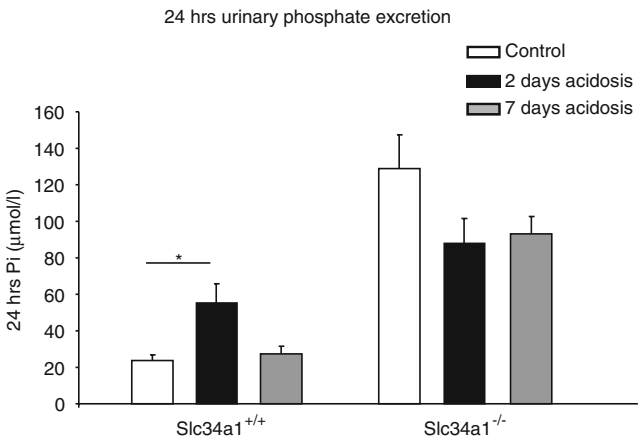

Fig. 1 Renal phosphate excretion during metabolic acidosis. Urine was collected over 24 h in metabolic cages from wild-type (*Slc34a1*+/+) control mice and mice receiving NH_4Cl for 2 or 7 days. Mice deficient for NaPi-IIa (*Slc34a1*−/−) were treated in parallel. Acid loading increased 24 h urinary phosphate excretion in wild-type mice after 2 days, but no effect was observed after 7 days. *Slc34a1*−/− mice had higher 24-h phosphate excretion, which was non-significantly reduced by acid loading for 2 or 7 days ($n = 5$ animals/group). All data are presented as mean ± SEM ($n = 5$). *$p < 0.05$

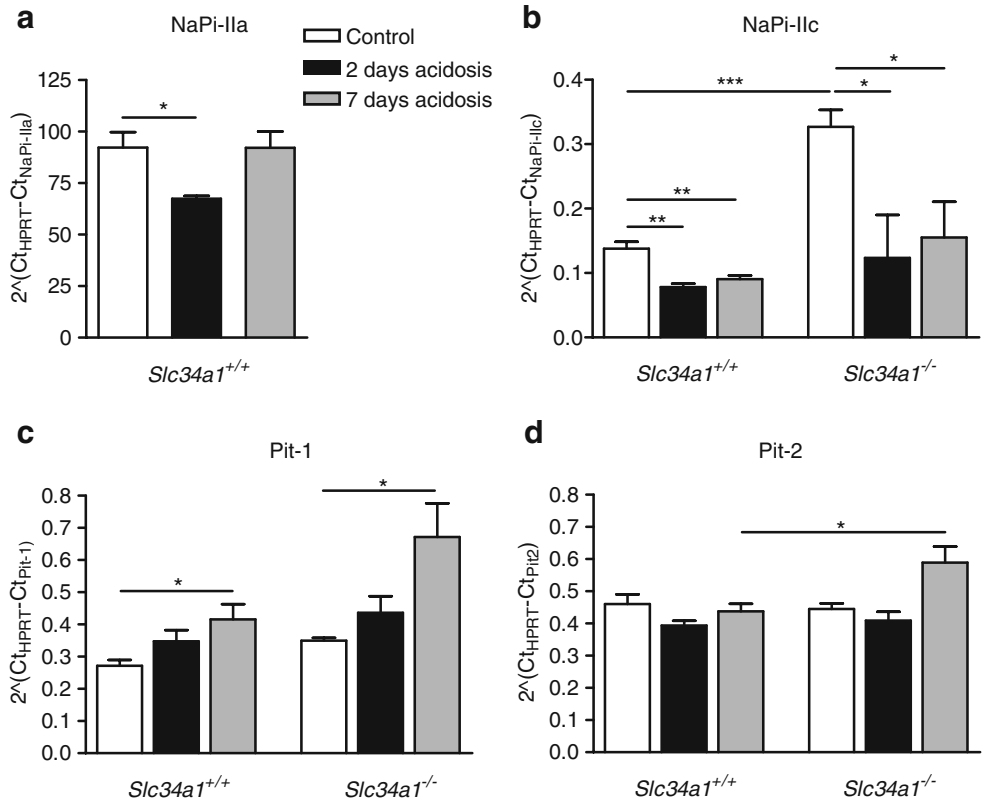

Fig. 2 Expression of genes encoding renal phosphate transporters. Real-time RT-PCR was used to assess NaPi-IIa, NaPi-IIc, Pit1, and Pit2 mRNA levels in kidneys from control and NH_4Cl-loaded animals (n = 5/group). **a** NaPi-IIa mRNA expression significantly decreased after 2 days acid loading and returned to normal values after 7 days. **b** NaPi-IIc mRNA expression decreased in normal and NaPi-IIa-deficient mice during MA. Under control conditions, NaPi-IIc expression was 2-fold higher in NaPi-IIa-deficient mice compared to wild-type animals. Expression of Pit1 was higher in the absence of NaPi-IIa and increased in both wild-type and *Slc34a1−/−*mice only after 7 days NH_4Cl loading (**c**), whereas Pit2 expression was not affected by acidosis in wild-type mice but increased after 7 days NH_4Cl loading in NaPi-IIa deficient mice (**d**). All data are presented as mean ± SEM (n = 5). *$p < 0.05$, **$p < 0.01$, ***$p < 0.001$

Metabolic acidosis affects brush border membrane Na/Pi cotransport activity

Sodium-dependent phosphate uptake was increased after 2 days of H_4Cl loading in BBMV from wild-type mice with metabolic acidosis and returned to normal values after 7 days (Fig. 4a). In contrast, in NaPi-IIa-deficient mice, sodium-dependent phosphate transport was progressively and significantly decreased in both acid-loaded KO mouse groups (Fig. 4b).

Metabolic acidosis does not alter distribution of renal Na^+/phosphate cotransporters

Immunohistochemistry was used to determine whether metabolic acidosis altered segmental and/or subcellular distribution of renal Na^+-dependent phosphate cotransporters NaPi-IIa and NaPi-IIc [20, 26, 30, 32]. Under standard dietary conditions, NaPi-IIa is expressed in convoluted (S1 + S2) and straight (S3) proximal tubules of superficial and juxtamedullary nephrons, whereas the expression of NaPi-IIc is restricted to the renal cortex in the S1 segment of deep and superficial proximal tubule (Fig. 5). The apparent renal distribution of NaPi-IIa and NaPi-IIc was not changed during metabolic acidosis in WT animals treated for 2 or 7 days. We also were not able to detect major signal intensity changes during acid loading in the kidneys of these animals (Fig. 5a and b). In NaPi-IIa $^{-/-}$ mice, NaPi-IIc was localized to apical brush border membranes of proximal S1 segments (Fig. 5c). Furthermore, the signal intensity of NaPi-IIc staining was stronger in superficial S1 proximal tubules than in wild-type animals (Fig. 5a vs. c). In addition, few S2 proximal tubules are expressed NaPi-IIc in NaPi-IIa $^{-/-}$ mice. Acidosis treatment for 2 or 7 days in these animals did not induce any change in NaPi-IIc signal intensity or its cortical distribution (Fig. 5c).

Effect of acute metabolic acidosis

We examined the effect of acute metabolic acidosis to determine whether direct interactions between protons and the phosphate transporters could reduce renal phosphate

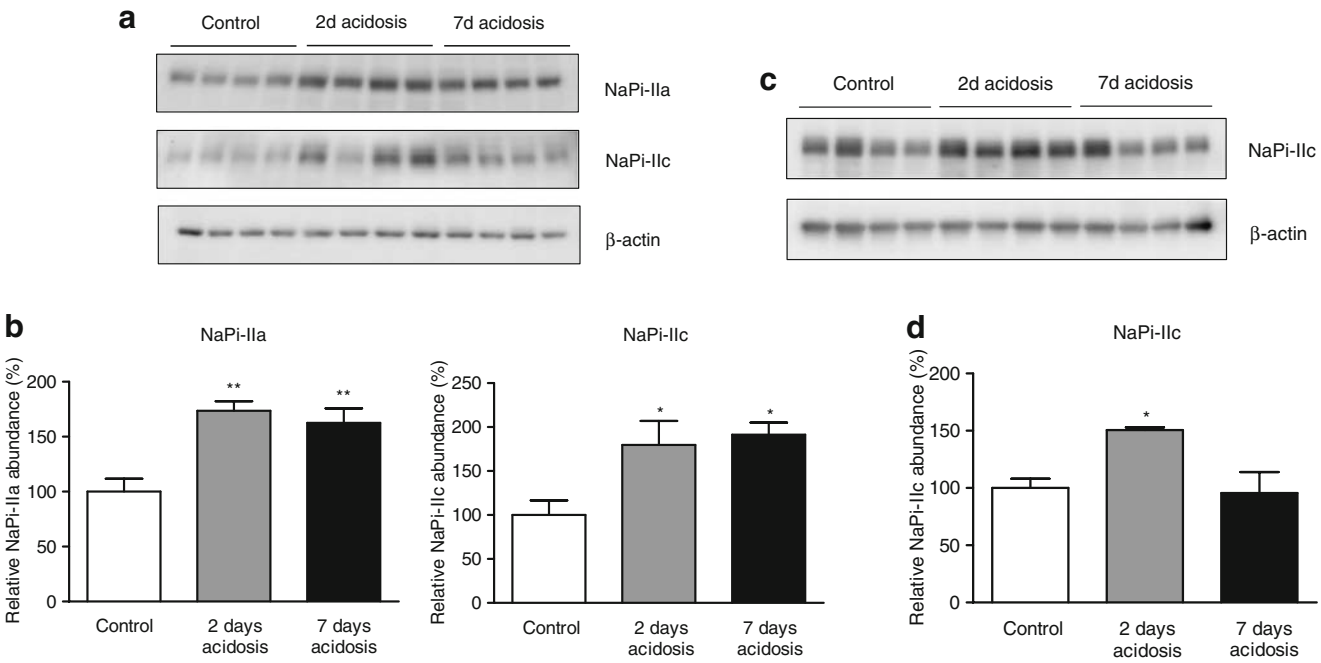

Fig. 3 Expression of NaPi-IIa and NaPi-IIc proteins during acid loading. **a** Immunoblotting for the Na^+/phosphate cotransporters NaPi-IIa and NaPi-IIc in brush border membranes from control and acid-loaded mice. All membranes were reprobed for β-actin. **b** Bar graphs summarizing data from immunoblotting. All data were normalized against β-actin, mean ± SEM (n = 5). Protein abundance of NaPi-IIa and NaPi-IIc was higher in wild-type mice after acid loading for 2 and 7 days. **c** In NaPi-IIa-deficient mice, NaPi-IIc expression increased only after 2 days NH_4Cl loading and normalized after 7 days. **d** Relative NaPi-Iic expression data in Slc34a3$^{-/-}$ mice. All data were normalized against β-actin, mean ± SEM (n = 5). *p < 0.05, **p < 0.01

reabsorption and thereby contribute to phosphaturia. The induction of acute metabolic acidosis was confirmed by the presence of lower blood pH and bicarbonate concentration, lower urine pH, and higher urinary ammonium excretion. Acute acidosis was also associated with significantly elevated urinary phosphate excretion (Table 3, Fig. 6a). However, NaPi-IIa and NaPi-IIc protein abundance in the brush border membrane fraction remained unchanged (Fig. 6b).

Discussion

Metabolic acidosis is associated with and causes increased renal acid elimination that requires adaptive changes in metabolic and transport pathways. Phosphate, working as a buffer in blood and as titratable acid in urine, greatly contributes to increased renal acid secretion [18], and its excretion into urine is elevated during MA. Previous transcriptome analysis of kidneys from acid-loaded mice

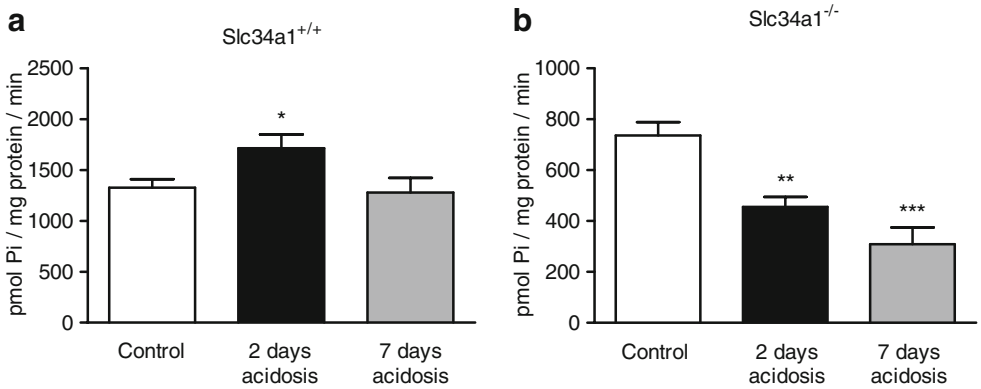

Fig. 4 BBM sodium-dependent phosphate (Na/Pi) transport activity in wild-type and NaPi-IIa-deficient mice. Na/Pi cotransport was determined by sodium-dependent ^{32}P-uptake in BBMV. **a** NH_4Cl loading reduced Na/Pi transport activity in BBMV from normal mice after 2 days but not after 7 days. **b** In NaPi-IIa-deficient mice, MA resulted in a significant decrease in Na/Pi cotransport activity after 2 and 7 days. n=5 per group. *p<0.05, **p<0.01, ***p<0.001

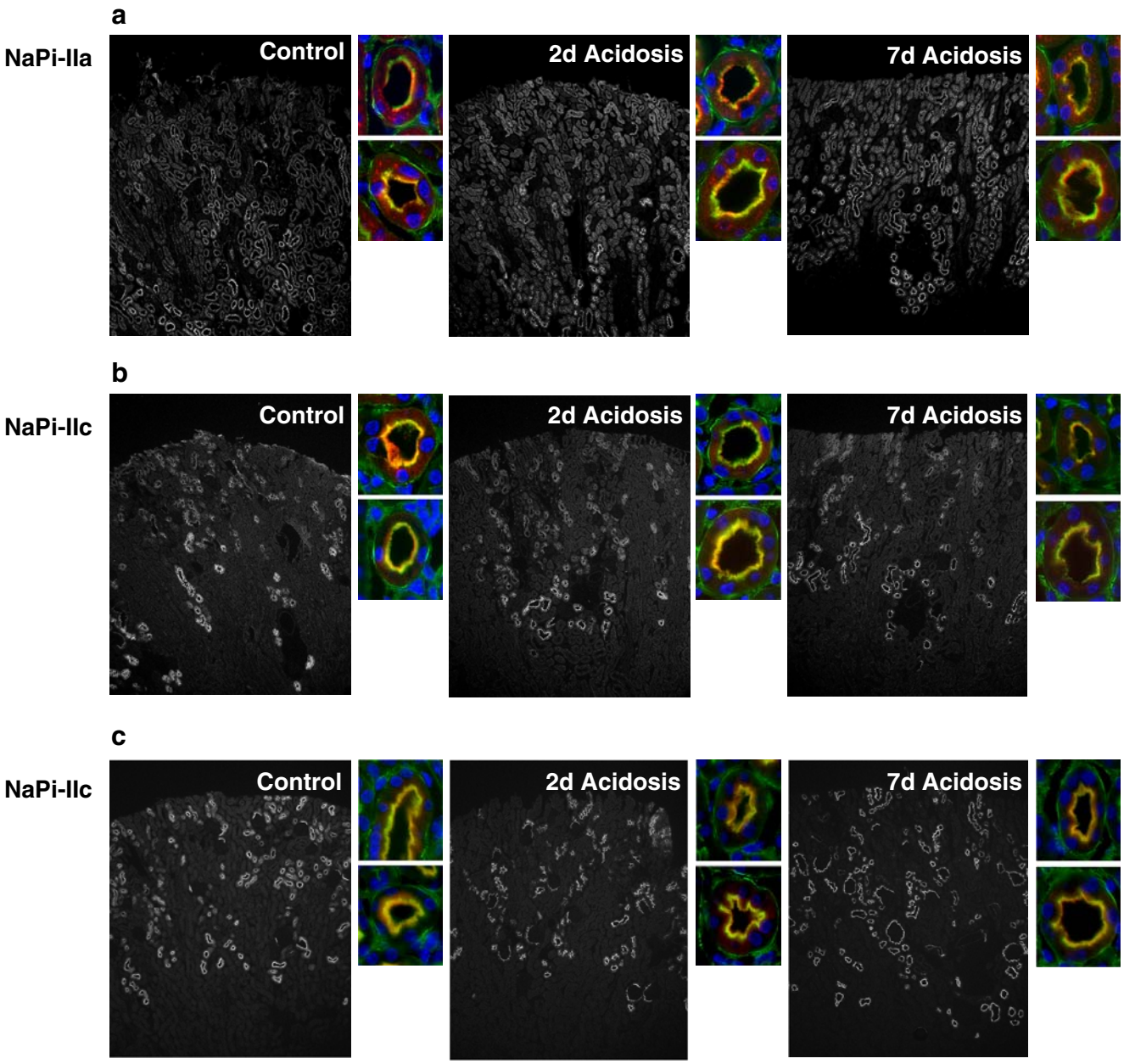

Fig. 5 Immunolocalization of type II Na/Pi cotransporters in kidneys from wild-type and NaPi-IIa-deficient mice after 2 and 7 days acid loading. NaPi-IIa (**a**) or NaPi-IIc (**b** and **c**) stainings on renal cortical overviews and single S1 proximal tubules (higher magnification) from wild-type (**a** and **b**) and NaPi-IIa-deficient mice (**c**) during acid loading. No difference in the localization of either NaPi-IIa or NaPi-IIc were detected in WT and NaPi-IIa-deficient mice after 2 and 7 days of acid loading

revealed a robust downregulation of the type IIc Na^+/Pi cotransporter NaPi-IIc mRNA [25], suggesting that it may be responsible for the phosphaturia observed.

In the present study, we analyzed the regulation of all known renal sodium-dependent phosphate cotransporters, namely, the type II NaPi-IIa and NaPi-IIc and the type III Pit1 and Pit2. NaPi-IIa-deficient mice served as an additional tool to distinguish between type IIa-dependent and IIa-independent transport activities in vivo and ex vivo and to test the contribution of renal mechanisms to acidosis-induced phosphaturia. Our findings demonstrate that during NH_4Cl-induced metabolic acidosis in mouse, (1) phosphaturia is only transient in wild-type mice and no acid-induced phosphaturia was observed in NaPi-IIa-deficient mice, (2) sodium-dependent phosphate transport activity is transiently increased in BBMV from wild-type mice and decreased in BBMV from NaPi-IIa deficient mice, (3) NaPi-IIa and NaPi-IIc protein are upregulated in wild-type mice and NaPi-IIc protein in KO mice, (4) NaPi-IIc mRNA is strongly reduced, (5) renal localization of NaPi-IIa and

Table 3 Summary of selected urine and blood values from mice receiving standard chow or NH_4Cl in food over a period of 6 hours

	Control	NH_4Cl in food
Blood		
pH	7.18 ± 0.01	6.97 ± 0.05**
$[HCO_3^-]$ (mM)	24.6 ± 1.0	13.4 ± 0.9 ***
[Pi] (mM)	2.60 ± 0.17	3.24 ± 0.27
Urine		
pH	5.95 ± 0.07	5.65 ± 0.03**
Creatinine (mg/dl)	62.8 ± 6.2	31.8 ± 2.5**
NH_3/NH_4^+/(mM)/crea (mg/dl)	1.4 ± 0.3	5.7 ± 0.3***
Pi (mM)/crea (mg/dl)	1.77 ± 0.16	2.80 ± 0.24**
6h Pi (μmol/l)	36.2 ± 3.9	51.4 ± 6.2*
Urine volume (ml/6h)	0.34 ± 0.04	0.59 ± 0.7*

All data are presented as mean ± SEM, n = 5 per group.
*$p < 0.05$; **$p < 0.01$; ***$p < 0.001$

NaPi-IIc is not affected, (6) phosphaturia in mice following induction of acute metabolic acidosis was not associated with changes in the abundance of the type IIa and IIc phosphate cotransporters in the brush border membrane, and (7) Pit1 and Pit2 mRNA are increased after 7 days.

Phosphaturia during metabolic acidosis has been attributed mainly to the release of phosphate from bone and subsequent renal excretion [17]. However, several causes may underlie phosphaturia independent from renal phosphate transporter protein abundance. The present demonstration that acidosis-induced phosphaturia is not observed in NaPi-IIa-deficient mice may suggest that phosphaturia in normal mice can be ascribed to decreased renal phosphate reabsorption via NaPi-IIa rather than originating from bone release. However, NaPi-IIa is also expressed in osteoclasts [13], and it has been suggested that NaPi-IIa-deficient osteoclasts are less active in bone resorption, which may also contribute to the reduced phosphaturia in acid-loaded KO mice. A third mechanism that may also contribute to the acidosis-induced phosphaturia is the direct interaction of protons with the phosphate transporter(s) in the brush border membrane of the proximal tubule. Amstutz et al. have demonstrated in rat isolated brush border membrane vesicles that a reduction in extracellular pH causes a decrease in sodium-dependent phosphate transport [2]. The function of the cloned and heterologously expressed type NaPi-IIa cotransporter is decreased by increasing extracellular proton concentrations, which interfere at

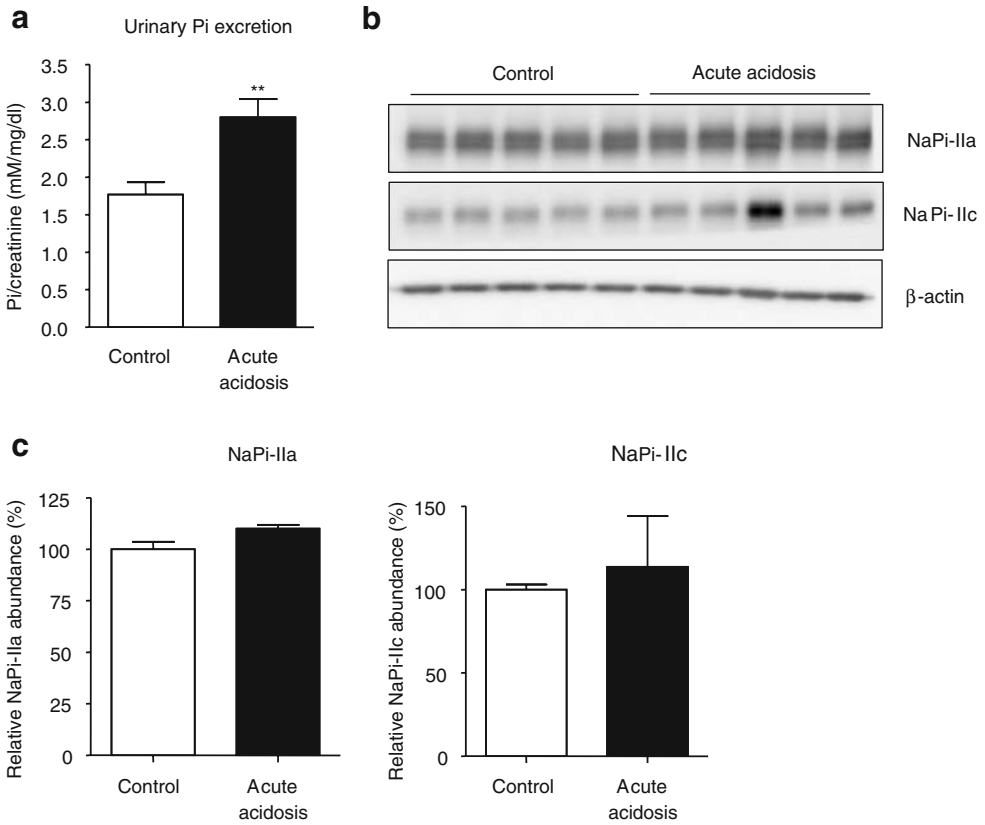

Fig. 6 Effects of acute metabolic acidosis. **a** Urinary phosphate excretion was increased during acute metabolic acidosis. **b** Western blotting for NaPi-IIa and NaPi-IIc abundance in brush border membranes from control and acidotic mice. All membranes were reprobed for β-actin. **c** Quantification of NaPi-IIa/β-actin and NaPi-IIc/β-actin ratios, n=5 for each group. All data are presented as mean ± SEM (n=5). **p<0.01

multiple stages of the transport cycle [9, 36]. Similarly, transport activity of mouse NaPi-IIc has been shown to be decreased by increasing extracellular proton concentrations from pH 7.5 to pH 6.5 [26]. The finding that acutely induced metabolic acidosis elicits phosphaturia without altering the abundance of brush border membrane NaPi-IIa and NaPi-IIc proteins supports the hypothesis that direct inhibition of transport activity contributes to the development of phosphaturia.

In contrast to the present findings, a previous study linked metabolic acidosis-induced phosphaturia to decreased activity and abundance of the renal Na^+/Pi cotransporter NaPi-IIa in rat kidney [1]. However, a subsequent study performed both in mouse and rat kidney could not confirm these observations and reported additionally elevated expression of the intestinal Na^+/Pi cotransporter NaPi-IIb [33]. Our data are in good agreement with the latter study, demonstrating that both transport activity and NaPi-IIa and NaPi-IIc protein abundance in the brush border membrane are increased during metabolic acidosis. Interestingly, mRNA levels of NaPi-IIa are reduced slightly after 2 days of acidosis, and NaPi-IIc mRNA expression is strongly decreased during metabolic acidosis. Similar discrepancies between NaPi-IIa mRNA expression, protein abundance, and transport activity have been observed in potassium-depleted rats [37]. There, changes in BBM lipid composition and fluidity were found to be linked to altered transport activity [37]. Also. Tenenhouse and colleagues observed the unexpected down-regulation of NaPi-IIc mRNA together with elevation of protein abundance in NaPi-IIa KO mice [34]. Thus, further investigation is required to delineate the underlying mechanism for the lack of concordance between cotransporter mRNA and protein abundance. Interestingly, we also observed the regulation of two additional sodium-dependent phosphate cotransporters, Pit1 and Pit2, at the mRNA level following the induction of metabolic acidosis. Pit1 and Pit2 mRNA were elevated after 7 days of metabolic acidosis, suggesting that both transporters could contribute to renal phosphate reabsorption. However, the exact localization of both transporters in kidney is not well studied. In situ hybridization for Pit1 (previously known as Glvr-1) described localization of Pit1 in most mouse kidney structures [35]. Interestingly, the transport activity of both Pit-1 and Pit-2 appears to be increased by extracellular acidification [15, 27].

In summary, we reanalyzed the regulation of renal sodium-phosphate cotransporters in mouse kidney during metabolic acidosis. Our data indicate that phosphaturia during metabolic acidosis cannot be explained by down-regulation of protein expression of luminal phosphate cotransporters. In contrast, we found evidence for increased renal expression of NaPi-IIa and NaPi-IIc proteins and Pit1 and Pit2 mRNAs. Thus, phosphaturia may be induced rather by direct interactions between protons and phosphate cotransporters IIa and IIc, thereby reducing transport activity. The role of skeletal phosphate release and increased delivery to the kidney may be less important than previously suggested.

Acknowledgments M. Nowik is the recipient of a PhD student fellowship from the Zurich Center for Integrative Human Physiology. This study was supported by grants from the Swiss National Science Research Foundation to J. Biber and H. Murer (31-65397.01) and C. A. Wagner (31-109677/1) and the 6th EU Frame work project EuReGene to J. Biber, H. Murer, and C. A. Wagner. The use of the ZIHP Core Facility for Rodent Physiology is gratefully acknowledged.

References

1. Ambuhl PM, Zajicek HK, Wang H, Puttaparthi K, Levi M (1998) Regulation of renal phosphate transport by acute and chronic metabolic acidosis in the rat. Kidney Int 53:1288–1298
2. Amstutz M, Mohrmann M, Gmaj P, Murer H (1985) Effect of pH on phosphate transport in rat renal brush border membrane vesicles. Am J Physiol 248:F705–F710
3. Beck L, Karaplis AC, Amizuka N, Hewson AS, Ozawa H, Tenenhouse HS (1998) Targeted inactivation of Npt2 in mice leads to severe renal phosphate wasting, hypercalciuria, and skeletal abnormalities. Proc Natl Acad Sci U SA 95:5372–5377
4. Bergwitz C, Roslin NM, Tieder M, Loredo-Osti JC, Bastepe M, Abu-Zahra H, Frappier D, Burkett K, Carpenter TO, Anderson D, Garabedian M, Sermet I, Fujiwara TM, Morgan K, Tenenhouse HS, Juppner H (2006) SLC34A3 mutations in patients with hereditary hypophosphatemic rickets with hypercalciuria predict a key role for the sodium-phosphate cotransporter NaPi-IIc in maintaining phosphate homeostasis. Am J Hum Genet 78:179–192
5. Berthelot M (1859) Violet d'aniline. Rep Chim App 1:284
6. Biber J, Stieger B, Haase W, Murer H (1981) A high yield preparation for rat kidney brush border membranes. Different behaviour of lysosomal markers. Biochim Biophys Acta 647:169–176
7. Biber J, Stieger B, Stange G, Murer H (2007) Isolation of renal proximal tubular brush-border membranes. Nature protocols 2:1356–1359
8. Brown AJ, Finch J, Slatopolsky E (2002) Differential effects of 19-nor-1,25-dihydroxyvitamin D(2) and 1,25-dihydroxyvitamin D (3) on intestinal calcium and phosphate transport. J Lab Clin Med 139:279–284
9. Busch AE, Wagner CA, Schuster A, Waldegger S, Biber J, Murer H, Lang F (1995) Properties of electrogenic Pi transport by a human renal brush border Na+/Pi transporter. J Am Soc Nephrol 6:1547–1551
10. Custer M, Lotscher M, Biber J, Murer H, Kaissling B (1994) Expression of Na-P(i) cotransport in rat kidney: localization by RT-PCR and immunohistochemistry. Am J Physiol 266:F767–F774
11. Dawson TP, Gandhi R, Le Hir M, Kaissling B (1989) Ecto-5′-nucleotidase: localization in rat kidney by light microscopic histochemical and immunohistochemical methods. J Histochem Cytochem 37:39–47
12. Guntupalli J, Eby B, Lau K (1982) Mechanism for the phosphaturia of NH4Cl: dependence on acidemia but not on diet PO4 or PTH. Am J Physiol 242:F552–F560

13. Gupta A, Tenenhouse HS, Hoag HM, Wang D, Khadeer MA, Namba N, Feng X, Hruska KA (2001) Identification of the type II Na(+)-Pi cotransporter (Npt2) in the osteoclast and the skeletal phenotype of Npt2−/− mice. Bone 29:467–476
14. Hattenhauer O, Traebert M, Murer H, Biber J (1999) Regulation of small intestinal Na–P(i) type IIb cotransporter by dietary phosphate intake. Am J Physiol 277:G756–G762
15. Kavanaugh MP, Kabat D (1996) Identification and characterization of a widely expressed phosphate transporter/retrovirus receptor family. Kidney Int 49:959–963
16. Kavanaugh MP, Miller DG, Zhang W, Law W, Kozak SL, Kabat D, Miller AD (1994) Cell-surface receptors for gibbon ape leukemia virus and amphotropic murine retrovirus are inducible sodium-dependent phosphate symporters. Proc Natl Acad Sci U S A 91:7071–7075
17. Lemann J Jr., Bushinsky DA, Hamm LL (2003) Bone buffering of acid and base in humans. Am J Physiol Renal Physiol 285:F811–F832
18. Levi M, Lotscher M, Sorribas V, Custer M, Arar M, Kaissling B, Murer H, Biber J (1994) Cellular mechanisms of acute and chronic adaptation of rat renal P(i) transporter to alterations in dietary P(i). Am J Physiol 267:F900–F908
19. Lorenz-Depiereux B, Benet-Pages A, Eckstein G, Tenenbaum-Rakover Y, Wagenstaller J, Tiosano D, Gershoni-Baruch R, Albers N, Lichtner P, Schnabel D, Hochberg Z, Strom TM (2006) Hereditary hypophosphatemic rickets with hypercalciuria is caused by mutations in the sodium-phosphate cotransporter gene SLC34A3. Am J Hum Genet 78:193–201
20. Madjdpour C, Bacic D, Kaissling B, Murer H, Biber J (2004) Segment specific expression of sodium-phosphate cotransporters NaPi-IIa and -IIc and interacting proteins in mouse renal proximal tubules. Pflugers Arch 448:402–410
21. Miyamoto K, Ito M, Kuwahata M, Kato S, Segawa H (2005) Inhibition of intestinal sodium-dependent inorganic phosphate transport by fibroblast growth factor 23. Ther Apher Dial 9:331–335
22. Murer H, Forster I, Biber J (2004) The sodium phosphate cotransporter family SLC34. Pflugers Arch 447:763–767
23. Murer H, Hernando N, Forster I, Biber J (2003) Regulation of Na/Pi transporter in the proximal tubule. Annu Rev Physiol 65:531–542
24. Murer H, Hernando N, Forster I, Biber J (2000) Proximal tubular phosphate reabsorption: molecular mechanisms. Physiol Rev 80:1373–1409
25. Nowik M, Lecca MR, Velic A, Rehrauer H, Brandli AW, Wagner CA (2008) Genome-wide gene expression profiling reveals renal genes regulated during metabolic acidosis. Physiol Genomics 32:322–334
26. Ohkido I, Segawa H, Yanagida R, Nakamura M, Miyamoto K (2003) Cloning, gene structure and dietary regulation of the type-IIc Na/Pi cotransporter in the mouse kidney. Pflugers Arch 446:106–115
27. Olah Z, Lehel C, Anderson WB, Eiden MV, Wilson CA (1994) The cellular receptor for gibbon ape leukemia virus is a novel high affinity sodium-dependent phosphate transporter. J Biol Chem 269:25426–25431
28. Radanovic T, Wagner CA, Murer H, Biber J (2005) Regulation of intestinal phosphate transport. I. Segmental expression and adaptation to low-P(i) diet of the type IIb Na(+)-P(i) cotransporter in mouse small intestine. Am J Physiol Gastrointest Liver Physiol 288:G496–G500
29. Seaton B, Ali A (1984) Simplified manual high performance clinical chemistry methods for developing countries. Med Lab Sci 41:327–336
30. Segawa H, Kaneko I, Takahashi A, Kuwahata M, Ito M, Ohkido I, Tatsumi S, Miyamoto K (2002) Growth-related renal type II Na/Pi cotransporter. J Biol Chem 277:19665–19672
31. Segawa H, Kawakami E, Kaneko I, Kuwahata M, Ito M, Kusano K, Saito H, Fukushima N, Miyamoto K (2003) Effect of hydrolysis-resistant FGF23-R179Q on dietary phosphate regulation of the renal type-II Na/Pi transporter. Pflugers Arch 446: 585–592
32. Segawa H, Yamanaka S, Ito M, Kuwahata M, Shono M, Yamamoto T, Miyamoto K (2005) Internalization of renal type IIc Na–Pi cotransporter in response to a high-phosphate diet. Am J Physiol Renal Physiol 288:F587–F596
33. Stauber A, Radanovic T, Stange G, Murer H, Wagner CA, Biber J (2005) Regulation of intestinal phosphate transport. II. Metabolic acidosis stimulates Na(+)-dependent phosphate absorption and expression of the Na(+)-P(i) cotransporter NaPi-IIb in small intestine. Am J Physiol Gastrointest Liver Physiol 288: G501–G506
34. Tenenhouse HS, Martel J, Gauthier C, Segawa H, Miyamoto K (2003) Differential effects of Npt2a gene ablation and X-linked Hyp mutation on renal expression of Npt2c. Am J Physiol Renal Physiol 285:F1271–F1278
35. Tenenhouse HS, Roy S, Martel J, Gauthier C (1998) Differential expression, abundance, and regulation of Na+-phosphate cotransporter genes in murine kidney. Am J Physiol 275:F527–F534
36. Virkki LV, Forster IC, Biber J, Murer H (2005) Substrate interactions in the human type IIa sodium-phosphate cotransporter (NaPi-IIa). Am J Physiol Renal Physiol 288:F969–F981
37. Zajicek HK, Wang H, Puttaparthi K, Halaihel N, Markovich D, Shayman J, Beliveau R, Wilson P, Rogers T, Levi M (2001) Glycosphingolipids modulate renal phosphate transport in potassium deficiency. Kidney Int 60:694–704

9.3 Induction of metabolic acidosis with ammonium chloride (NH_4Cl) in mice and rats – species differences and technical considerations

Marta Nowik, Marija Mihailova, Dominique Eladari, Carsten A. Wagner

Manuscript submitted

Induction of metabolic acidosis with ammonium chloride (NH_4Cl) in mice and rats – species differences and technical considerations

Marta Nowik[1], Marija Mihailova[1], Dominique Eladari[2], Carsten A. Wagner[1]

[1] Institute of Physiology and Zurich Center for Human Integrative Physiology (ZHIP), University of Zurich, Zurich, Switzerland; [2] UMRS 872 (CRC) INSERM, Equipe 3; Université Paris Descartes; Departement de Physiologie, HEGP, AP-HP, Paris, France

Corresponding author:
Carsten A. Wagner
Institute of Physiology and Zurich Center for Integrative Human Physiology
University of Zurich
Winterthurerstrasse 190
CH-8057 Zurich
Phone: +41-44-63 50659
Fax: +41-44-63 56814
Email: Wagnerca@access.uzh.ch

ABSTRACT

Ammonium chloride addition to drinking water is often used to induce metabolic acidosis (MA) in rodents but may also cause mild dehydration. Previous microarray screening of acidotic mouse kidneys showed upregulation of genes involved in renal water handling. Thus, we compared two protocols to induce metabolic acidosis in mice and rats: standard 0.28M NH_4Cl in drinking water or an equivalent amount of NH_4Cl in food. Both treatments induced MA in mice and rats. In rats, NH_4Cl in water caused dehydration, reduced mRNA abundance of the vasopression receptor 2 (V2R), and increased protein abundance of the aquaporin water channels AQP2 and AQP3. In contrast, NH_4Cl in food induced massive diuresis, decreased mRNA levels of V2R, AQP2, and AQP3 and did not affect protein abundance of the water channels. In mice, NH_4Cl in drinking water stimulated urine concentration, increased AQP2 and V2R mRNA levels, and enhanced AQP2 and AQP3 protein expression. Addition of NH_4Cl to food, stimulated diuresis, had no effect on mRNA levels of AQP2, AQP3, and V2R, and enhanced only AQP3 protein abundance. Similarly, AQP2 staining was more intense and luminal in kidney from mice with NH_4Cl in water but not in food. Pendrin, SNAT3 and PEPCK mRNA expression in mouse kidney were not affected by the route of NH_4Cl application. Thus, NH_4Cl in water but not MA induces dehydration and regulation of proteins involved in water homeostasis. The standard protocol adding NH_4Cl to drinking water may be problematic and application of NH_4Cl in food should be considered. Moreover, mice and rats

respond differently to NH_4Cl loading, and increased water intake and diuresis may be a compensatory mechanism during MA.

keywords: Ammonium chloride, metabolic acidosis, rodents, aquaporins, pendrin, ammoniagenesis

INTRODUCTION

The kidney plays a central role in maintaining the composition of body fluids by regulating water, NaCl, acid-base, and solute reabsorption and excretion, respectively. The role of specific genes in these processes have been studied extensively over the last decade using genetically modified animals, often requiring provocation tests to uncover defects. The standard protocol to induce metabolic acidosis in experimental animals involves application of ammonium chloride (NH_4Cl), which is supplied most frequently in drinking water [1-11], but also in food or fixed amount of gelled diet [6, 12-16]. Administration of NH_4Cl in both, drinking water and food is also used [17, 18].The first report describing the effect of ammonium chloride ingestion on acid-base balance dates back to 1921 [19].

Metabolic acidosis induced by NH_4Cl administered in food and drinking solution has been associated with decreased reabsorption of NaCl and water in the proximal tubule of dog and rat [17, 20, 21]. In the collecting duct in rats, MA (NH_4Cl provided in gelled diet or standard 0.28M NH_4Cl solution) has been linked to altered expression and activity of the epithelial sodium channel ENaC [13, 22]. Moreover, altered expression of the vasopressin-regulated water channel AQP2 and a concomitant increase of circulating levels of vasopressin in response to 0.28M NH_4Cl loading have been described in rats [9]. In contrast, Nanogutchi and colleagues suggested that elevated expression of AQP2 in rats was due to dehydration and not MA itself [16]. Similarly, a study on the aquaporin 6 water

channel revealed elevated abundance of AQP6 only in rats receiving NH_4Cl in water but not in food [6]. The authors suggested that changes in water intake and not disturbed acid-base status of animals would be responsible. Recently microarray screening of kidneys from 2 and 7 days acidotic mice revealed the upregulation of a number of genes involved in water homeostasis (AQP1, AQP2, AQP3, AQP4, the vasopressin receptor V2R, and the urea transporter Slc14a2) [23]. Acidotic mice, however, consumed around 20% water less than control animals.

Thus, the effects of acidosis and particularly the application of NH_4Cl have remained controversial with respect to its effects on renal water handling. Most authors used the standard protocol, adding 0.28M NH_4Cl to drinking water [9, 21, 24-28]. Nonoguchi et al. added NH_4Cl to food [16]. Therefore discrepancies observed in these studies may be explained by different routes of NH_4Cl application, variable degrees of dehydration in studies adding NH_4Cl to drinking water, and species differences between rats and mice.

Therefore, we wanted to clarify if the route of NH_4Cl application affects the physiologic response of the kidney and examined the induction of metabolic acidosis in response to standard 0.28M NH_4Cl in drinking water and compared it with NH_4Cl addition to food. Both protocols were tested in mice and rats to test also for species specific responses. Our data indicate that NH_4Cl in drinking water induces dehydration in addition to MA and that some of the effects ascribed previously to MA may be rather the consequences of dehydration.

Moreover, distinct differences between mice and rats exist in their response to NH_4Cl-loading.

METHODS

Animals

All experiments were performed on 12 weeks old C57BL/6J male mice (25-30 g) and male Wistar rats (160-200 g). All experiments were performed according to Swiss Animal Welfare laws and approved by the local veterinary authority (Veterinäramt Zürich). All animals received standard rodent chow GLP 3433 (PROVIMI KLIBA, Kaiseraugst, Switzerland)

Induction of metabolic acidosis

Two experimental protocols were used:

***Protocol 1: Experimental protocol for acid load in drinking water*.** C57BL/6J male mice and Wistar rats were given 0.28 M NH_4Cl + 0.5% sucrose in drinking water (tap water) for 3 days. Control animals received tap water + 0.5% sucrose ad libitum. All animals had free access to standard rodent chow. This acid load averaged 6.74 ± 0.49 mmoles NH_4Cl/day/rat and 1.06 ± 0.06 mmoles NH_4Cl/day/mouse.

Protocol 2: Experimental protocol for acid load in food. C57BL/6J male mice and Wistar rats were given NH_4Cl mixed with standard rodent chow for 3 days in the following proportion: 2 g (mice) or 3 g (rats) of NH_4Cl / 100 g of standard rodent chow. All animals received tap water + 0.5% sucrose ad libitum and had free access to the chow. Control animals received the same diet but without NH_4Cl. This acid load averaged 9.41 ± 0.24 mmoles NH_4Cl/day/rat and 1.19 ± 0.04 mmoles NH_4Cl/day/mice.

Metabolic cages studies

All animals were adapted to metabolic cages for 3 days before data collection. In total, 4 rats and 6 mice were acid-loaded using *Protocol 1*, 4 rats and 6 mice were acid-loaded using *Protocol 2*, and 4 rats and 6 mice served as controls. Daily chow, water intake and body weights were measured and urine was collected under mineral oil. At the end of experiments, animals were anesthetized with isoflurane/O_2 and heparinised arterial blood was collected from the tail artery in rats and heparinised mixed venous blood was collected in mice (anesthesized with ketamine/xylazine) and analyzed immediately for pH, blood gases and electrolytes on a Radiometer ABL 505 (Radiometer, Copenhagen, Denmark) blood gas analyzer. Serum was collected and frozen until further analysis. Both kidneys were harvested, rapidly frozen in liquid nitrogen, and stored at -80°C until mRNA extraction.

Urine and serum analysis was performed as described previously [23]. Aldosterone in urine was measured with a radioimmunoassay using a commercially available kit (DPC Dade Behring, La Défense, France). Briefly, 24 hour urines were collected in metabolic cages and kept at -20°C until use. For each sample, 50 µl urine were hydrolized overnight with 3.2 N HCl, treated with ethyl acetate to extract aldosterone and evaporated. Dried extracts were resuspended in the appropriate solvent following the manufacturer's recommandations and aldosterone were then measured by radioimmunoassay.

RNA extraction, reverse transcription, and real-time quantitative PCR

Kidneys were harvested and rapidly frozen in liquid nitrogen. Total snap-frozen kidneys were homogenized in RLT-Buffer/1% ß-mercaptoethanol (Qiagen, Basel, Switzerland). Total RNA was extracted using the RNeasy Mini Kit (Qiagen) according to the manufacturer's instructions. Quality and concentration of the isolated RNA preparations were analyzed by the ND-1000 spectrophotometer (NanoDrop Technologies). 300 ng of RNA was used as a template for reverse transcription using the TaqMan Reverse Transcription Kit (Applied Biosystems, Forster City, CA, USA). Real time RT-PCR was performed as described previously [23].

Western Blot Analysis

Preparation of crude membrane proteins from the total kidneys was performed as described elsewhere [27]. 50 µg of crude membrane proteins were solubilised in Laemmli sample buffer and SDS-PAGE was performed on a 10 % polyacrylamide gel. Immunoblotting and image analysis was performed as described previously [23, 29]. The primary antibodies used were: rabbit anti aquaporin 2 (1:5000) (kindly provided by J. Loffing, Institute of Anatomy, University of Zurich, Switzerland [30], rabbit anti aquaporin 3 (1:200) (Alomone Labs, Jerusalem, Israel) and mouse monoclonal anti-β-actin antibody (42 kD; Sigma, St. Louis, MO; 1:5000); secondary antibodies used were: donkey anti-rabbit or sheep anti-mouse antibodies linked to horseradish peroxidase (1:10000)

(GE Healthcare, Little Chalfont Buckinghamshire, UK) or goat anti-rabbit antibody (1:5000) linked to alkaline phosphatase (Promega, USA).

Immunohistochemistry

Mouse kidneys were perfusion fixed through the right ventricle with a PFA fixative solution and subsequent immunohistochemistry were performed as described previously [26, 31]. Primary antibodies used were: polylonal goat anti-human aquaporin 2 (1:1000) (Santa Cruz Biotechnology). Secondary antibody: Alexa 488-conjugated donkey anti-goat antibody (1:400) (Invitrogen, Basel, Switzerland).

Statistical analysis

Results are expressed as mean ± SEM. All data were tested for significance using the one way ANOVA and Turkey post test or unpaired student's test where appropriate.

RESULTS

NH_4Cl in water induces metabolic acidosis and dehydration in rats

In rats acid-loading with NH_4Cl either in drinking water or food resulted in induction of metabolic acidosis, as evident from the reduction of blood pH and bicarbonate levels (Table 2). However, the degree of metabolic acidosis was less pronounced in rats ingesting NH_4Cl with food despite receiving even a slightly higher load (6.74 ± 0.49 mM NH_4Cl/day/rat. for *Protocol 1*; 9.41 ± 0.24 mM NH_4Cl/day/rat for *Protocol 2*). As expected serum chloride was elevated in both acidotic rat groups, however, animals ingesting NH_4Cl in food had significantly lower chloride levels than animals with NH_4Cl in water. Plasma sodium concentration and hematocrit were not changed in both experimental rat groups (Table 2). Plasma urea concentration and osmolality were elevated only in rats NH_4Cl-loaded with water (Table 2). During acid-loading rats gained less weight when receiving NH_4Cl in drinking water and their food intake was lower comparing to control (Table 2). Water consumption increased significantly in the group receiving NH_4Cl in food paralleled by higher urinary output.

Urine analysis revealed that rats from both acidotic groups acidified their urine to the similar extend and ammonium excretion was increased accordingly. NH_4Cl-loading in water did not influence water intake and urine output but increased urine osmolality. NH_4Cl-loading in food, however increased urine volume without changing urine osmolality. Urinary urea was elevated in both acidotic rat groups as well as urine aldosterone levels were elevated, however 3-fold higher in animals receiving NH_4Cl in water than in food (Table 2).

Changes in AQP2, AQP3 and V2R mRNA and protein expression in rat kidney depend on the route of NH_4Cl application.

Induction of MA for 3 days with 0.28M NH_4Cl in the drinking water in rats had no effect on mRNA expression of both aquaporins AQP2 and AQP3, but decreased V2R mRNA expression (Figure 1). In contrast, addition of NH_4Cl to food decreased mRNA expression of both aquaporins and the V2R (Figure 1).

Induction of metabolic acidosis using NH_4Cl-containing drinking solution resulted in elevated abundance of both, glycosylated and non-glycosylated AQP2 species and AQP3 in rat kidney (Figure 2A,B). Application of NH_4Cl in food had no apparent effect on AQP2 and AQP3 protein abundance (Figure 2A,B).

NH_4Cl in water induces more pronounced metabolic acidosis and decreases diuresis in mice

In mice acid-loading with both protocols resulted in a fall of blood pH, however, only mice drinking NH_4Cl-containing solution had lowered HCO_3^- and increased Cl^- and Na^{2+} concentrations in blood. Neither serum urea nor osmolality were affected by acid-loading, but hematocrit was significantly lower in mice ingesting NH_4Cl in food. Mice with NH_4Cl in drinking water lost more body weight than mice on normal diet or receiving NH_4Cl in food (Table 3); however food intake was not changed by either way of acid-loading. Water consumption was elevated in mice receiving NH_4Cl in food paralleled by higher urinary output.

In mice acid loading with both protocols resulted in urinary acidification and elevated ammonium excretion. Interestingly mice ingesting NH_4Cl in food showed much higher urine ammonium excretion than NH_4Cl-loaded in water, although NH_4Cl intake was not significantly different between protocols (1.06 ± 0.06 mmoles NH_4Cl/day/mouse for NH_4Cl in water; 1.19 ± 0.04 mmoles NH_4Cl/day/mice for NH_4Cl in food). Elevated urine osmolality in mice acid-loaded in water was paralleled by lower urine output despite normal water intake. NH_4Cl-loading in food, however, increased water consumption and urine volume without changing urine osmolality. Both protocols of NH_4Cl loading increased urinary aldosterone excretion to a similar extent.

NH_4Cl in water increases AQP2 and AQP3 mRNA and protein abundance

In mice acid-loading with NH_4Cl in water resulted in increased AQP2 and V2R mRNA abundance but had no effect on expression of AQP3 mRNA (Figure 3). In contrast to rats, mice ingesting NH_4Cl in food did not show any changes in mRNA abundance of AQP2, AQP3, or V2R (Figure 3). Also only mice ingesting NH_4Cl in water but not in food had elevated abundance of glycosylated and non-glycosylated AQP2 (Figure 4A,B). Moreover, both acidotic mice groups exhibited elevated AQP3 abundance (Figure 4A,B).

Only NH_4Cl-loading in water alters distribution of AQP2 water channel

Immunohistochemistry was used to examine whether NH_4Cl-loadnig alters segmental and/or subcellular distribution of the aquaporin 2 water channel in

mouse kidney. AQP2 is predominantly expressed on the apical side of principal cells along the entire connecting tubule and collecting duct system [32]. Increased staining and more pronounced luminal AQP2 labeling was observed in mouse kidneys after addition of NH_4Cl to drinking water but not to food consistent with more concentrated urine in the NH_4Cl water group (Figure 4C).

NH_4Cl in food and water alters abundance of acidosis regulated genes

We and others have previously shown that the anion exchanger pendrin, the glutamine transporter SNAT3, and phospho-enol pyruvate carboxy kinase (PEPCK) are regulated on mRNA levels during metabolic acidosis induced by NH_4Cl [10, 23, 33-35]. qPCR demonstrated that pendrin mRNA abundance was similarly reduced in mice receiving NH_4Cl in food or drinking water (Figure 5). Also, SNAT3 and PEPCK mRNA levels were increased in both mouse groups irrespective of the route of NH_4Cl administration (Figure 5).

DISCUSSION

The purpose of this study was to compare the induction of metabolic acidosis with NH_4Cl added either to drinking water or food. Application of NH_4Cl with drinking water is a well established and extensively used method to induce metabolic acidosis [1-4, 7, 8, 10, 28]. In our hands, both protocols induced MA in rats and mice as evident from lower blood pH, increased urinary acidification, and acid excretion. Both acidotic mice and rat groups were also able to acidify their urine to a similar extend regardless of the diet (Tables 2-3). It seems, however, that animals receiving NH_4Cl in food were less acidotic compared to the group receiving NH_4Cl in drinking water as their bicarbonate levels in blood were not as low (rats) or even unchanged (mice). Total NH_4Cl intake was similar in both groups suggesting that the route of application affects compensatory mechanisms.

The major findings of our comparison of different NH_4Cl-loading protocols are: 1) both protocols induced metabolic acidosis in mice and rats, 2) differences between rats and mice exist with respect to their renal compensatory responses as evident from different expression levels of AQP2, AQP3, and V2R mRNA and protein, 3) NH_4Cl in drinking water induces a mild but clear dehydration in rats, as demonstrated by higher aldosterone levels and urine osmolality, 4) NH_4Cl in water stimulated urinary concentration in mice without other signs of dehydration, and 5) dehydration and MA affect independently expression patterns of genes and proteins involved in renal water handling.

Dehydration and extracellular volume contraction activates the renin-angiotensin-aldosterone system and stimulates secretion of aldosterone. Induction of MA resulted in elevation of urine aldosterone excretion in both acidotic rat and mice groups; however, aldosterone levels were 3-fold lower in rats receiving NH_4Cl in food compared to the NH_4Cl/water group. Hematocrit and plasma sodium concentration were unchanged in both rat groups. In contrast, in mice we observed increased plasma sodium concentration in animals subjected to acid-loading with NH_4Cl in water. Additionally NH_4Cl ingestion in food resulted in increased water intake and urine output and decreased urine osmolality in both mice and rats which is in agreement with observations of Mori et al [15]. Collectively, these data indicate mild dehydration in animals receiving NH_4Cl in drinking water resulting in elevated aldosterone levels and upregulation of several components of the urinary concentration machinery. The regulation of AQP3 observed also in the NH_4Cl/ food group may be at least in part due to the slightly increased levels of aldosterone which has been shown to increase AQP3 expression [36].

Our results of NH_4Cl-loading in drinking water are similar to those of Amlal et al [9] suggesting that the results reported there are mainly due to dehydration but not MA of rats. Ingestion of equivalent amounts of NH_4Cl in food had no effect on AQP2 protein levels in our hands. Also immunohistochemistry analysis of mouse kidneys showed more pronounced AQP2 staining only in the NH_4Cl in water group. Concomitant with increased protein abundance was mRNA expression of AQP2 in mice loaded with NH_4Cl in water. Interestingly there was

no change in AQP2 mRNA expression in rats subjected to NH_4Cl in water, and in animals ingesting NH_4Cl in food expression of AQP2 was even decreased. Thus, not urinary concentration but increased diuresis may even be part of the renal compensatory response to metabolic acidosis.

Taken together, our study demonstrates that the route of NH_4Cl application – drinking water versus food – strongly affects the regulation of renal genes and proteins, particularly those involved in water handling. NH_4Cl in drinking water causes mild dehydration and upregulation of several components of the urinary concentrative mechanism. Moreover, our study shows that distinct species differences exist between mice and rats in their response to NH_4Cl-loading in drinking water. Future studies should consider NH_4Cl addition to food rather than to drinking water and species differences between rats and mice may be more pronounced than previously anticipated. Moreover, it may be of interest to consider similar studies in humans assessing urinary concentration and water balance.

Acknowledgements

This study was supported by grants to C A Wagner from the Swiss National Science Foundation (31-109677), the 6th EU Frame work project EuReGene, and a ZIHP PhD student fellowship to M Nowik. The use of the ZIHP Core Facility for Rodent Physiology is gratefully acknowledged. The authors thanks Françoise

Leviel and the technicians from the Department of Physiology of Hopital Européen Georges Pompidou for their skillful technical assistance in aldosterone measurements.

Table 1. Primers and probes used for real-time PCR

Gene	Acc. No.	Primers	Probe
AQP2 (M)	NM_009699	F: 5'-TGGTGCTGTGCATCTTTGCCT-3' (503-523) R: 5'-ACTTGCCAGTGACAACTGCTG-3' (655-673)	5'-ACCTCCTTGGGATCTATTTCACCGG-3' (596-620)
AQP2 (R)	NM_012909	F: 5'-TGGTGCTGTGCATCTTTGCCT-3' (506-526) R: 5'-ACTTGCCAGTGACAACTGCTG-3' (658-676)	5'-ACCTCCTTGGGATCTATTTCACCGG-3' (599-623)
AQP3 (M)	NM_016689	F: 5'-TCAGAAGTCTTCACGACTGGCC-3' (763-784) R: 5'-ATGTGGGCCAGCTTCACATTC-3' (903-923)	5'-TGGTGTCTTCGTGTACCAGCTCATG-3' (834-858)
AQP3 (R)	NM_031703	F: 5'-AGAAGTCTTTACGACTGGCCAG-3' (775-796) R: 5'-ATGTGGGCCAGCTTCACATTC-3' (913-933)	5'-TGGTGTCTTCGTGTACCAGCTCATG-3' (844-868)
V2R (M)	NM_019404	F: 5'-CGTGGGATCCAGAAGCTCC-3' (1026-1044) R: 5'-AGGCTACGCAACTCCGAGG-3' (1140-1158)	5'-CCTTTGTGTTGCTCATGCTGCTGGCTAG-3' (1059-1086)
V2R (R)	NM_019136	F: 5'-CGTGGGATCCAGAAGCTCC-3' (884-902) R: 5'-AGGCTACGCAACTCCGAGG-3' (998-1016)	5'-CCTTTGTGTTGCTCATGCTGCTGGCTAG-3' (917-944)
HPRT (M)	NM_013556	F: 5'-TTATCAGACTGAAGAGCTACTGTAAGATC-3' (442-471) R: 5'-TTACCAGTGTCAATTATATCTTCAACAATC-3' (539-568)	5'-TGAGAGATCATCTCCACCAATAACTTTTATGTCCC-3' (481-515)

HPRT (R)	NM_012583	F: 5'-GCTGAAGATTTGGAAAAGGTGTTTA-3' R: 5'-ACACAGAGGGCCACAATGTGA-3'	5'-TTATGGACAGGACTGAAAGACTTGCTCGAG ATG-3'

Table 2: Induction of metabolic acidosis in rats

	Control	NH_4Cl in water	NH_4Cl in food
Blood			
pH	7.41 ± 0.02	7.16 ± 0.02 ***	7.25 ± 0.02 *** #
pCO_2 mmHg	41.4 ± 3.0	49.9 ± 2.6	49.7 ± 1.7
$[HCO_3^-]$ mM	25.4 ± 1.1	17.2 ± 1.0 **	20.9 ± 1.2 *
$[Na^+]$ mM	135.0 ± 2.3	139.5 ± 0.9	138.8 ± 0.3
$[K^+]$ mM	5.1 ± 0.1	4.5 ± 0.2 *	4.4 ± 0.1 *
$[Cl^-]$ mM	99.8 ± 0.9	112.0 ± 0.9 ***	105.3 ± 0.9 ** ##
[Pi] mM	0.72 ± 0.02	0.85 ± 0.06	0.90 ± 0.08
$[Ca^{2+}]$ mM	1.02 ± 0.14	1.49 ± 0.04 **	1.22 ± 0.04 ##
Hematorit %	41.7 ± 0.9	43.7 ± 0.8	43.1 ± 0.8
Urea (mg/dl)	27.2 ± 3.8	54.9 ± 2.0 ***	25.3 ± 1.2 ###
Osmolality (mOsm/kg H_2O)	294.5 ± 0.3	302.0 ± 2.9 *	284.5 ± 2.2 ##
Urine			
pH	8.67 ± 0.05	5.73 ± 0.06 ***	5.79 ± 0.04 ***
Creatinine (mg/dl)	30.4 ± 4.9	43.4 ± 3.9	13.7 ± 1.6 * ###
NH_3/NH_4^+ (mM)/crea (mg/dl)	2.45 ±0.19	7.45 ± 0.58 ***	5.97 ± 0.73 **
Na^+ (mM)/crea (mg/dl)	1.13 ± 0.25	1.63 ± 0.23	2.94 ± 0.42 ** ##
K^+ (mM)/crea (mg/dl)	2.69 ± 0.56	3.61 ± 0.30	5.95 ± 0.74 ** #
Ca^{2+} (mM)/crea (mg/dl)	0.091 ± 0.022	0.193 ± 0.042	0.305 ± 0.036 **
Mg^{2+} (mM)/crea (mg/dl)	0.081 ± 0.027	0.430 ± 0.053 **	0.635 ± 0.092 ***
Cl^- (mM)/crea (mg/dl)	2.14 ± 0.72	13.38 ± 2.01 **	13.25 ± 1.59 **
Pi (mM)/crea (mg/dl)	0	0.20 ± 0.02 ***	0.33 ± 0.04 *** #
24 h Aldosterone (nM)	0.008 ± 0.003	0.199 ± 0.030 ***	0.047 ± 0.005 *** ###
Urea (mg/dl)/crea (mg/dl)	40.3 ± 4.3	74.4 ± 6.0 *	100.5 ± 9.9 ***
Osmolality (mOsm/kg H_2O)	563 ± 100	1783 ± 124 ***	820 ± 47 ###
Urine volume (ml)/g BW	0.069 ± 0.014	0.045 ± 0.007	0.107 ± 0.005 * ##
Water intake (ml)/g BW	0.18 ± 0.02	0.14 ± 0.01	0.22 ± 0.01 ##
Food intake (g)/g BW	0.095 ± 0.005	0.072 ± 0.005 **	0.089 ± 0.002 #
Body weight (% change)	+14.6 ± 0.8	+2.6 ± 1.4 ***	+8.0 ± 1.0 **#
NH_4Cl load (mM/day)	n.a.	6.74 ±0.49	9.41 ± 0.24 **

Table 3: Induction of metabolic acidosis in mice

	Control	NH_4Cl in water	NH_4Cl in food
Blood			
pH	7.22 ± 0.02	7.12 ± 0.03 *	7.14 ± 0.03 *
pCO_2 mmHg	46.2 ± 2.1	45.6 ± 4.7	46.7 ± 4.2
$[HCO_3^-]$ mM	18.1 ± 1.1	13.9 ± 1.2 *	15.3 ± 1.8
$[Na^+]$ mM	143.6 ± 1.0	147.2 ± 1.1 *	142.6 ± 0.5 ##
$[K^+]$ mM	3.5 ± 0.1	3.2 ± 0.1	3.5 ± 0.1
$[Cl^-]$ mM	113.2 ± 1.0	122.4 ± 1.4 ***	113.8 ± 0.9 ###
$[Ca^{2+}]$ mM	1.24 ± 0.03	1.27 ± 0.06	1.21 ± 0.03
Hematorit %	41.6 ± 0.2	43.6 ± 1.4	38.8 ± 0.7 ** #
Urea (mg/dl)	42.9 ± 2.1	43.0 ± 5.0	39.9 ± 4.2
Osmolality (mOsm/kg H_2O)	301.6 ± 1.7	300.2 ± 2.4	302.5 ± 2.7
Urine			
pH	6.38 ± 0.05	5.30 ± 0.04 ***	5.42 ± 0.02 ***
Creatinine (mg/dl)	35.7 ± 4.7	54.6 ± 10.8	17.1 ± 1.3 ** ##
NH_3/NH_4^+ (mM)/crea (mg/dl)	0.66 ± 0.05	8.78 ± 1.12 ***	16.15 ± 1.10 *** ###
Na^+ (mM)/crea (mg/dl)	3.86 ± 0.29	3.88 ± 0.47	6.04 ± 0.49 ** ##
K^+ (mM)/crea (mg/dl)	12.89 ± 0.56	11.05 ± 1.03	16.51 ± 0.89 * ##
Ca^{2+} (mM)/crea (mg/dl)	0.043 ± 0.007	0.080 ± 0.018	0.236 ± 0.017 *** ###
Mg^{2+} (mM)/crea (mg/dl)	0.50 ± 0.06	0.63 ± 0.09	1.09 ± 0.1 *** ##
Cl^- (mM)/crea (mg/dl)	7.58 ± 0.44	22.42 ± 2.64 ***	30.97 ± 1.97 *** #
Pi (mM)/crea (mg/dl)	1.66 ± 0.13	1.39 ± 0.21	2.37 ± 0.23 * ##
24 h Aldosterone (nM)	0.022 ± 0.001	0.031 ± 0.002 **	0.027 ± 0.001 *
Urea (mg/dl)/crea (mg/dl)	205.9 ± 20.5	161.8 ± 23.5	329.2 ± 14.8 ** ###
Osmolality (mOsm/kg H_2O)	2565 ± 316	4360 ± 543 *	2100 ± 158 ##
Urine volume (ml)/g BW	0.059 ± 0.005	0.049 ± 0.004	0.086 ± 0.008 * ##
Water intake (ml)/g BW	0.161 ± 0.006	0.167 ± 0.010	0.222 ± 0.027 *
Food intake (g)/g BW	0.154 ± 0.005	0.153 ± 0.007	0.144 ± 0.006
Body weight (% change)	-3.7 ± 0.7	-4.7 ± 1.3	-8.3 ± 1.2 *
NH_4Cl load (mM/day)	n.a.	1.06 ± 0.06	1.19 ± 0.04

FIGURE LEGENDS

Table 1

Primers and probes used for quantitative real-time PCR in mice (M) and rats (R). All primers and probes were designed using Primer Express software (Applied Biosystems). Either primers or probes are spanning intron-exon boundries to exclude genomic DNA contamination. The nucleotide numbers of the primers and probes are given in brackets.

Table 2

Blood gas status and electrolytes in blood and urine data from Wistar rats under control conditions and after 3 days acid-loading (0.28 M NH_4Cl + 0.5% sucrose in drinking water or 3g NH_4Cl / 100g in food + 0.5% sucrose in drinking water). Control rats received only 0.5% sucrose in their drinking water. Values are means ± SEM, n = 4 per group. * $p \leq 0.05$, ** $p \leq 0.01$, *** $p \leq 0.001$, $^{\#}$ significantly different between two acidotic groups.

Table 3

Blood gas status and electrolytes in blood and urine data from C57BL/6 mice under control conditions and after 3 days acid-loading (0.28 M NH_4Cl + 0.5% sucrose in drinking water or 2g NH_4Cl/ 100g food + 0.5 % sucrose in drinking water). Control mice received only 0.5% sucrose in their drinking water. Values are means ± SEM, n = 6 per group. * $p \leq 0.05$, ** $p \leq 0.01$, *** $p \leq 0.001$, $^{\#}$ significantly different between two acidotic groups.

Figure 1

AQP2, AQP3 and V2R mRNA abundance in rat kidney.

Real-time RT-PCR was used to assess AQP2, AQP3 and V2R mRNA levels in kidneys from control and NH_4Cl-loaded animals (n = 4 rats/group). In rat kidney, AQP2, AQP3, and V2R mRNA was reduced in animals receiving NH_4Cl in food. NH_4Cl in drinking water decreased only V2R mRNA. * $p \leq 0.05$, ** $p \leq 0.01$.

Figure 2

Expression of AQP2 and AQP3 proteins during acid-loading in rat kidney.

A) Immunobloting for glycosylated and non-glycosylated variants of AQP2 and AQP3 water channels in total membrane fractions from control and NH_4Cl-loaded rats (n = 4 animals/group). All membranes were reprobed for β-actin. **(B)** Bar graphs summarizing data from immunoblotting. All data were normalized against β-actin. * $p \leq 0.05$, *** $p \leq 0.001$.

Figure 3

AQP2, AQP3 and V2R mRNA abundance in mouse kidney.

Real-time RT-PCR was used to assess AQP2, AQP3 and V2R mRNA levels in kidneys from control and NH_4Cl-loaded animals (n = 6 mice/group). In mouse kidney, expression of AQP2 water channel and V2R mRNA was increased only in mice receiving NH_4Cl in water, but not in food. AQP3 expression remained unchanged in both groups. * $p \leq 0.05$.

Figure 4

Expression of AQP2 and AQP3 proteins during acid-loading in mouse kidney.

A) Immunobloting for glycosylated and non-glycosylated variants of AQP2 and AQP3 water channels in total membrane fractions from control and NH_4Cl-loaded mice. All membranes were reprobed for β-actin, 4 representative animals/ group are shown. **(B)** Bar graphs summarizing data from immunoblotting. All data were normalized against β-actin. **(C)** Immunolocalization of AQP2 water channel in kidneys from control and acid-loaded mice shows higher intensity in kidneys from mice loaded with NH_4Cl in water. Pictures were taken from the inner medulla at an original magnification of 200 x. * $p \leq 0.05$, ** $p \leq 0.01$.

Figure 5

Regulation of SNAT3, PEPCK, and Pendrin in kidneys from NH_4Cl-loaded mice. Real-time RT-PCR was used to assess SNAT3, PEPCK, and pendrin mRNA levels in kidneys from control and NH_4Cl-loaded animals (n = 6 mice/group). All three mRNAs were regulated irrespective of the route of NH_4Cl application. *** $p \leq 0.001$.

REFERENCES

1. Chambrey R, Goossens D, Bourgeois S*, et al.*: Genetic ablation of Rhbg in the mouse does not impair renal ammonium excretion. *Am J Physiol Renal Physiol* 289:F1281-1290, 2005

2. Quentin F, Chambrey R, Trinh-Trang-Tan MM*, et al.*: The Cl^-/HCO_3^- exchanger pendrin in the rat kidney is regulated in response to chronic alterations in chloride balance. *Am J Physiol Renal Physiol* 287:F1179-1188, 2004

3. Ambuhl PM, Amemiya, M, Danczkay, M, Lotscher, M, Kaissling, B, Moe, O W, Preisig, P A, Alpern, R J: Chronic metabolic acidosis increases NHE3 protein abundance in rat kidney. *Am J Physiol* 271:F917-925, 1996

4. Ambuhl PM, Zajicek, H K, Wang, H, Puttaparthi, K, Levi, M: Regulation of renal phosphate transport by acute and chronic metabolic acidosis in the rat. *Kidney Int* 53:1288-1298, 1998

5. Wang T, Egbert, A L, Jr, Aronson, P S, Giebisch, G: Effect of metabolic acidosis on NaCl transport in the proximal tubule. *Am J Physiol* 274:F1015-1019, 1998

6. Promeneur D, Kwon TH, Yasui M*, et al.*: Regulation of AQP6 mRNA and protein expression in rats in response to altered acid-base or water balance. *Am J Physiol Renal Physiol* 279:F1014-1026, 2000

7. Frische S, Kwon, T H, Frokiaer, J, Madsen, K M, Nielsen, S: Regulated expression of pendrin in rat kidney in response to chronic NH_4Cl or $NaHCO_3$ loading. *Am J Physiol Renal Physiol* 284:F584-593, 2003

8. Stehberger PA, Shmukler BE, Stuart-Tilley AK*, et al.*: Distal renal tubular acidosis in mice lacking the AE1 (band3) Cl^-/HCO_3^- exchanger (slc4a1). *J Am Soc Nephrol* 18:1408-1418., 2007

9. Amlal H, Sheriff S, Soleimani M: Upregulation of collecting duct aquaporin-2 by metabolic acidosis: role of vasopressin. *Am J Physiol Cell Physiol* 286:C1019-1030, 2004

10. Curthoys NP, Taylor L, Hoffert JD*, et al.*: Proteomic analysis of the adaptive response of rat renal proximal tubules to metabolic acidosis. *Am J Physiol Renal Physiol* 292:F140-147, 2007

11. Nijenhuis T, Renkema KY, Hoenderop JG*, et al.*: Acid-base status determines the renal expression of Ca2+ and Mg2+ transport proteins. *J Am Soc Nephrol* 17:617-626, 2006

12. Windus DW, Cohn DE, Klahr S*, et al.*: Glutamine transport in renal basolateral vesicles from dogs with metabolic acidosis. *Am J Physiol* 246:F78-86, 1984

13. Kim GH, Martin SW, Fernandez-Llama P*, et al.*: Long-term regulation of renal Na-dependent cotransporters and ENaC: response to altered acid-base intake. *Am J Physiol Renal Physiol* 279:F459-467, 2000

14. Tashima Y, Kohda Y, Nonoguchi H*, et al.*: Intranephron localization and regulation of the V1a vasopressin receptor during chronic metabolic acidosis and dehydration in rats. *Pflugers Arch* 442:652-661, 2001

15. Mori T, Inoue T, Nanoguchi H*, et al.*: Reduced urinary excretion of aquaporin 2 in metabolic acidosis (Abstract). *J Am Soc Nephrol*:273A, 2002

16. Nonoguchi H, Inoue T, Mori T*, et al.*: Regulation of aquaporin-2 by metabolic acidosis. *Am J Physiol Cell Physiol* 287:C824; author reply C814-825, 2004

17. Levine DZ, Nash LA: Effect of chronic NH4Cl acidosis on proximal tubular H2O and HCO3 reabsorption. *Am J Physiol* 225:380-384, 1973

18. Ikebe M, Nonoguchi H, Nakayama Y*, et al.*: Upregulation of the secretory-type Na(+)/K(+)/2Cl(-)-cotransporter in the kidney by metabolic acidosis and dehydration in rats. *J Am Soc Nephrol* 12:423-430, 2001

19. Haldane JB: Experiments on the regulation of the blood's alkalinity: II. *J Physiol* 55:265-275, 1921

20. Safirstein R, Glassman VP, DiScala VA: Effects of an NH4Cl-induced metabolic acidosis on salt and water reabsorption in dog kidney. *Am J Physiol* 225:805-809, 1973

21. Wang T, Egbert AL, Jr., Aronson PS*, et al.*: Effect of metabolic acidosis on NaCl transport in the proximal tubule. *Am J Physiol* 274:F1015-1019, 1998

22. Faroqui S, Sheriff S, Amlal H: Metabolic acidosis has dual effects on sodium handling by rat kidney. *Am J Physiol Renal Physiol* 291:F322-331, 2006

23. Nowik M, Lecca MR, Velic A*, et al.*: Genome-wide gene expression profiling reveals renal genes regulated during metabolic acidosis. *Physiol Genomics* 32:322-334, 2008

24. Ambuhl PM, Amemiya M, Danczkay M*, et al.*: Chronic metabolic acidosis increases NHE3 protein abundance in rat kidney. *Am J Physiol* 271:F917-925, 1996

25. Ambuhl PM, Zajicek HK, Wang H*, et al.*: Regulation of renal phosphate transport by acute and chronic metabolic acidosis in the rat. *Kidney Int* 53:1288-1298, 1998

26. Moret C, Dave MH, Schulz N*, et al.*: Regulation of renal amino acid transporters during metabolic acidosis. *Am J Physiol Renal Physiol* 292:F555-566, 2007

27. Stehberger PA, Schulz N, Finberg KE*, et al.*: Localization and regulation of the ATP6V0A4 (a4) vacuolar H+-ATPase subunit defective in an inherited form of distal renal tubular acidosis. *J Am Soc Nephrol* 14:3027-3038, 2003

28. Rizzo M, Capasso G, Bleich M*, et al.*: Effect of chronic metabolic acidosis on calbindin expression along the rat distal tubule. *J Am Soc Nephrol* 11:203-210, 2000

29. Mohebbi N, Kovacikova J, Nowik M*, et al.*: Thyroid hormone deficiency alters expression of acid-base transporters in rat kidney. *Am J Physiol Renal Physiol* 293:F416-427, 2007

30. Wagner CA, Loffing-Cueni D, Yan Q*, et al.*: Mouse Model of Type II Bartters Syndrome. II. Altered Expression of Renal Sodium- and Water-Transporting Proteins. *Am J Physiol Renal Physiol*, 2008

31. Dawson TP, Gandhi R, Le Hir M*, et al.*: Ecto-5'-nucleotidase: localization in rat kidney by light microscopic histochemical and immunohistochemical methods. *J Histochem Cytochem* 37:39-47, 1989

32. Nielsen S, DiGiovanni SR, Christensen EI*, et al.*: Cellular and subcellular immunolocalization of vasopressin-regulated water channel in rat kidney. *Proc Natl Acad Sci U S A* 90:11663-11667, 1993

33. Solbu TT, Boulland JL, Zahid W*, et al.*: Induction and targeting of the glutamine transporter SN1 to the basolateral membranes of cortical kidney tubule cells during chronic metabolic acidosis suggest a role in pH regulation. *J Am Soc Nephrol* 16:869-877, 2005

34. Frische S, Kwon TH, Frokiaer J*, et al.*: Regulated expression of pendrin in rat kidney in response to chronic NH4Cl or NaHCO3 loading. *Am J Physiol Renal Physiol* 284:F584-593, 2003

35. Wagner CA, Finberg KE, Stehberger PA*, et al.*: Regulation of the expression of the Cl-/anion exchanger pendrin in mouse kidney by acid-base status. *Kidney Int* 62:2109-2117, 2002

36. Kwon TH, Nielsen, J, Masilamani, S, Hager, H, Knepper, M A, Frokiar, J, Nielsen, S: Regulation of collecting duct AQP3 expression: response to mineralocorticoid. *Am J Physiol Renal Physiol* 283:F1403-F1421, 2002

Figure 1

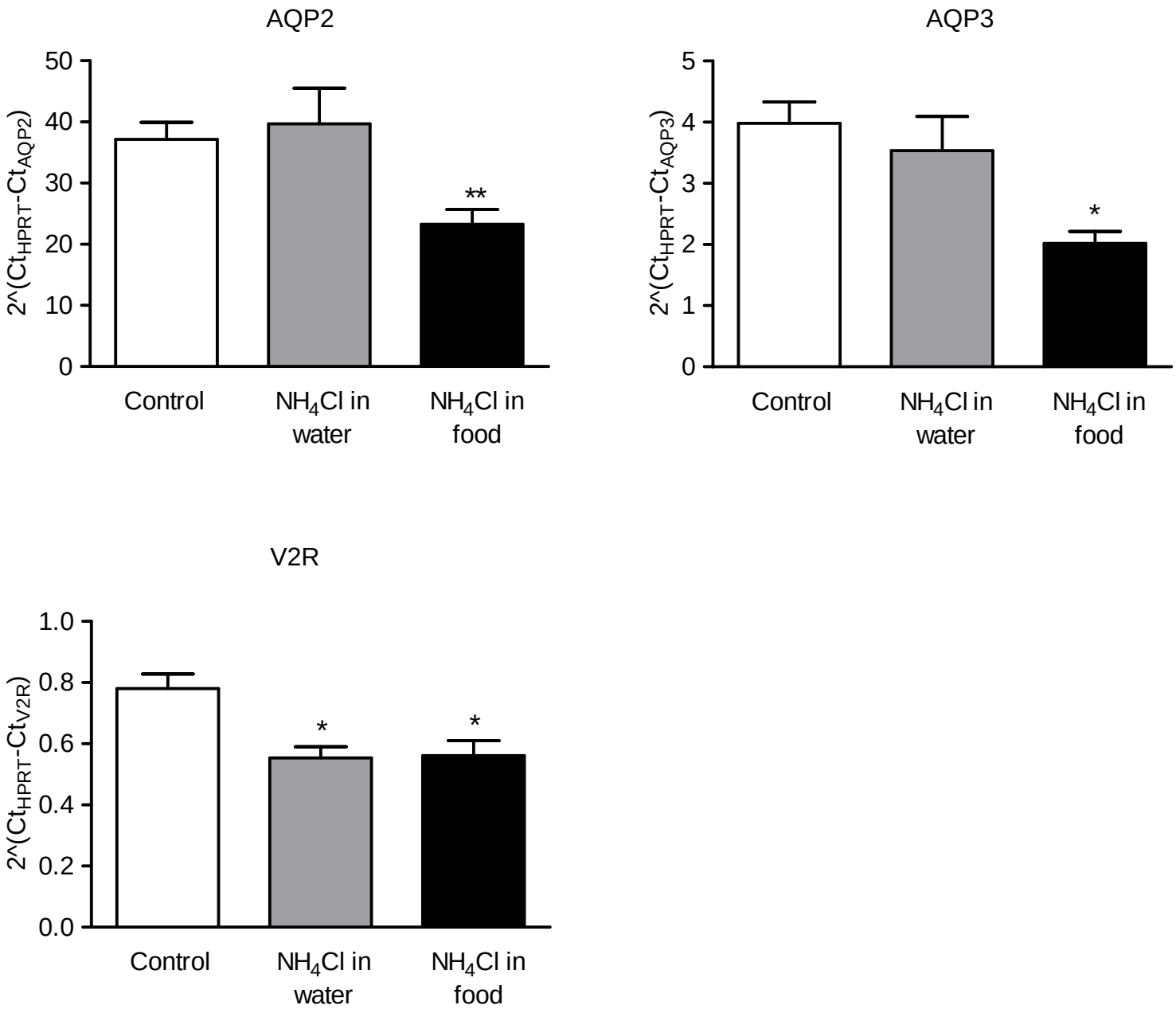
AQP2
2^(Ct_HPRT-Ct_AQP2)
50
40
30
20
10
0
**
Control
NH4Cl in water
NH4Cl in food
AQP3
2^(Ct_HPRT-Ct_AQP3)
5
4
3
2
1
0
*
Control
NH4Cl in water
NH4Cl in food
V2R
2^(Ct_HPRT-Ct_V2R)
1.0
0.8
0.6
0.4
0.2
0.0
*
*
Control
NH4Cl in water
NH4Cl in food

Figure 2 A

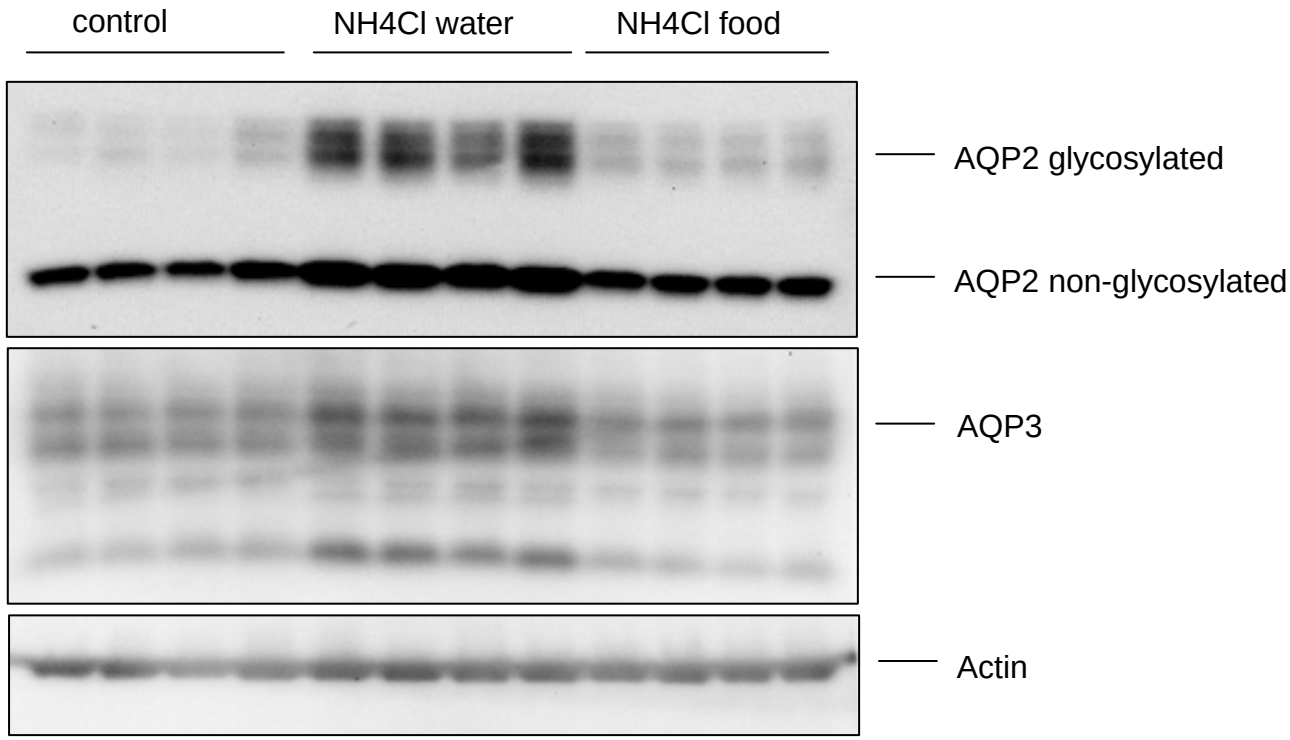
control
NH4Cl water
NH4Cl food
AQP2 glycosylated
AQP2 non-glycosylated
AQP3
Actin

Figure 2 B

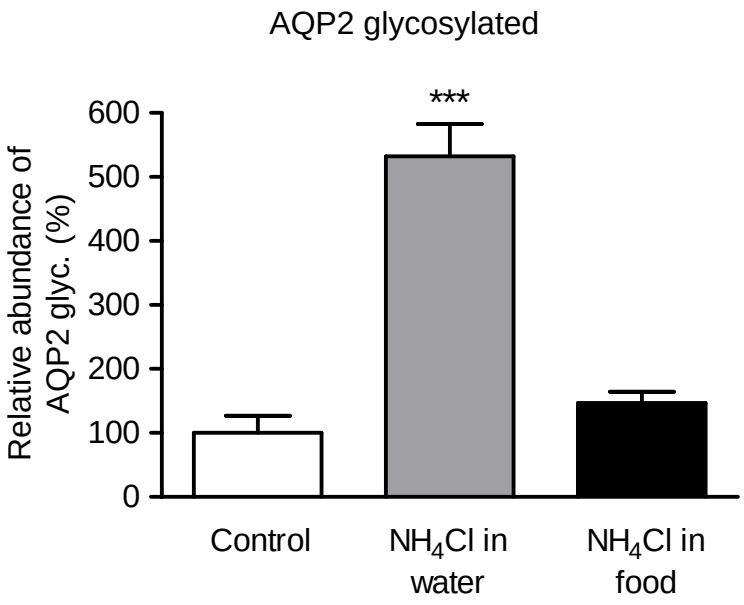
AQP2 glycosylated
Relative abundance of AQP2 glyc. (%)
600
500
400
300
200
100
0
***
Control
NH4Cl in water
NH4Cl in food

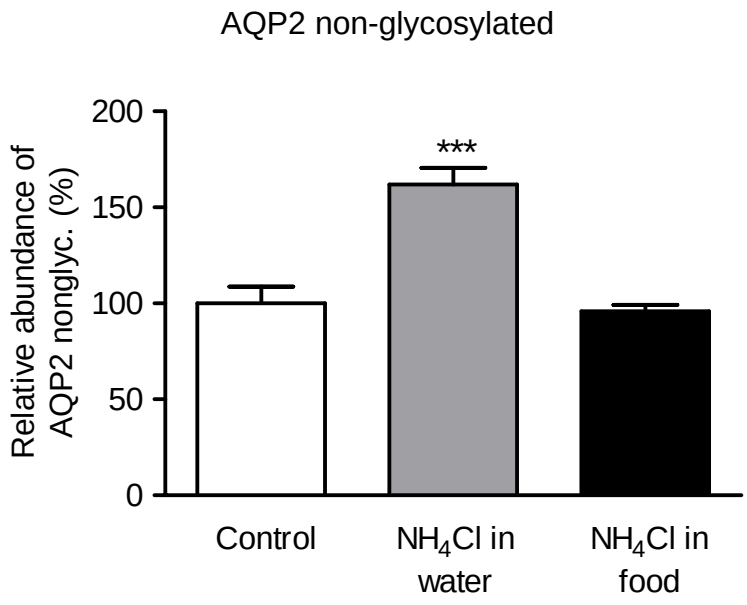
AQP2 non-glycosylated
Relative abundance of AQP2 nonglyc. (%)
200
150
100
50
0
***
Control
NH4Cl in water
NH4Cl in food

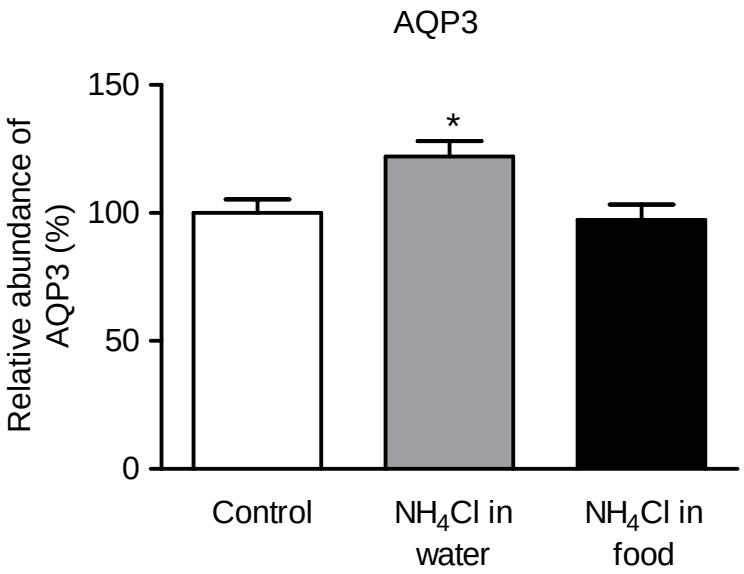
AQP3
Relative abundance of AQP3 (%)
150
100
50
0
*
Control
NH4Cl in water
NH4Cl in food

Figure 3

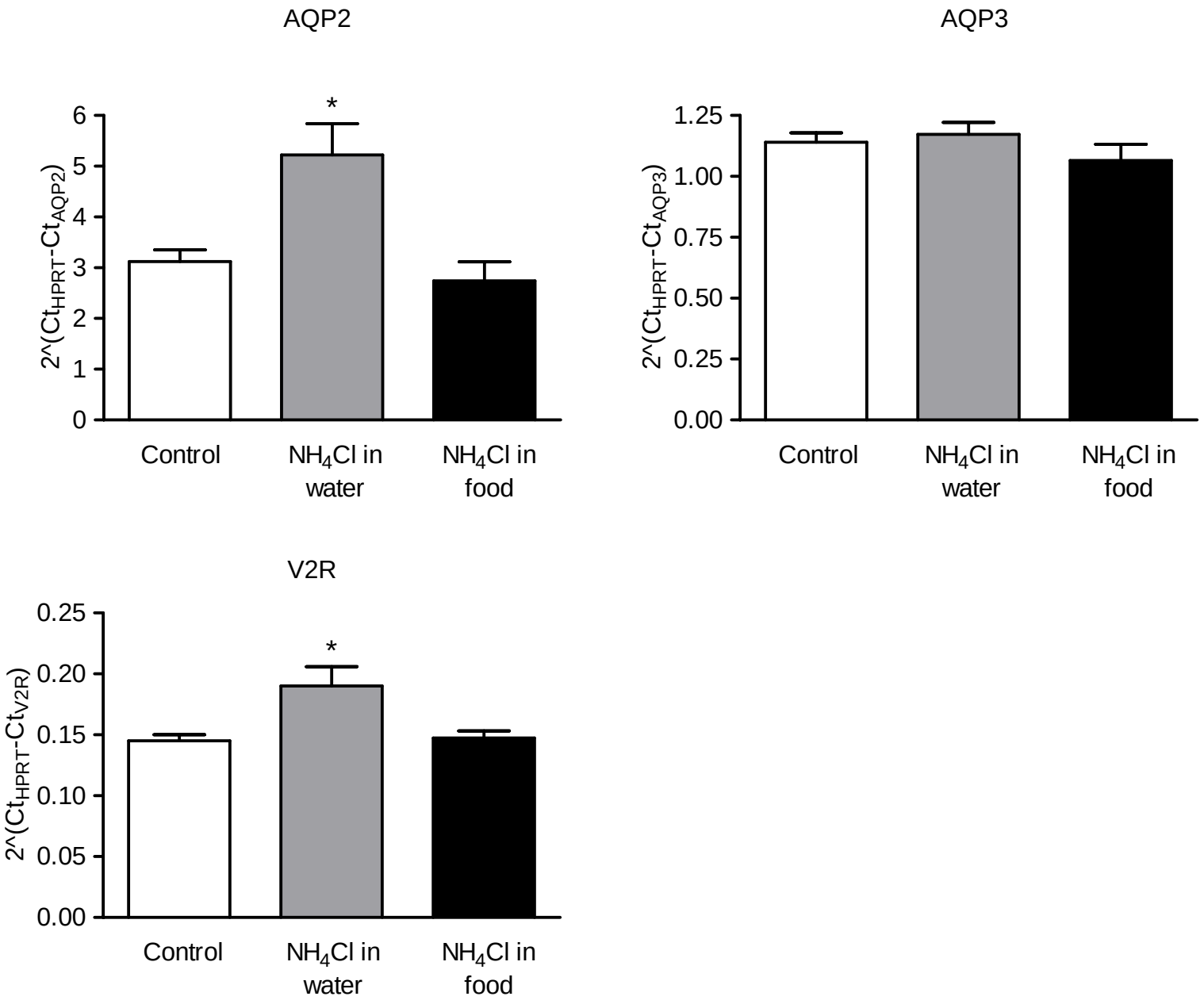
AQP2
2^(Ct$_{HPRT}$-Ct$_{AQP2}$)
0
1
2
3
4
5
6
*
Control
NH$_4$Cl in water
NH$_4$Cl in food
AQP3
2^(Ct$_{HPRT}$-Ct$_{AQP3}$)
0.00
0.25
0.50
0.75
1.00
1.25
Control
NH$_4$Cl in water
NH$_4$Cl in food
V2R
2^(Ct$_{HPRT}$-Ct$_{V2R}$)
0.00
0.05
0.10
0.15
0.20
0.25
*
Control
NH$_4$Cl in water
NH$_4$Cl in food

Figure 4 A

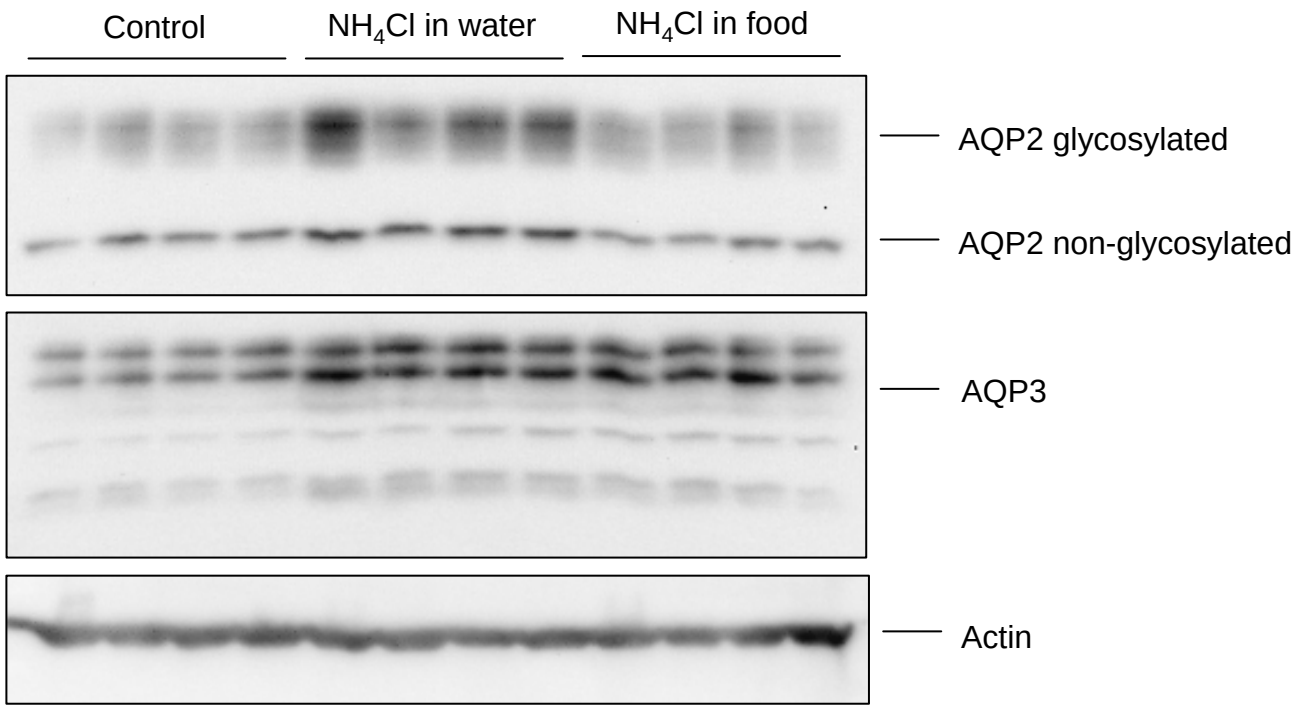
Control
NH4Cl in water
NH4Cl in food
AQP2 glycosylated
AQP2 non-glycosylated
AQP3
Actin

Figure 4 continued

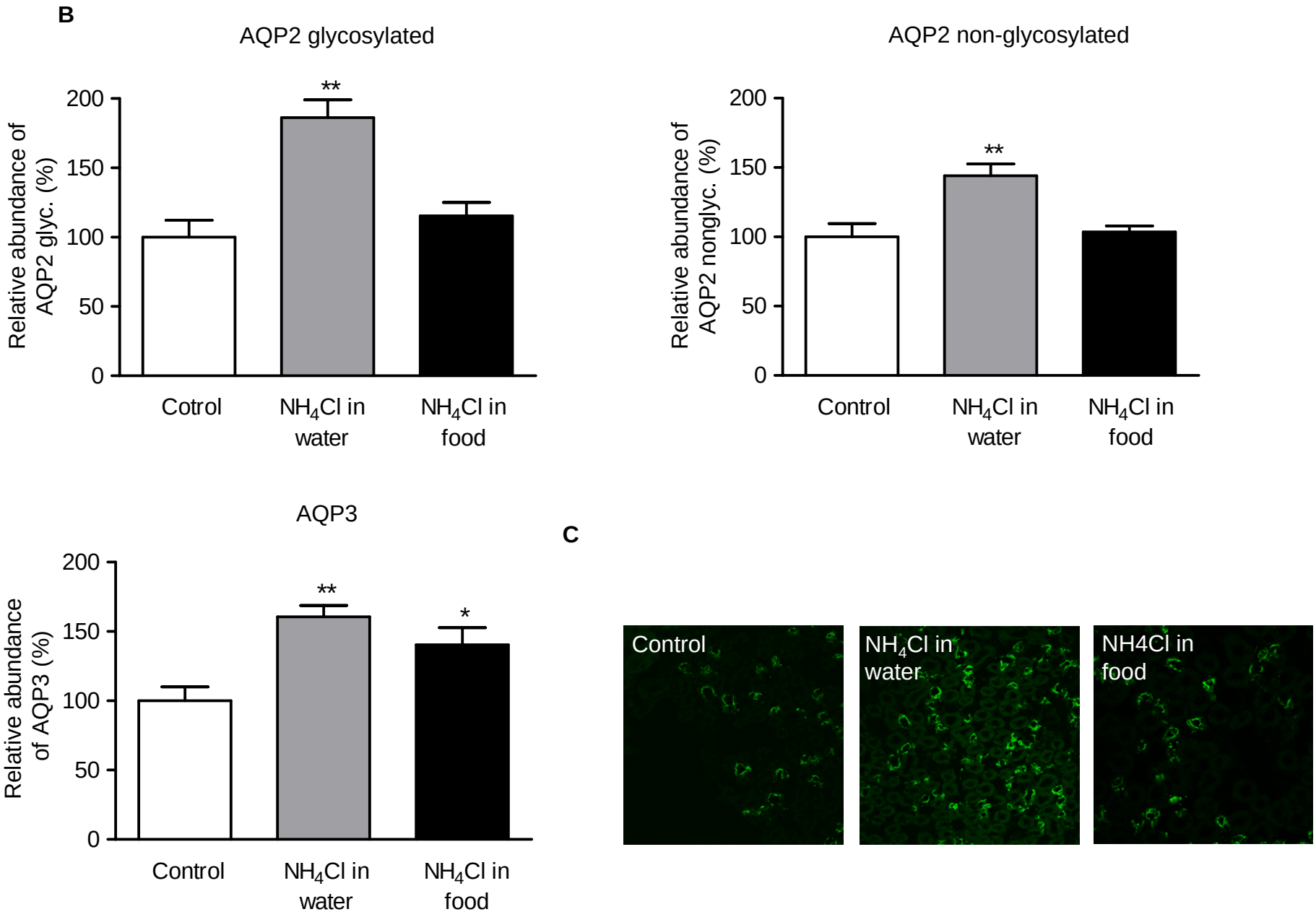

Figure 5

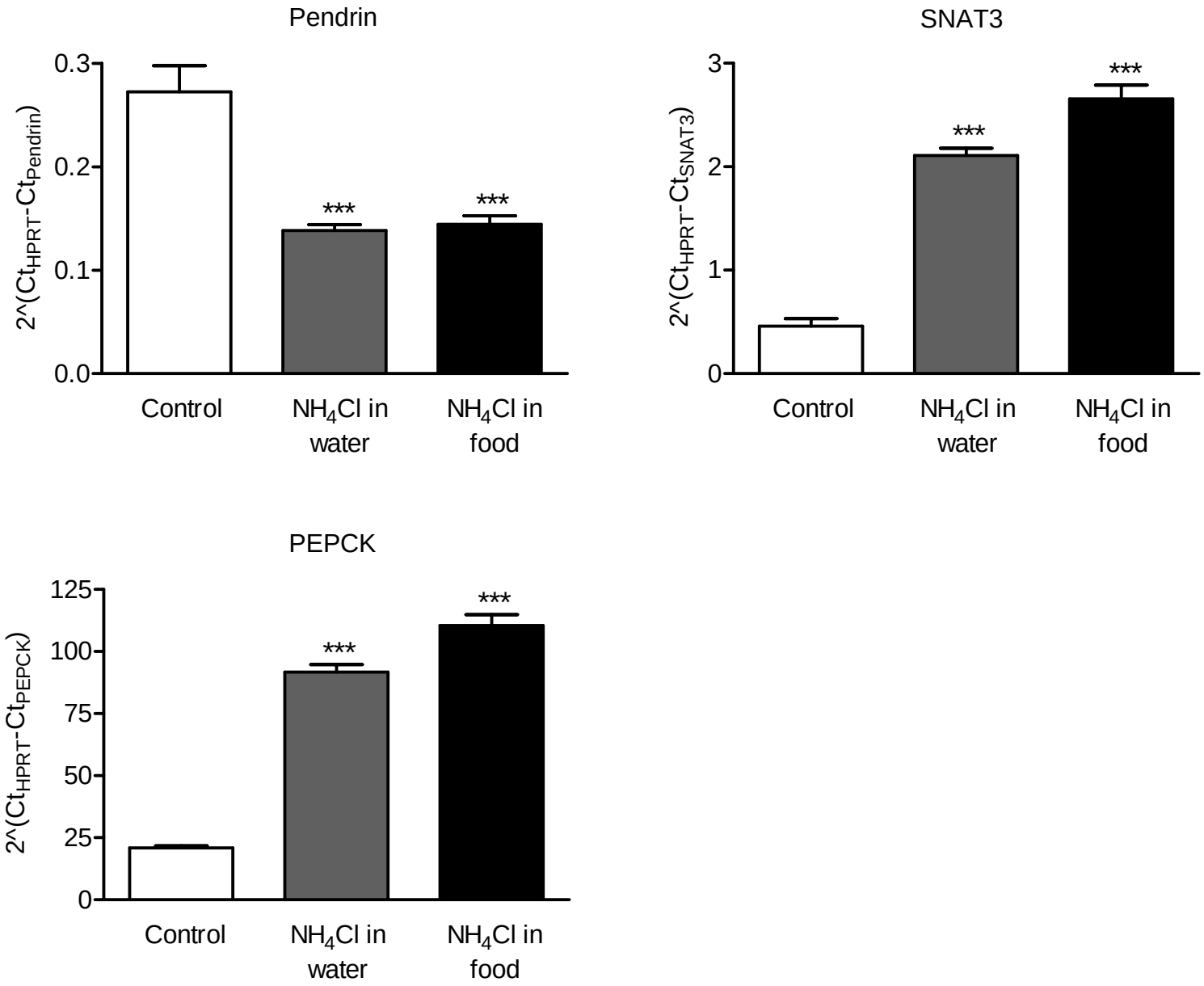
Pendrin
2^(Ct_HPRT-Ct_Pendrin)
0.3
0.2
0.1
0.0
***
***
Control
NH4Cl in water
NH4Cl in food
SNAT3
2^(Ct_HPRT-Ct_SNAT3)
3
2
1
0
***
***
Control
NH4Cl in water
NH4Cl in food
PEPCK
2^(Ct_HPRT-Ct_PEPCK)
125
100
75
50
25
0
***
***
Control
NH4Cl in water
NH4Cl in food

10. SUMMARY OF THE RESULTS

10.1 Genome wide detection of renal genes regulated during metabolic acidosis

To date little is known about global changes in expression of renal genes and proteins in response to metabolic acidosis. Here, we used microarray-based gene expression profiling to perform a genome-wide analysis of altered transcripts in response to acute (2 days) and chronic (7 days) MA in mouse kidneys.

Using microarray approach we found that nearly one third of all genes (approximately 12,000 transcripts) present on the chip could be detected in the kidney. Expression of over 4,000 genes was affected by acid-loading representing 30% of all expressed genes. Interestingly, the majority of acutely regulated genes after 2 days, returned to normal values after 7 days, suggesting that adaptation had occurred. Besides these temporal changes, we also detected differential regulation of selected genes (SNAT3, PEPCK, and PDG) between early and late proximal tubule. Pathway analysis revealed that a large group of transcripts, which expression was affected by acid-loading, belonged to oxidative phosphorylation, cell growth, proliferation, apoptosis, water homeostasis, and ammoniagenesis. Among them genes coding for solute carrier transporters (SLCs) were most represented.

In conclusion, the mammalian kidney responds to MA by temporally and spatially altering the expression of a large number of genes. Our analysis suggests that many of these genes may participate in various processes leading to adaptation and restoration of normal systemic acid-base and electrolyte homeostasis.

10.2 Molecular mechanisms for decreased renal phosphate reabsorption during metabolic acidosis

Increased phosphate secretion observed during MA belongs to one of the adaptive mechanism to increase titratable acid secretion. However, molecular mechanisms of phosphaturia have remained unclear. During microarray screening of kidneys from 2 and 7 days acidotic mice we found a strong downregulation of NaPi-IIc mRNA which may explain, at least partially, the phosphaturia observed. To further investigate the contribution of renal transporter regulation to phosphaturia, we induced MA for 2 and 7 days in normal and NaPi-IIa KO mice and analyzed the regulation of all known renal Na^+-dependent Pi cotransporters, namely, the type II NaPi-IIa and NaPi-IIc, and the type III, Pit1 and Pit2.

Our findings demonstrate that during NH_4Cl-induced metabolic acidosis in mouse 1) phosphaturia is only transient in wildtype mice and not further increased in NaPi-IIa deficient mice, 2) sodium-dependent phosphate transport activity is transiently increased in BBMV from wildtype mice and decreased in BBMV from NaPi-IIa deficient mice 3) NaPi-IIa and NaPi-IIc protein are upregulated, 4) NaPi-IIc mRNA strongly reduced, 5) NaPi-IIa and NaPi-IIc localization are not affected, and 6) Pit1 and Pit2 mRNA is increased after 7 days.

Our data indicate that phosphaturia during metabolic acidosis cannot be explained by downregulation of protein expression of luminal phosphate cotransporters. Thus, phosphaturia may be induced rather by direct interactions between protons and phosphate cotransporters reducing transport activity. The role of skeletal phosphate release and increased delivery to the kidney may be less important than previously suggested.

10.3 Induction of metabolic acidosis with ammonium chloride – some technical considerations

Microarray analysis of kidneys from 2 and 7 days acidotic mice revealed upregulation of a large number of genes involved in renal water transport, namely aquaporins 1-4 (AQP1-4), vasopressin receptor 2 (V2R), and the urea transporter (Slc14a2). However, acidotic mice consumed approximately 20% less water, which could have contributed to the regulation. Therefore, we wanted to clarify if the route of NH_4Cl application affects the physiologic response of the kidney and examined in rats and mice the induction of metabolic acidosis in response to the standard protocol 0.28M NH_4Cl in drinking water and compared it with equivalent NH_4Cl addition to food.

The major findings of our comparison of different NH_4Cl-loading protocols are: 1) both protocols induced metabolic acidosis in mice and rats, 2) differences between rats and mice exist with respect to their renal compensatory responses, 3) NH_4Cl in drinking water induces a mild, but clear dehydration in rats and mice, and 4) dehydration, but not MA affects expression patterns of genes and proteins involved in renal water handling.

These data demonstrate that the standard protocol inducing MA with NH_4Cl in drinking water is problematic and that application of NH_4Cl in food should be considered. Moreover, mice and rats respond differently to NH_4Cl loading, and increased water intake and diuresis and not antidiuresis may be a compensatory mechanism during MA.

10.4 Renal adaptation to metabolic acidosis – outlook and an integrative view

The kidney is a primary organ responsible for maintaining acid-base homeostasis. Under normal physiological condition the production and excretion of acids is balanced. However, during metabolic acidosis acid is accumulated that leads to a fall in plasma pH. The renal response to MA is complex and involves

increased synthesis and excretion of ammonia and other titratable acids, stimulation of proton excretion and bicarbonate reclamation, changes in electrolyte and water handling, and remodelling of the nephron.

Our findings confirm that the kidney adapts to changes in acid-base status on many different levels. Microarray profiling confirmed the pivotal role of ammoniagenesis and ATP synthesis in that process. Moreover, the regulation of a large number of genes involved in cytoskeleton organization, cell proliferation, cell differentiation and apoptosis highlights the importance of nephron remodelling / plasticity phenomenon in renal response. However, the role of specific pathways remains to be investigated. Although we successfully verified results of transcriptome profiling, it has to be emphasized that it is difficult to correlate mRNA expression levels with protein abundance. The sodium dependent Pi cotransporter NaPi-IIc was found to be strongly downregulated during microarray screening, but was surprisingly upregulated on protein level (88). Several studies similarly failed to detect a correlation between mRNA and protein expression (25, 49, 76, 119). However, an overall correlation of metabolic pathways and complexes of proteins that function together has been found indicating transcriptional control not at single loci, but of entire protein pathways (119). Furthermore, we observed spatial differences in regulation of genes involved in ammoniagenesis (PEPCK, SNAT3, PDG) between S1/S2 and S3 segment of the proximal tubule (87). Therefore we decided to investigate changes in protein abundance in proximal tubule (S1/S2 and S3 segment separately) during acute adaptation to MA.

To this end, we employed the SILAC mouse to study proximal tubule (S1/S2 and S3 segment) specific changes in protein expression after 2 days of NH_4Cl-induced MA. We identified and quantified more than 1,000 proteins in each of the two different subsegments of the proximal tubule, many of which were membrane proteins. Preliminary analysis indicates that SILAC technology combined with cDNA microarray will provide us with complex information about renal adaptation to MA. Selected pathways will be studied in more detail and their relevance tested using appropriate cell culture or preferably animal models.

PUBLICATIONS THAT DID NOT CONTRIBUTE TO THIS STUDY

11.1 Thyroid hormone deficiency alters expression of acid-base transporters in rat kidney

Nilufar Mohebbi, Jana Kovacikova, **Marta Nowik**, Carsten A. Wagner

Am J Physiol Renal Physiol (2007); 293(1):F416-27

Abstract:
Hypothyroidism in humans is associated with incomplete distal renal tubular acidosis, presenting as the inability to respond appropriately to an acid challenge by excreting less acid. Here, we induced hypothyroidism in rats with methimazole (HYPO) and in one group substituted with l-thyroxine (EU). After 4 wk, acid-base status was similar in both groups. However, after 24 h acid loading with NH_4Cl HYPO rats displayed a more pronounced metabolic acidosis. The expression of the Na^+/H^+ exchanger NHE3, the Na^+-phosphate cotransporter NaPi-IIa, and the B2 subunit of the vacuolar H^+-ATPase was reduced in the brush-border membrane of the proximal tubule of the HYPO group, paralleled by a lower abundance of the Na^+/HCO_3^- cotransporter NBCe1 and a higher expression of the acid-secretory type A intercalated cell-specific Cl^-/HCO_3^- exchanger AE1. In contrast to control conditions, the expression of NBCe1 was increased in the HYPO group during metabolic acidosis. In addition, net acid excretion was similar in both groups. The relative number of type A intercalated cells was increased in the connecting tubule and cortical collecting duct of the HYPO group during acidosis. Thus, thyroid hormones modulate the renal response to an acid challenge and alter the expression of several key acid-base transporters. Mild hypothyroidism is associated only with a very mild defect in renal acid handling, which appears to be mainly located in the proximal tubule and is compensated by the distal nephron.

11.2 Role of Rhesus factor RhCG in renal ammonium excretion and male fertility

Sophie Biver, Hendrica Belge, Soline Bourgeois, Pascale Van Vooren, **Marta Nowik**, Sophie Scohy, Pascal Houillier, Josiane Szpirer, Claude Szpirer, Carsten A. Wagner, Olivier Devuyst, Anna Maria Marini

Nature; manuscript in press

Abstract:
The kidney plays a major role in the regulation of acid-base homeostasis. Renal ammonium production and excretion are essential for net acid excretion under basal conditions and during metabolic acidosis. Ammonium is secreted into the urine by the collecting duct, a distal nephron segment, where ammonium transport is believed to occur through non-ionic NH_3 diffusion coupled to H^+ secretion. Here we show that this process is largely mediated by the Rhesus factor RhCG. Mice lacking RhCG display abnormal urinary acidification due to impaired ammonium excretion upon acid loading, a feature of distal renal tubular acidosis. *In vitro* microperfused collecting ducts of *Rhcg*$^{-/-}$ acid-loaded mice show reduced luminal permeability to NH_3 and impaired transepithelial NH_3 transport. Furthermore, RhCG is localized in epididymal epithelial cells and is required for normal fertility and epididymal fluid pH. We demonstrate that RhCG is important in the ammonium handling and pH homeostasis both in the kidney and the male reproductive tract.

11.3 Calcium-sensing receptor-mediated urinary acidification prevents renal stone formation

Kirsten Y. Renkema, Ana Velic, Henry B. Dijkman, Sjoerd Verkaart, Annemiete W. van der Kemp, **Marta Nowik**, Kim Timmermans, Alain Doucet, Carsten A. Wagner, René J. Bindels, and Joost G. Hoenderop

Proc Natl Acad Sci U S A; revision under consideration

Abstract:
Kidney stones form a major socio-economic problem in humans, involving severe pain, recurrent treatment, and eventually renal insufficiency. Hypercalciuria is a risk factor for urolithiasis and renal adaptive mechanisms are crucial in the prevention of renal stones. Transient receptor potential vanilloid 5 (TPRV5) knockout (TRPV5$^{-/-}$) mice exhibit robust urinary calcium (Ca^{2+}) wasting and concomitant hyperphosphaturia, but lack kidney stones. These hypercalciuric mice display significant polyuria and increased urinary acidification, pointing toward adaptation mechanisms preventing renal stone formation. Here, we demonstrated that exposure of dissected mouse outer medullary collecting ducts to 5.0 mM Ca^{2+} stimulates H^+-ATPase activity and increases the intracellular pH recovery rates compared with 0.1 mM Ca^{2+}. Ca^{2+}-sensing receptor (CaSR)-mediated activation of H^+-ATPase provoked urinary acidification, whereas downregulation of aquaporin-2 water channels induced polyuria in the TRPV5$^{-/-}$ mice. Gene ablation of the collecting duct-specific B1-subunit of H^+-ATPase in TRPV5$^{-/-}$ mice abolished the increased urinary acidification resulting in severe tubular precipitations of Ca^{2+}-phosphate in the renal medulla. In conclusion, activation of CaSR by augmented urinary Ca^{2+} levels triggers urinary acidification and polyuria. These beneficial adaptations facilitate the excretion of large amounts of soluble Ca^{2+}, which is crucial in the prevention of kidney stones.

11.4 Proliferation of acid-secretory cells in the kidney during adaptive remodelling of the collecting duct

Desa Bacic, **Marta Nowik**, Brigitte Kaissling, Carsten A. Wagner

Manuscript in preparation

Abstract:
The collecting duct is the main site controlling final urinary acidification through the activity of intercalated cells. At least two types of intercalated cells exist, type A (A-IC) and non-type A (B-IC). Acid secretory A-IC express apical H-ATPases and the basolateral bicarbonate exchanger AE1, whereas bicarbonate secretory B-IC express basolateral (and apical) H-ATPases and the apical bicarbonate exchanger pendrin. During metabolic acidosis the relative number of A-IC increases and B-IC is reduced, a phenomenon termed plasticity. It is thought that B-IC alter their phenotype and are converted into A-IC. We used markers of proliferation (PCNA, BrdU incorporation) and cell-specific markers for A-IC (AE1) and B-IC (pendrin) to investigate if proliferation of A-IC could provide an additional or alternative explanation for plasticity. Induction of remodelling in rats with metabolic acidosis (with NH_4Cl for 12 hrs, 4 and 7 days) or treatment with acetazolamide for 10 days resulted in a larger portion of AE1 positive cells in the cortical collecting duct. A large number of AE1 expressing A-IC was labelled with proliferative markers in the cortical and outer medullary collecting duct, whereas no staining was found in B-IC. Thus, during chronic acidosis proliferation of AE1 containing acid-secretory cells occurs and may contribute to the remodelling of the collecting duct.

REFERENCES

1. **Akiba T, Rocco VK, and Warnock DG**. Parallel adaptation of the rabbit renal cortical sodium/proton antiporter and sodium/bicarbonate cotransporter in metabolic acidosis and alkalosis. *The Journal of clinical investigation* 80: 308-315, 1987.

2. **Al-Awqati Q**. Plasticity in epithelial polarity of renal intercalated cells: targeting of the H(+)-ATPase and band 3. *The American journal of physiology* 270: C1571-1580, 1996.

3. **Al-Awqati Q, Norby LH, Mueller A, and Steinmetz PR**. Characteristics of stimulation of H+ transport by aldosterone in turtle urinary bladder. *The Journal of clinical investigation* 58: 351-358, 1976.

4. **Al-Awqati Q, Vijayakumar S, Takito J, Hikita C, Yan L, and Wiederholt T**. Phenotypic plasticity and terminal differentiation of the intercalated cell: the hensin pathway. *Experimental nephrology* 8: 66-71, 2000.

5. **Alper SL**. Genetic diseases of acid-base transporters. *Annual review of physiology* 64: 899-923, 2002.

6. **Alper SL, Natale J, Gluck S, Lodish HF, and Brown D**. Subtypes of intercalated cells in rat kidney collecting duct defined by antibodies against erythroid band 3 and renal vacuolar H+-ATPase. *Proceedings of the National Academy of Sciences of the United States of America* 86: 5429-5433, 1989.

7. **Ambuhl PM, Amemiya M, Danczkay M, Lotscher M, Kaissling B, Moe OW, Preisig PA, and Alpern RJ**. Chronic metabolic acidosis increases NHE3 protein abundance in rat kidney. *The American journal of physiology* 271: F917-925, 1996.

8. **Ambuhl PM, Zajicek HK, Wang H, Puttaparthi K, and Levi M**. Regulation of renal phosphate transport by acute and chronic metabolic acidosis in the rat. *Kidney international* 53: 1288-1298, 1998.

9. **Amlal H, Sheriff S, and Soleimani M**. Upregulation of collecting duct aquaporin-2 by metabolic acidosis: role of vasopressin. *Am J Physiol Cell Physiol* 286: C1019-1030, 2004.

10. **Balagura S, and Pitts RF**. Excretion of ammonia injected into renal artery. *The American journal of physiology* 203: 11-14, 1962.

11. **Barreto-Chaves ML, and Mello-Aires M**. Effect of luminal angiotensin II and ANP on early and late cortical distal tubule HCO3- reabsorption. *The American journal of physiology* 271: F977-984, 1996.

12. **Bastani B, Purcell H, Hemken P, Trigg D, and Gluck S**. Expression and distribution of renal vacuolar proton-translocating adenosine triphosphatase in response to chronic acid and alkali loads in the rat. *The Journal of clinical investigation* 88: 126-136, 1991.

13. **Beck L, Karaplis AC, Amizuka N, Hewson AS, Ozawa H, and Tenenhouse HS**. Targeted inactivation of Npt2 in mice leads to severe renal phosphate wasting, hypercalciuria, and skeletal abnormalities. *Proceedings of the National Academy of Sciences of the United States of America* 95: 5372-5377, 1998.

14. **Biver S, Belge H, Bourgeois S, Van Vooren P, Nowik M, Scohy S, Houillier P, Szpirer J, Szpirer C, Wagner CA, Devuyst O, and Marini AM**. Role of Rhesus factor RhCG in renal ammonium excretion and male fertility. *Nature* Accepted: 2008.

15. **Boron W**. Acid-base physiology. In: *Medical Physiology*, edited by Boron W, Boulpaep, ELElsevier Science (USA), 2003, p. 633-653.

16. **Brandes A, Oehlke O, Schumann A, Heidrich S, Thevenod F, and Roussa E**. Adaptive redistribution of NBCe1-A and NBCe1-B in rat kidney proximal tubule and striated ducts of salivary glands during acid-base disturbances. *Am J Physiol Regul Integr Comp Physiol* 293: R2400-2411, 2007.

17. **Brown D, Hirsch S, and Gluck S**. An H+-ATPase in opposite plasma membrane domains in kidney epithelial cell subpopulations. *Nature* 331: 622-624, 1988.

18. **Bruce LJ, Cope DL, Jones GK, Schofield AE, Burley M, Povey S, Unwin RJ, Wrong O, and Tanner MJ**. Familial distal renal tubular acidosis is associated with mutations in the red cell anion exchanger (Band 3, AE1) gene. *The Journal of clinical investigation* 100: 1693-1707, 1997.

19. **Bushinsky DA, Chabala JM, Gavrilov KL, and Levi-Setti R**. Effects of in vivo metabolic acidosis on midcortical bone ion composition. *The American journal of physiology* 277: F813-819, 1999.

20. **Bushinsky DA, Smith SB, Gavrilov KL, Gavrilov LF, Li J, and Levi-Setti R**. Chronic acidosis-induced alteration in bone bicarbonate and phosphate. *American journal of physiology* 285: F532-539, 2003.

21. **Capasso G, Unwin R, Agulian S, and Giebisch G**. Bicarbonate transport along the loop of Henle. I. Microperfusion studies of load and inhibitor sensitivity. *The Journal of clinical investigation* 88: 430-437, 1991.

22. **Capasso G, Unwin R, Rizzo M, Pica A, and Giebisch G**. Bicarbonate transport along the loop of Henle: molecular mechanisms and regulation. *Journal of nephrology* 15 Suppl 5: S88-96, 2002.

23. **Chambrey R, Paillard M, and Podevin RA**. Enzymatic and functional evidence for adaptation of the vacuolar H(+)-ATPase in proximal tubule apical membranes from rats with chronic metabolic acidosis. *The Journal of biological chemistry* 269: 3243-3250, 1994.

24. **Chan YL, and Giebisch G**. Relationship between sodium and bicarbonate transport in the rat proximal convoluted tubule. *The American journal of physiology* 240: F222-230, 1981.

25. **Chen G, Gharib TG, Huang CC, Taylor JM, Misek DE, Kardia SL, Giordano TJ, Iannettoni MD, Orringer MB, Hanash SM, and Beer DG**. Discordant protein and mRNA expression in lung adenocarcinomas. *Mol Cell Proteomics* 1: 304-313, 2002.

26. **Chen Y, Cann MJ, Litvin TN, Iourgenko V, Sinclair ML, Levin LR, and Buck J**. Soluble adenylyl cyclase as an evolutionarily conserved bicarbonate sensor. *Science (New York, NY* 289: 625-628, 2000.

27. **Cheval L, Morla L, Elalouf JM, and Doucet A**. Kidney collecting duct acid-base "regulon". *Physiological genomics* 27: 271-281, 2006.

28. **Chobanian MC, and Julin CM**. Angiotensin II stimulates ammoniagenesis in canine renal proximal tubule segments. *The American journal of physiology* 260: F19-26, 1991.

29. **Curthoys NP, and Gstraunthaler G**. Mechanism of increased renal gene expression during metabolic acidosis. *American journal of physiology* 281: F381-390, 2001.

30. **Curthoys NP, Taylor L, Hoffert JD, and Knepper MA**. Proteomic analysis of the adaptive response of rat renal proximal tubules to metabolic acidosis. *American journal of physiology* 292: F140-147, 2007.

31. **Dinour D, Chang MH, Satoh J, Smith BL, Angle N, Knecht A, Serban I, Holtzman EJ, and Romero MF**. A novel missense mutation in the sodium bicarbonate cotransporter (NBCe1/SLC4A4) causes proximal tubular acidosis and glaucoma through ion transport defects. *The Journal of biological chemistry* 279: 52238-52246, 2004.

32. **DuBose TJ, Alpern, RJ**. Renal tubular acidosis. In: *The metabolic and molecular bases of inherited disease*, edited by Scriver CR B, L, Sly WS, Valle, D. New York: McGraw-Hill, 2001, p. 4983-5021.

33. **Duggan DJ, Bittner M, Chen Y, Meltzer P, and Trent JM**. Expression profiling using cDNA microarrays. *Nature genetics* 21: 10-14, 1999.

34. **Duong JP, Huyen V, Cheval L, Bloch-Faure M, Belair MF, Heudes D, Bruneval P, and Doucet A**. GDF15 Triggers Homeostatic Proliferation of Acid-Secreting Collecting Duct Cells. *J Am Soc Nephrol* 2008.

35. **Eladari D, Cheval L, Quentin F, Bertrand O, Mouro I, Cherif-Zahar B, Cartron JP, Paillard M, Doucet A, and Chambrey R**. Expression of RhCG, a new putative NH(3)/NH(4)(+) transporter, along the rat nephron. *J Am Soc Nephrol* 13: 1999-2008, 2002.

36. **Faroqui S, Sheriff S, and Amlal H**. Metabolic acidosis has dual effects on sodium handling by rat kidney. *American journal of physiology* 291: F322-331, 2006.

37. **Fejes-Toth G, and Naray-Fejes-Toth A**. Differentiation of renal beta-intercalated cells to alpha-intercalated and principal cells in culture. *Proceedings of the National Academy of Sciences of the United States of America* 89: 5487-5491, 1992.

38. **Field M, Pollock, C, Harris, D**. Acid-base balance and regulation of pH. In: *The renal system*2001, p. 49-61.

39. **Frische S, Kwon TH, Frokiaer J, Madsen KM, and Nielsen S**. Regulated expression of pendrin in rat kidney in response to chronic NH4Cl or NaHCO3 loading. *American journal of physiology* 284: F584-593, 2003.

40. **Fry AC, and Karet FE**. Inherited renal acidoses. *Physiology (Bethesda, Md* 22: 202-211, 2007.

41. **Furuya H, Breyer MD, and Jacobson HR**. Functional characterization of alpha- and beta-intercalated cell types in rabbit cortical collecting duct. *The American journal of physiology* 261: F377-385, 1991.

42. **Garvin JL**. Angiotensin stimulates bicarbonate transport and Na+/K+ ATPase in rat proximal straight tubules. *J Am Soc Nephrol* 1: 1146-1152, 1991.

43. **Gawenis LR, Bradford EM, Prasad V, Lorenz JN, Simpson JE, Clarke LL, Woo AL, Grisham C, Sanford LP, Doetschman T, Miller ML, and Shull GE**. Colonic anion secretory defects and metabolic acidosis in mice lacking the NBC1 Na+/HCO3- cotransporter. *The Journal of biological chemistry* 282: 9042-9052, 2007.

44. **Geibel J, Giebisch G, and Boron WF**. Angiotensin II stimulates both Na(+)-H+ exchange and Na+/HCO3- cotransport in the rabbit proximal tubule. *Proceedings of the National Academy of Sciences of the United States of America* 87: 7917-7920, 1990.

45. **Gibson G**. Microarray analysis: genome-scale hypothesis scanning. *PLoS biology* 1: E15, 2003.

46. **Giebisch G, Windhager, E**. Organization of the urinary system. In: *Medical physiology*, edited by Boron F, Boulpaep, ELElsevier Science (USA), 2003, p. 737-756.

47. **Giebisch G, Windhager, E**. Transport of acids and bases. In: *Medical physiology*, edited by Boron F, Boulpaep, ELElsevier Science (USA), 2003, p. 845-860.

48. **Guntupalli J, Eby B, and Lau K**. Mechanism for the phosphaturia of NH4Cl: dependence on acidemia but not on diet PO4 or PTH. *The American journal of physiology* 242: F552-560, 1982.

49. **Gygi SP, Rochon Y, Franza BR, and Aebersold R**. Correlation between protein and mRNA abundance in yeast. *Molecular and cellular biology* 19: 1720-1730, 1999.

50. **Gyorke ZS, Sulyok E, and Guignard JP**. Ammonium chloride metabolic acidosis and the activity of renin-angiotensin-aldosterone system in children. *European journal of pediatrics* 150: 547-549, 1991.

51. **Haldane JB**. Experiments on the regulation of the blood's alkalinity: II. *J Physiol* 55: 265-275, 1921.

52. **Henger A, Tutt P, Riesen WF, Hulter HN, and Krapf R**. Acid-base and endocrine effects of aldosterone and angiotensin II inhibition in metabolic acidosis in human patients. *The Journal of laboratory and clinical medicine* 136: 379-389, 2000.

53. **Horita S, Yamada H, Inatomi J, Moriyama N, Sekine T, Igarashi T, Endo Y, Dasouki M, Ekim M, Al-Gazali L, Shimadzu M, Seki G, and Fujita T**. Functional analysis of NBC1 mutants associated with proximal renal tubular acidosis and ocular abnormalities. *J Am Soc Nephrol* 16: 2270-2278, 2005.

54. **Hwang JJ, and Curthoys NP**. Effect of acute alterations in acid-base balance on rat renal glutaminase and phosphoenolpyruvate carboxykinase gene expression. *The Journal of biological chemistry* 266: 9392-9396, 1991.

55. **Hwang JJ, Perera S, Shapiro RA, and Curthoys NP**. Mechanism of altered renal glutaminase gene expression in response to chronic acidosis. *Biochemistry* 30: 7522-7526, 1991.

56. **Ibrahim H, Lee YJ, and Curthoys NP**. Renal response to metabolic acidosis: role of mRNA stabilization. *Kidney international* 73: 11-18, 2008.

57. **Ikebe M, Nonoguchi H, Nakayama Y, Tashima Y, and Tomita K**. Upregulation of the secretory-type Na(+)/K(+)/2Cl(-)-cotransporter in the kidney by metabolic acidosis and dehydration in rats. *J Am Soc Nephrol* 12: 423-430, 2001.

58. **Kaiser S, Hwang JJ, Smith H, Banner C, Welbourne TC, and Curthoys NP**. Effect of altered acid-base balance and of various agonists on levels of renal glutamate dehydrogenase mRNA. *The American journal of physiology* 262: F507-512, 1992.

59. **Karet FE, Finberg KE, Nelson RD, Nayir A, Mocan H, Sanjad SA, Rodriguez-Soriano J, Santos F, Cremers CW, Di Pietro A, Hoffbrand BI, Winiarski J, Bakkaloglu A, Ozen S, Dusunsel R, Goodyer P, Hulton SA, Wu DK, Skvorak AB, Morton CC, Cunningham MJ, Jha V, and Lifton RP**. Mutations in the gene encoding B1 subunit of H+-ATPase cause renal tubular acidosis with sensorineural deafness. *Nature genetics* 21: 84-90, 1999.

60. **Karet FE, Gainza FJ, Gyory AZ, Unwin RJ, Wrong O, Tanner MJ, Nayir A, Alpay H, Santos F, Hulton SA, Bakkaloglu A, Ozen S, Cunningham MJ, di Pietro A, Walker WG, and Lifton RP**. Mutations in the chloride-bicarbonate exchanger gene AE1 cause autosomal dominant but not autosomal recessive distal renal tubular acidosis. *Proceedings of the National Academy of Sciences of the United States of America* 95: 6337-6342, 1998.

61. **Karinch AM, Lin CM, Wolfgang CL, Pan M, and Souba WW**. Regulation of expression of the SN1 transporter during renal adaptation to chronic metabolic acidosis in rats. *American journal of physiology* 283: F1011-1019, 2002.

62. **Kim GH, Martin SW, Fernandez-Llama P, Masilamani S, Packer RK, and Knepper MA**. Long-term regulation of renal Na-dependent cotransporters and ENaC: response to altered acid-base intake. *American journal of physiology* 279: F459-467, 2000.

63. **Kim J, Kim YH, Cha JH, Tisher CC, and Madsen KM**. Intercalated cell subtypes in connecting tubule and cortical collecting duct of rat and mouse. *J Am Soc Nephrol* 10: 1-12, 1999.

64. **Kinsella JL, and Aronson PS**. Interaction of NH4+ and Li+ with the renal microvillus membrane Na+-H+ exchanger. *The American journal of physiology* 241: C220-226, 1981.

65. **Kruger M, Moser M, Ussar S, Thievessen I, Luber CA, Forner F, Schmidt S, Zanivan S, Fassler R, and Mann M**. SILAC mouse for quantitative proteomics uncovers kindlin-3 as an essential factor for red blood cell function. *Cell* 134: 353-364, 2008.

66. **Kunau RT, Jr., Hart JI, and Walker KA**. Effect of metabolic acidosis on proximal tubular total CO2 absorption. *The American journal of physiology* 249: F62-68, 1985.

67. **Kurella M, Hsiao LL, Yoshida T, Randall JD, Chow G, Sarang SS, Jensen RV, and Gullans SR**. DNA microarray analysis of complex biologic processes. *J Am Soc Nephrol* 12: 1072-1078, 2001.

68. **Laghmani K, Borensztein P, Ambuhl P, Froissart M, Bichara M, Moe OW, Alpern RJ, and Paillard M**. Chronic metabolic acidosis enhances NHE-3 protein abundance and transport activity in the rat thick ascending limb by increasing NHE-3 mRNA. *The Journal of clinical investigation* 99: 24-30, 1997.

69. **Lemann J, Jr., Litzow JR, and Lennon EJ**. The effects of chronic acid loads in normal man: further evidence for the participation of bone mineral in the defense against chronic metabolic acidosis. *The Journal of clinical investigation* 45: 1608-1614, 1966.

70. **Levine DZ, Iacovitti M, Buckman S, Hincke MT, Luck B, and Fryer JN**. ANG II-dependent HCO3- reabsorption in surviving rat distal tubules: expression/activation of H(+)-ATPase. *The American journal of physiology* 272: F799-808, 1997.

71. **Levine DZ, Iacovitti M, Luck B, Hincke MT, Burns KD, and Fryer JN**. Surviving rat distal tubule bicarbonate reabsorption: effects of chronic AT(1) blockade. *American journal of physiology* 278: F476-483, 2000.

72. **Levine DZ, and Nash LA**. Effect of chronic NH4Cl acidosis on proximal tubular H2O and HCO3 reabsorption. *The American journal of physiology* 225: 380-384, 1973.

73. **Li HC, Szigligeti P, Worrell RT, Matthews JB, Conforti L, and Soleimani M**. Missense mutations in Na+:HCO3- cotransporter NBC1 show abnormal trafficking in polarized kidney cells: a basis of proximal renal tubular acidosis. *American journal of physiology* 289: F61-71, 2005.

74. **Li S, Sato S, Yang X, Preisig PA, and Alpern RJ**. Pyk2 activation is integral to acid stimulation of sodium/hydrogen exchanger 3. *The Journal of clinical investigation* 114: 1782-1789, 2004.

75. **Liang M, Cowley AW, Jr., Hessner MJ, Lazar J, Basile DP, and Pietrusz JL**. Transcriptome analysis and kidney research: toward systems biology. *Kidney international* 67: 2114-2122, 2005.

76. **Lichtinghagen R, Musholt PB, Lein M, Romer A, Rudolph B, Kristiansen G, Hauptmann S, Schnorr D, Loening SA, and Jung K**. Different mRNA and protein expression of matrix metalloproteinases 2 and 9 and tissue inhibitor of metalloproteinases 1 in benign and malignant prostate tissue. *European urology* 42: 398-406, 2002.

77. **Liu FY, and Cogan MG**. Angiotensin II: a potent regulator of acidification in the rat early proximal convoluted tubule. *The Journal of clinical investigation* 80: 272-275, 1987.

78. **Ludwig MG, Vanek M, Guerini D, Gasser JA, Jones CE, Junker U, Hofstetter H, Wolf RM, and Seuwen K**. Proton-sensing G-protein-coupled receptors. *Nature* 425: 93-98, 2003.

79. **Makhanova N, Lee G, Takahashi N, Sequeira Lopez ML, Gomez RA, Kim HS, and Smithies O**. Kidney function in mice lacking aldosterone. *American journal of physiology* 290: F61-69, 2006.

80. **Merot J, Giebisch G, and Geibel J**. Intracellular acidification induces Cl/HCO3 exchange activity in the basolateral membrane of beta-intercalated cells of the rabbit cortical collecting duct. *The Journal of membrane biology* 159: 253-262, 1997.

81. **Moret C, Dave MH, Schulz N, Jiang JX, Verrey F, and Wagner CA**. Regulation of renal amino acid transporters during metabolic acidosis. *American journal of physiology* 292: F555-566, 2007.

82. **Mori T, Inoue T, Nanoguchi H, Nakayama Y, Kohda Y, Machida K, and Tomita K**. Reduced urinary excretion of aquaporin 2 in metabolic acidosis (Abstract). *J Am Soc Nephrol* 273A, 2002.

83. **Murer H, Hernando N, Forster I, and Biber J**. Regulation of Na/Pi transporter in the proximal tubule. *Annual review of physiology* 65: 531-542, 2003.

84. **Nagami G**. Renal ammonia production and excretion. In: *The kidney: physiology and pathophysiology*, edited by Seldin D, Giebisch, G. New York, London: Lippincott Williams & Wilkins, 2000, p. 1995-2013.

85. **Nijenhuis T, Renkema KY, Hoenderop JG, and Bindels RJ**. Acid-base status determines the renal expression of Ca2+ and Mg2+ transport proteins. *J Am Soc Nephrol* 17: 617-626, 2006.

86. **Nonoguchi H, Inoue T, Mori T, Nakayama Y, Kohda Y, and Tomita K**. Regulation of aquaporin-2 by metabolic acidosis. *Am J Physiol Cell Physiol* 287: C824; author reply C814-825, 2004.

87. **Nowik M, Lecca MR, Velic A, Rehrauer H, Brandli AW, and Wagner CA**. Genome-wide gene expression profiling reveals renal genes regulated during metabolic acidosis. *Physiological genomics* 32: 322-334, 2008.

88. **Nowik M, Picard N, Stange G, Capuano P, Tenenhouse HS, Biber J, Murer H, and Wagner CA**. Renal phosphaturia during metabolic acidosis revisited: molecular mechanisms for decreased renal phosphate reabsorption. *Pflugers Arch* 2008.

89. **Ong SE, Blagoev B, Kratchmarova I, Kristensen DB, Steen H, Pandey A, and Mann M**. Stable isotope labeling by amino acids in cell culture, SILAC, as

a simple and accurate approach to expression proteomics. *Mol Cell Proteomics* 1: 376-386, 2002.

90. **Orloff J, and Berliner RW**. The mechanism of the excretion of ammonia in the dog. *The Journal of clinical investigation* 35: 223-235, 1956.

91. **Pastor-Soler N, Beaulieu V, Litvin TN, Da Silva N, Chen Y, Brown D, Buck J, Levin LR, and Breton S**. Bicarbonate-regulated adenylyl cyclase (sAC) is a sensor that regulates pH-dependent V-ATPase recycling. *The Journal of biological chemistry* 278: 49523-49529, 2003.

92. **Paunescu TG, Da Silva N, Russo LM, McKee M, Lu HA, Breton S, and Brown D**. Association of soluble adenylyl cyclase with the V-ATPase in renal epithelial cells. *American journal of physiology* 294: F130-138, 2008.

93. **Pitts R**. Renal excretion of acid. *Federation Proc* 7: 418-426, 1948.

94. **Porter R, Kaplan, JL, Homeier, BP, Beers, MH**. Acid-base disorders Merck Research Laboratories. http://www.merck.com/mmpe/sec12/ch157/ch157b.html.

95. **Promeneur D, Kwon TH, Yasui M, Kim GH, Frokiaer J, Knepper MA, Agre P, and Nielsen S**. Regulation of AQP6 mRNA and protein expression in rats in response to altered acid-base or water balance. *American journal of physiology* 279: F1014-1026, 2000.

96. **Quentin F, Eladari D, Cheval L, Lopez C, Goossens D, Colin Y, Cartron JP, Paillard M, and Chambrey R**. RhBG and RhCG, the putative ammonia transporters, are expressed in the same cells in the distal nephron. *J Am Soc Nephrol* 14: 545-554, 2003.

97. **Rizzo M, Capasso G, Bleich M, Pica A, Grimaldi D, Bindels RJ, and Greger R**. Effect of chronic metabolic acidosis on calbindin expression along the rat distal tubule. *J Am Soc Nephrol* 11: 203-210, 2000.

98. **Rothenberger F, Velic A, Stehberger PA, Kovacikova J, and Wagner CA**. Angiotensin II stimulates vacuolar H+ -ATPase activity in renal acid-secretory intercalated cells from the outer medullary collecting duct. *J Am Soc Nephrol* 18: 2085-2093, 2007.

99. **Schena M, Shalon D, Heller R, Chai A, Brown PO, and Davis RW**. Parallel human genome analysis: microarray-based expression monitoring of 1000 genes. *Proceedings of the National Academy of Sciences of the United States of America* 93: 10614-10619, 1996.

100. **Schoolwerth AC, deBoer PA, Moorman AF, and Lamers WH**. Changes in mRNAs for enzymes of glutamine metabolism in kidney and liver during

ammonium chloride acidosis. *The American journal of physiology* 267: F400-406, 1994.

101. **Schuster VL**. Function and regulation of collecting duct intercalated cells. *Annual review of physiology* 55: 267-288, 1993.

102. **Schwartz GJ, and Al-Awqati Q**. Regulation of transepithelial H+ transport by exocytosis and endocytosis. *Annual review of physiology* 48: 153-161, 1986.

103. **Schwartz GJ, Barasch J, and Al-Awqati Q**. Plasticity of functional epithelial polarity. *Nature* 318: 368-371, 1985.

104. **Segawa H, Kaneko I, Takahashi A, Kuwahata M, Ito M, Ohkido I, Tatsumi S, and Miyamoto K**. Growth-related renal type II Na/Pi cotransporter. *The Journal of biological chemistry* 277: 19665-19672, 2002.

105. **Seuwen K, Ludwig MG, and Wolf RM**. Receptors for protons or lipid messengers or both? *Journal of receptor and signal transduction research* 26: 599-610, 2006.

106. **Sly W, Shah, GN**. The carbonic anhydrase II deficiency syndrome: osteopetrosis with renal tubular acidosis and cerebral calcification. In: *Thr metabolic and molecular bases of inherited desease*, edited by Scriver CR B, L, Sly WS, Valle, D. New York: McGraw Hill, 2001, p. 5331-5343.

107. **Smith AN, Skaug J, Choate KA, Nayir A, Bakkaloglu A, Ozen S, Hulton SA, Sanjad SA, Al-Sabban EA, Lifton RP, Scherer SW, and Karet FE**. Mutations in ATP6N1B, encoding a new kidney vacuolar proton pump 116-kD subunit, cause recessive distal renal tubular acidosis with preserved hearing. *Nature genetics* 26: 71-75, 2000.

108. **Solbu TT, Boulland JL, Zahid W, Lyamouri Bredahl MK, Amiry-Moghaddam M, Storm-Mathisen J, Roberg BA, and Chaudhry FA**. Induction and targeting of the glutamine transporter SN1 to the basolateral membranes of cortical kidney tubule cells during chronic metabolic acidosis suggest a role in pH regulation. *J Am Soc Nephrol* 16: 869-877, 2005.

109. **Stauber A, Radanovic T, Stange G, Murer H, Wagner CA, and Biber J**. Regulation of intestinal phosphate transport. II. Metabolic acidosis stimulates Na(+)-dependent phosphate absorption and expression of the Na(+)-P(i) cotransporter NaPi-IIb in small intestine. *Am J Physiol Gastrointest Liver Physiol* 288: G501-506, 2005.

110. **Stehberger PA, Schulz N, Finberg KE, Karet FE, Giebisch G, Lifton RP, Geibel JP, and Wagner CA**. Localization and regulation of the ATP6V0A4 (a4) vacuolar H+-ATPase subunit defective in an inherited form of distal renal tubular acidosis. *J Am Soc Nephrol* 14: 3027-3038, 2003.

111. **Stehberger PA, Shmukler BE, Stuart-Tilley AK, Peters LL, Alper SL, and Wagner CA**. Distal renal tubular acidosis in mice lacking the AE1 (band3) Cl-/HCO3- exchanger (slc4a1). *J Am Soc Nephrol* 18: 1408-1418, 2007.

112. **Tashima Y, Kohda Y, Nonoguchi H, Ikebe M, Machida K, Star RA, and Tomita K**. Intranephron localization and regulation of the V1a vasopressin receptor during chronic metabolic acidosis and dehydration in rats. *Pflugers Arch* 442: 652-661, 2001.

113. **Wagner CA, Finberg KE, Breton S, Marshansky V, Brown D, and Geibel JP**. Renal vacuolar H+-ATPase. *Physiological reviews* 84: 1263-1314, 2004.

114. **Wagner CA, and Geibel JP**. Acid-base transport in the collecting duct. *Journal of nephrology* 15 Suppl 5: S112-127, 2002.

115. **Wagner CA, Giebisch G, Lang F, and Geibel JP**. Angiotensin II stimulates vesicular H+-ATPase in rat proximal tubular cells. *Proceedings of the National Academy of Sciences of the United States of America* 95: 9665-9668, 1998.

116. **Wagner CA, Kovacikova J, Stehberger PA, Winter C, Benabbas C, and Mohebbi N**. Renal acid-base transport: old and new players. *Nephron Physiol* 103: p1-6, 2006.

117. **Wall SM, Knepper MA, Hassell KA, Fischer MP, Shodeinde A, Shin W, Pham TD, Meyer JW, Lorenz JN, Beierwaltes WH, Dietz JR, Shull GE, and Kim YH**. Hypotension in NKCC1 null mice: role of the kidneys. *American journal of physiology* 290: F409-416, 2006.

118. **Wang T, Egbert AL, Jr., Aronson PS, and Giebisch G**. Effect of metabolic acidosis on NaCl transport in the proximal tubule. *The American journal of physiology* 274: F1015-1019, 1998.

119. **Washburn MP, Koller A, Oshiro G, Ulaszek RR, Plouffe D, Deciu C, Winzeler E, and Yates JR, 3rd**. Protein pathway and complex clustering of correlated mRNA and protein expression analyses in Saccharomyces cerevisiae. *Proceedings of the National Academy of Sciences of the United States of America* 100: 3107-3112, 2003.

120. **Weiner ID, New AR, Milton AE, and Tisher CC**. Regulation of luminal alkalinization and acidification in the cortical collecting duct by angiotensin II. *The American journal of physiology* 269: F730-738, 1995.

121. **Wesson DE, and Dolson GM**. Endothelin-1 increases rat distal tubule acidification in vivo. *The American journal of physiology* 273: F586-594, 1997.

122. **Wesson DE, Simoni J, and Green DF**. Reduced extracellular pH increases endothelin-1 secretion by human renal microvascular endothelial cells. *The Journal of clinical investigation* 101: 578-583, 1998.

123. **Windus DW, Cohn DE, Klahr S, and Hammerman MR**. Glutamine transport in renal basolateral vesicles from dogs with metabolic acidosis. *The American journal of physiology* 246: F78-86, 1984.

124. **Winter C, Schulz N, Giebisch G, Geibel JP, and Wagner CA**. Nongenomic stimulation of vacuolar H+-ATPases in intercalated renal tubule cells by aldosterone. *Proceedings of the National Academy of Sciences of the United States of America* 101: 2636-2641, 2004.

125. **Wu MS, Biemesderfer D, Giebisch G, and Aronson PS**. Role of NHE3 in mediating renal brush border Na+-H+ exchange. Adaptation to metabolic acidosis. *The Journal of biological chemistry* 271: 32749-32752, 1996.

126. **Yip KP, and Kurtz I**. NH3 permeability of principal cells and intercalated cells measured by confocal fluorescence imaging. *The American journal of physiology* 269: F545-550, 1995.

ACKNOWLEDGMENTS

I would like to thank:

- Prof. Carsten A. Wagner, my thesis supervisor and boss, for giving me the opportunity to work in his group, for his guidance and support through the years of my thesis;

- Prof. Jürg Biber and Prof. André W. Brändli, the members of my thesis committee, for helpful discussions and advice concerning my project;

- All of the people who contributed with their work and expertise to the completion of my thesis: Rita M. Lecca, Hubert Rehrauer, Nicolas Picard, Ana Velic, Paola Capuano, Gerti Stange and Marija Mihailova;

- All current and former members of the Wagner Group, for discussions, advice and support;

- All of the people working on J-floor of the Institute of Physiology, for creating a great working atmosphere;

Further I would like to thank:

- Zurich Center for Integrative Human Physiology “ZIHP”, for the PhD student Fellowship;
- European Renal Genome Project “EuReGene”, for financial support of this project.

Surname	**NOWIK**
First name	**MARTA**
Date of birth:	3 April, 1980
Nationality:	Polish
Current address:	Winterthurerstrasse 292 8057 Zurich, Switzerland
Phone:	(+41/44/63-55036)
E-mail address:	martan@physiol.unizh.ch

EDUCATION:

2005-	University of Zurich, Faculty of Science, Institute of Physiology
1999-2004	University of Warmia and Mazury in Olsztyn, Faculty of Biology, Department of Biotechnology; **M.Sc. in Biotechnology**
1995-2000	C.K. Norwid High School in Monki; **Matura**

RESEARCH EXPERIENCE:

2005-	Ph.D. student, Institute of Physiology, University of Zürich, Switzerland (Group Prof. Carsten A. Wagner); Ph.D. Project: *"Identification of renal genes regulated during metabolic acidosis"*
1998-1999	MSc student, Institute of Animal Reproduction and Food Research, Polish Academy of Sciences, Olsztyn, Poland (Group Jan Kotwica); MSc Project: "*Expression of 3β-hydroxysteroid dehydrogenase (3β-HSD) gene in bovine luteal cells: effect of luteinizing hormone, progesterone, prostaglandin E_2, noradrenaline and S-NAP"*

OTHER PROFESSIONAL ACTIVITIES:

- Course for working with experimental animals 2006
- Course in "Introduction in Bioethics and Biopatents" 2007

CURRENT RESEARCH INTERESTS:

- Main project about identification of renal genes regulated during metabolic acidosis using microarray approach
- Technical study about different methods of induction of metabolic acidosis in rodents
- Collaboration on the quantitative proteomic profiling of the mouse proximal tubule during metabolic acidosis

PREVIOUS RESEARCH INTERESTS:

- Supervision of the student on the project investigating regulation of organic anions/cations transporters during metabolic acidosis
- Collaboration on the project investigating role of Rhesus factor RhCG in renal ammonium excretion
- Collaboration on the project investigating adaptive remodeling of the collecting duct during metabolic acidosis

SKILLS (hands-on experience)**:**

- Enzymatic isolation of nephron segments (proximal S1/S2 and S3)
- Mouse and rat phenotype characterization
- Standard immunoblotting, immunostaining and PCR methods
- Real-time quantitative PCR (TaqMan Primer/Probe design and optimalization)
- Cell culture
- Transcriptome and proteome data mining (pathway analysis: WebGestalt, KEGG, Biocarta etc)

HONORS/SCHOLARSHIPS/FELLOWSHIPS:

2006: Fellowship from the University of Zürich Research Priority Program "Integrative Human Physiology" covering 2 years salary
2004: Faculty's of Biology Dean Award for the Master Dissertation

PRESENTATIONS ON CONGRESSES AND MEETINGS:

- Annual Meeting of American Society of Nephrology, Philadelphia 4.-9.11.2008
- Annual Meeting of German Society of Nephrology, Tübingen 27.-30.09.2008
- Summer School of European Renal Genome Project, Edinburgh 29.-31.08.2008
- Annual Meeting of German Physiological Society, Köln 02.-05.03.2008
- Annual Meeting of German Physiological Society, Hannover 27. - 30. 03. 2007
- Annual Meeting of German Physiological Society, München 24. - 27.03.2006
- Annual Meeting of European Renal Genome Project, Berlin 01.-02.02.2006

Biver S, Belge H, Bourgeois S, Van Vooren P, **Nowik M**, Scohy S, Houillier P, Szpirer J, Szpirer C, Wagner CA, Devuyst O, Marini AM (2008). “Role of Rhesus factor RhCG in renal ammonium excretion and male fertility” Nature 456(7220):339-43

Nowik M, Picard N, Stange G, Capuano P, Tenenhouse HS, Biber J, Murer H, Wagner CA (2008). ”Renal phosphaturia during metabolic acidosis revisited: molecular mechanisms for decreased renal phosphate reabsorption” Pflugers Arch 457(2):539-49

Nowik M, Lecca MR, Velic A, Rehrauer H, Brändli AW, Wagner CA (2008). ”Genome-wide gene expression profiling reveals renal genes regulated during metabolic acidosis” Physiol Genomics 32(3):322-34

Mohebbi N, Kovacikova J, **Nowik M**, Wagner CA (2007). ”Thyroid hormone deficiency alters expression of acid-base transporters in rat kidney” Am J Physiol Renal Physiol 293(1):F416-27

Rekawiecki R, **Nowik M**, Kotwica J (2005). “Stimulatory effect of LH, PGE2 and progesterone on StAR protein, cytochrome P450 cholesterol side chain cleavage and 3beta hydroxysteroid dehydrogenase gene expression in bovine luteal cells” Prostaglandins Other Lipid Mediat 78(1-4):169-84